SHAPE REALIZATION USING A FLEXIBLE SURFACE TOOLING SYSTEM

by

P. V. MADHUSUDHAN RAO

DEPARTMENT OF MECHANICAL ENGINEERING

INDIAN INSTITUTE OF TECHNOLOGY KANPUR

DECEMBER, 1995

SHAPE REALIZATION USING A FLEXIBLE SURFACE TOOLING SYSTEM

A Thesis Submitted
in Partial Fulfilment of the Requirements
for the Degree of
Doctor of Philosophy

by

P. V. Madhusudhan Rao

to the

DEPARTMENT OF MECHANICAL ENGINEERING
INDIAN INSTITUTE OF TECHNOLOGY KANPUR

December, 1995

CERTIFICATE

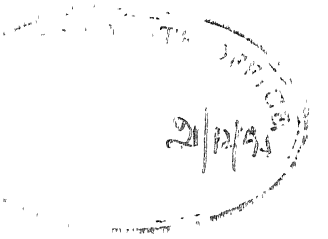

It is certified that the work contained in the thesis entitled **Shape Realization Using A Flexible Surface Tooling System** by **P. V. Madhusudhan Rao** has been carried out under my supervision and it has not been submitted elsewhere for a degree.

Dr. Sanjay G. Dhande
Professor
Department of Mechanical Engineering
IIT Kanpur

December, 1995

ABSTRACT

Shape Realization Using A Flexible Surface Tooling System

A Thesis Submitted
in Partial Fulfilment of the Requirements
for the Degree of
Doctor of Philosophy
by
P. V. Madhusudhan Rao
to the
Department of Mechanical Engineering
Indian Institute of Technology, Kanpur
December, 1995

In a class of shape realization processes, the product shape is realized by making the original material in the form of a deformable sheet to *conform* to a relatively rigid surface of the tool. Such shape conformance involves an elastic/plastic deformation of the material by one or more of the modes of deformation, namely, bending, stretching and in-plane shear. As the shape realization here is due to close conformance of one surface to another, these processes can be called as *shape conforming processes*. Press brake bending of sheet metal components, stretch forming, deep drawing, spinning, composite layup, compression molding with sheet molding compound (SMC), some of the preforming techniques used in resin transfer molding and thermoforming are some of the examples in this category.

Tooling is an important aspect in all shape conforming processes. Tooling in the form of molds and dies provide a single or multiple base surfaces required for shaping the metallic sheet or the combination of reinforcing and matrix materials. If we neglect the

the shape variations due to springback and thermal effects, the shape of the product obtained in these processes is completely defined by the shape of the mold or die used. In an ideal situation the problem of shape realization in these processes reduces to that of realization of a tool surface.

All shape conforming processes suffer from a limitation in the sense that a tool is required as a precursor for manufacturing an object. For trial production runs and prototyping work, when the shape changes are frequent, a considerable time and money is spent on the development of a tooling. For example, in the case of composites the mold design and fabrication often involves a slow and labour intensive stage of master preparation. In a typical prototyping environment, where the accuracy requirements of the product shapes are not very critical, the hard tooling is generally expensive and can be substituted by a flexible tooling for a class of component shapes. One such tooling which has been proposed for shape conforming processes is *discrete surface tooling.*

The discrete surface tooling is based on the concept of discrete approximation to a continuous surface of a mold or a die. It consists of a number of closely spaced multiple rigid surface tool elements, each of which is a surface element of an expected contour. The heights of the tool elements can be adjusted to approximate the desired surface shapes. The positioning of each surface tool element can be carried out either manually or using a computer control. The discrete nature of the tool can be overcome by placing a deformable elastomeric sheet over the surface tool elements. The flexible sheet draped over the discrete surface provides with a continuous surface required for the tooling applications. The advantage of such a tooling is that it is adjustable. A variety of surface shapes can be realized by properly adjusting the heights of surface tool elements.

The concept of discrete surface tooling was first given by Nakajima (1969). The concept was used to fabricate complicated dies for press work and electrodes for electrochemical machining. Here, one set of surface tool elements form one half of the mold surface which is held in a press and the other set of tool elements form a second half of the mold whose motion is controlled by the a ram. An extensive research work on the concept of discrete surface tooling has been carried out by Hardt et. al at the Laboratory

for Manufacturing and Productivity at Massachusetts Institute of Technology. They propose the use of a variable configuration discrete element die, which is similar to Nakajima's flexible die. Unlike the forming system proposed by Nakajima, they propose the use of discrete element die in a closed loop shape control system. The system forms a workpiece by an iterative procedure involving forming, measuring and die shape change until the shape convergence occurs.

A modified version of the above scheme of tooling has been proposed as part of the present work which is meant for those processes which can provide a single finished surface of the product, such as composite layup. The tool in this case consists of a rubber-like sheet constrained partially or fully along its edges and lifted by a set of surface tool elements deforming the flexible sheet to the required shape. The tooling in this case is known as *flexible surface tool* and the surface tool elements here are referred as *indentors*. One side of the deformed flexible sheet conforms to discrete surface formed by the indentors and the other side of the sheet can be used for tooling applications.

The present research is motivated by the need to explore the possibilities of using the proposed flexible surface tooling for shape conforming processes in general, and for composite layup in particular. Before a flexible surface tooling machine based on the proposed concept is built, it is necessary to evaluate such an idea computationally. This will help in identifying the the class of shapes which can be realized. The shape accuracies which can be obtained with such a tooling is another important aspect. The computational simulation of the proposed concept also forms a basis for the successful design and the fabrication of the flexible surface tooling machine.

The successful realization of the desired shapes by a flexible surface tooling depends on many tooling parameters. These include the size, the thickness, and the material of the flexible elastomeric sheet, the layout of indentors, the contact and the section geometries of the indentors etc. The study of these tooling parameters and their effect on the shapes obtainable is necessary. An experimental study of these parameters is a time consuming and also not cost effective.

The overall objective of the present work is to carry out the numerical study of the flexible surface tooling concept in order to evaluate its applicability to composite layup process in a prototyping environment. The specific objective of this research can be stated as follows:

- To identify the shape conforming processes and to propose the use of discrete surface tooling concept to this class of processes in general and composite layup in particular.

A class of manufacturing processes have been identified where the shape realization is due to geometric transformation from an original shape to a tool shape. A discrete surface tooling which is based on the concept of discrete approximation to a continuous surface, has been extended for shape conforming processes in general and composite manufacturing processes in particular.

- A computational study of the realizability of a class of shapes by flexible surface tooling.

A numerical study of the realizability of simple and complex shapes by the proposed flexible surface tool has been carried out. A computer program which deals with the deformation analysis of nonlinear elastic membranes in multiple contact has been written and used for this purpose.

- To study the effect of tooling parameters on the surface shape accuracies.

The effect geometric and material properties of the flexible sheet on the shape accuracies has been studied with an objective to identify the range of these parameter for a given application.

- A study of the parameters associated with discrete approximation to a continuous surface.

The tooling parameters related to surface discretization such as the number and the layout of indentors, the section and the contact geometries of the indentors play a

major role in obtaining accurate surface shapes. The effect of these parameters on the accuracy of surface shapes has been studied with an objective to identify the suitable range of theses values for fabricating a flexible surface tooling machine.

- To study the static shape optimization of the flexible sheet in the proposed tooling.

The static shape of the deformed flexible sheet in the proposed tooling is used as a base surface for tooling applications. Apart from the other parameters associated with the tooling, the deformed shape of the flexible sheet depends on the heights by which indentors are raised. The sensitivity of the static shape to the indentor heights is an important aspect. This has been dealt with an objective to improve the shape accuracies obtainable.

- To study the realizability of shapes having negative Gaussian curvature.

The proposed scheme of tooling has been modified for realizing the shapes having negative Gaussian curvature. A numerical study of this scheme of tooling has been carried out in order to evaluate the realizability of shapes.

Chapter 1 of the thesis introduces the shape conforming processes and the importance of tooling in these processes. The concept of adjustable discrete tooling is discussed and its applicability for shape conforming processes in general is discussed. A modified version of the discrete surface tooling namely, flexible surface tooling is proposed for shape conforming processes where a single finished surface is desired. The need for a computational analysis of this version of tooling is discussed.

In the proposed tooling system, deformed configuration of the flexible elastomeric sheet is used as the mold surface. Hence, the deformation analysis of the flexible sheet forms the central idea of the present work. This involves solving a finite elasto-static contact problem with multiple contacts. Chapter 2 presents the formulation and the numerical scheme used for solving this problem. The chapter also presents the validation of the computer code developed for the purpose of analysis.

Chapter 3 discusses the description of the steps involved in the shape realization proce-

dure in terms of a preprocessor, analysis and the post processor. The chapter presents the results of the numerical experiments in terms of realization of singly and doubly curved surface shapes. The results of the study of various parameters associated with the flexible sheet such as geometric and material properties of the sheet, sheet dimensions etc. on the accuracy of realized shapes are presented. The effect of external loading on the realized shapes is also dealt as a part of this chapter.

Chapter 4 is concerned with the study of parameters involved in discrete approximation of a continuous surface. These include the number of indentors, the indentor layout, the section and contact geometries of the indentors etc. The objective of this study is twofold. The main purpose of this study is to know the effect of discretization parameters in order to improve the accuracy of realizable shapes. The secondary objective of such a study is to identify the range of discretization parameters in order to fabricate a flexible surface tooling machine.

Chapter 5 of the thesis deals with the static shape optimization of the flexible sheet for the indentor heights. The presence of a flexible sheet on the discrete surface of the mold changes the effective mold shape. In such cases, the sensitivity of the static shape of the flexible sheet for indentor heights forms an important and interesting aspect of the present study. This aspect has been investigated with an objective to minimize the error between the desired and realized surface.

An alternate version of the flexible surface tooling for realizing shapes having both synclastic and anticlastic regions is discussed. A numerical study of this version of tooling forms the contents of Chapter 6. The main objective of this study is to evaluate the realizability of shapes having considerable negative Gaussian curvature. A secondary objective of this study is to compare this version of tooling with the earlier version dealt as a part of Chapter 3.

The conclusions of this work are presented in Chapter 7. The future scope of the work in terms of analysis, design and fabrication of the proposed tooling are discussed in detail. The possibility of extending the concepts and results which are the outcome of the present work to applications in other areas of engineering is also discussed.

ACKNOWLEDGEMENTS

I would like to express my sincere gratitude to my thesis supervisor **Prof. Sanjay G. Dhande** for his guidance and support over the past few years and for patience and ability to motivate the progress. He was and continues to be a model of teaching and research administration that I still strive to emulate.

A portion of the present work is based on the projects supported by Planning Commission, Govt. of India (Technology Mission on *Integrated Design & Competitive Manufacturing*) and Aeronautical Development Agency (ADA), Bangalore. My thanks go to **Dr. Kota Harinarayana, Sri T.G.A. Simha** and **Dr. B.G. Prakash** of ADA for their support.

I am grateful to **Prof. J.T. Oden**, Director, Texas Institute of Computational and Applied Mathematics (TICAM), University of Texas, Austin and **Prof. Shiv G. Kapoor** of Department of Mechanical and Industrial Engineering, University of Illinois, Urbana-Champaign for their assistance with some of the technical aspects of this research. I wish to thank **Prof. B. Sahay, Prof. Prashant Kumar, Prof. N.N. Kishore, Dr. P.M. Dixit, Dr. Gautam Biswas, Dr. Amitabha Mukerjee** and **Dr. Kalyanmoy Deb**, the faculty members for their help and the useful discussions which I had with them during the course of present research work.

Special thanks are due to **Prof. Y.V.N. Rao** and **Prof. C.R. Rao** presently with Kakatiya Institute of Technology and Science, Warangal, **Prof. S.B.L. Garg, Prof. R.K. Bharadwaj** and **Prof. R. Yadav**, Motilal Nehru Regional Engineering College, Allahabad and **Prof. P.C. Upadhyay**, Institute of Technology, Banaras Hindu University, Varanasi. They have been a constant source of encouragement and of valuable assistance.

I wish to thank all my friends, colleagues and ex-colleagues, Piyush Agrawal (Computervision, Pune), A. Ambekar, Chaitanya Babu, A.D. Bhat, Mrs. S. Biswas (BITS, Pilani), Dr. A. Chawla (IIT, Delhi), V.N. Dubey (Univ. of Sothampton), A.R. Har-

ish, Jitendra Das, Shankar Dhar (Jadavpur Univ., Calcutta), Dr. K.P. Karunakaran (IIT, Bombay), A.K. Mittal (MNREC, Allahabad), Dr. T.R. Muralidharan (Govt. of Brunei), A. Palanisamy, B.S.S Pradhan (Swiss Federal Institute, Lausanne), T.S. Rajpathak, K.V.N.D. Ramesh (Ramco, Madras), Dr. B. Ravindra (Hong Kong Univ.), N.V. Reddy, Dr. K.G. Sastry (ADA, Bangalore), S. Kishore, Manish Srikhande, N. Srinivas (Cambridge Univ.), Nivedan Tiwari, J. Venkatesh (Computervision, Pune), and Dr. Ravi Voruganti (VPI & SU) for their help in various ways during the course of my thesis work.

Finally, I wish to express my heartfelt thanks to my parents, grandparents and sisters for their endless love, encouragement and endurance during my course of study.

(P.V. Madhusudhan Rao)

Contents

List of Figures

List of Tables

List of Symbols

A, B, C	Nodes of an undeformed triangular element.
C_1, C_2	First and second Mooney constants.
$\langle \mathbf{E_1}\ \mathbf{E_2}\ \mathbf{E_3} \rangle$	Triad of unit vectors defining local coordinate system of an undeformed element.
$\left[F^G\right]$	Nodal force vector in a global coordinate system.
$\left[F^L\right]$	Nodal force vector in a local coordinate system.
I_1, I_2, I_3	First, second and third strain invariants.
N_A, N_B, N_C	Shape functions of a triangular element.
$[R]$	Transformation matrix relating global coordinate system and local coordinate system of an undeformed element.
U	Strain energy of the deformed membrane.
W	Virtual work of the external traction forces.
$\mathbf{X}$, (X_1, X_2, X_3)	Position vector (Undeformed).
a, b, c	Nodes of a deformed triangular element.
$\langle \mathbf{e_1}\ \mathbf{e_2}\ \mathbf{e_3} \rangle$	Triad of unit vectors defining local coordinate system of a deformed element.
h_0	Undeformed thickness of the flexible sheet.
h	Deformed thickness of the flexible sheet.

$\langle \mathbf{i_1}\ \mathbf{i_2}\ \mathbf{i_3} \rangle$	Triad of unit vectors defining global coordinate system.
p	Applied pressure load.
$[r]$	Transformation matrix relating global coordinate system and local coordinate system of a deformed element.
$\mathbf{t}$	Traction load vector.
$\mathbf{u}$, $(u_1,\ u_2,\ u_3)$	Displacement vector.
$\{u_A\ u_B\ u_C\}$	Nodal displacements of an element in $\mathbf{e_1}$ direction.
$u,\ v$	Parameters describing a bi-parametric surface patch.
$\mathbf{v}$	Kinematically admissible displacement field.
$\{v_A\ v_B\ v_C\}$	Nodal displacements of an element in $\mathbf{e_2}$ direction.
w	Strain energy density function.
$\mathbf{x}$, $(x_1,\ x_2,\ x_3)$	Position vector (Deformed).
$\{x_A\ x_B\ x_C\}$	x-coordinates of nodes of a triangular element.
$\{y_A\ y_B\ y_C\}$	y-coordinates of nodes of a triangular element.
Δ	Area of an undeformed triangular element.
Δ_d	Area of a deformed triangular element.
Π	Potential energy of the deformed membrane.
$\mathbf{\Omega_0}$	Initial or undeformed configuration of the membrane.
$\mathbf{\Omega}$	Deformed configuration of the membrane.
$\mathbf{\Omega_0}^e$	Initial or undeformed configuration of an element.
$\mathbf{\Omega}^e$	Deformed configuration of an element.
γ_{ij}	Lagrangian strain tensor.
δ_{ij}	Kronecker delta.
λ	Extension ratio of the membrane.

Chapter 1

INTRODUCTION

1.1 Shape Realization

In an environment of concurrent engineering, the physical realizability of a designed shape by a manufacturing process is of primary concern. The shape realization by a manufacturing process often involves achieving the desired shape of a product or a component from an original shape by using a proper tool shape and the associated machine tool kinematics (Fig. 1.1). Most of the shape realization processes can be classified into two major groups, namely, *shape generation processes* and *shape formation* or *shape transformation processes* (Tavakkoli, 1991; Dhande and Karunakaran, 1993).

In a shape generation process, the product shape is realized by the removal of material. In general, such material removal requires movement of a cutting tool through the volume of a blank (Fig. 1.2). The tool shape as well as the kinematics of machine tool play an important role in the process of shape realization. Processes such as milling, gear hobbing, electric discharge machining and sheet metal punching can be classified as shape generation processes. The realizability of a given shape by shape generation processes has been studied extensively by Voruganti (1990), Karunakaran (1993) and

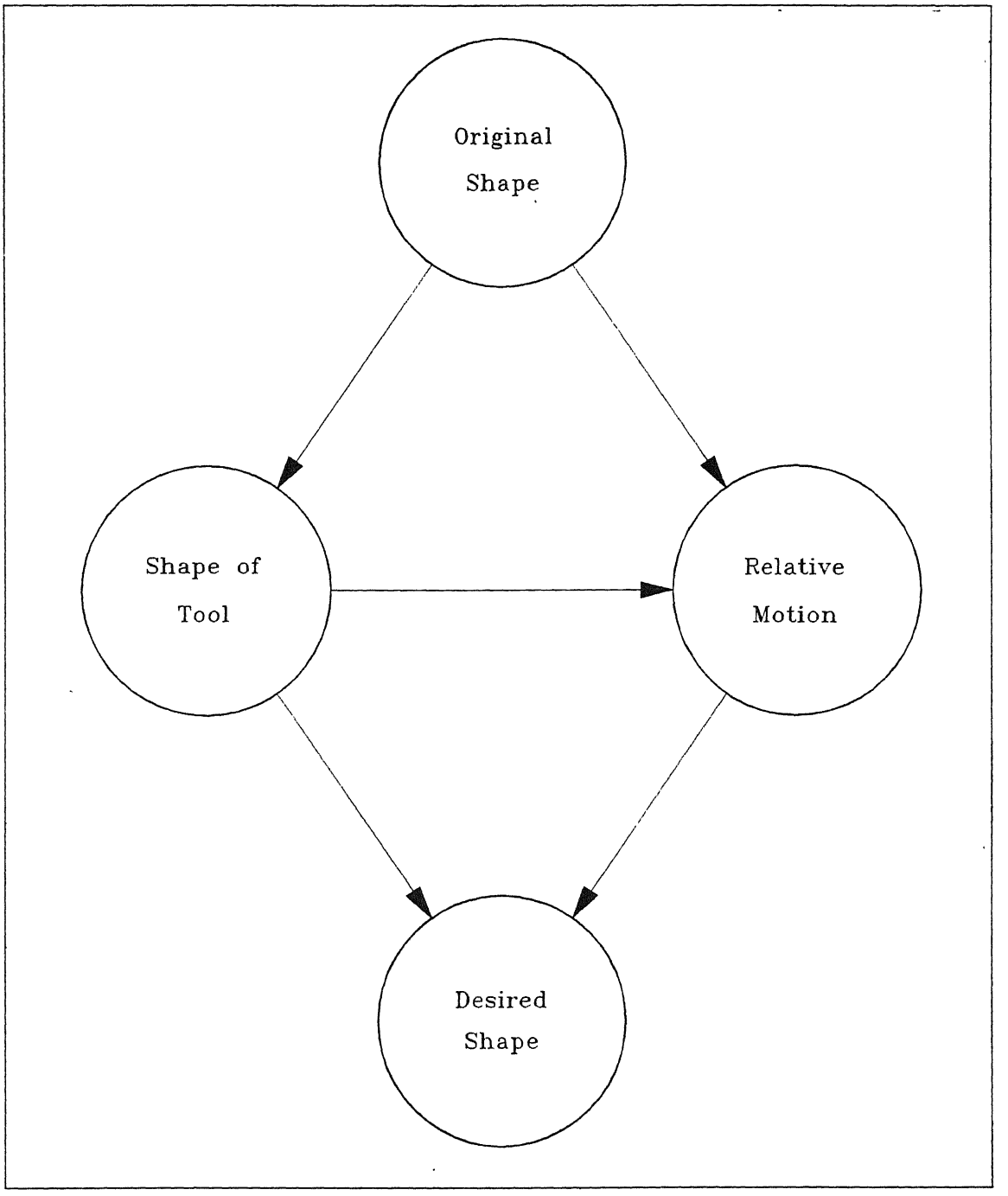

Figure 1.1. Shape Realization.

Misra (1993).

A shape forming process, on the other hand, involves a geometric transformation of a shape from its original state to a desired state (Fig. 1.2). Such transformations often involve a permanent or plastic deformation of the material. In a shape forming process, the tool shape plays a major role in realizing the shape of a product. The associated machine tool kinematics is relatively simple and its role is to bring the original material in contact with the tool surface by deforming it. In a shape forming process, the shape transformations can be idealized either at a volume level when they are called as bulk forming processes or at a surface level when they are called as sheet forming processes. The processes such as forging, rolling and extrusion can be classified as bulk forming processes, whereas sheet bending, deep drawing and roll forming are some of the processes which can be categorized as sheet forming processes (Alting, 1982).

1.2 Shape Conforming Processes

In a class of sheet forming processes, the shape is realized by making the original material in the form of a deformable sheet to *conform* to a relatively rigid surface of the tool. Such shape conformance involves an elastic/plastic deformation of the material by one or more of the modes of deformation, namely, bending, stretching and in-plane shear. As the shape realization here is due to close conformance of one surface to another, these processes can be called as *shape conforming processes.* In other words, in all shape conforming processes the product shape is dictated by the shape of a tool. The following paragraphs describe some of the important shape conforming processes and the role of tool/mold in shape realization.

A number of sheet metal forming processes used with metallic materials can be classified as shape conforming processes. In these processes, the sheet metal in the form of a blank undergoes a permanent deformation by the application of force to conform to complicated die shapes. Press brake bending of sheet metal components, stretch forming, deep drawing and spinning are some of the examples in this category (Fig.

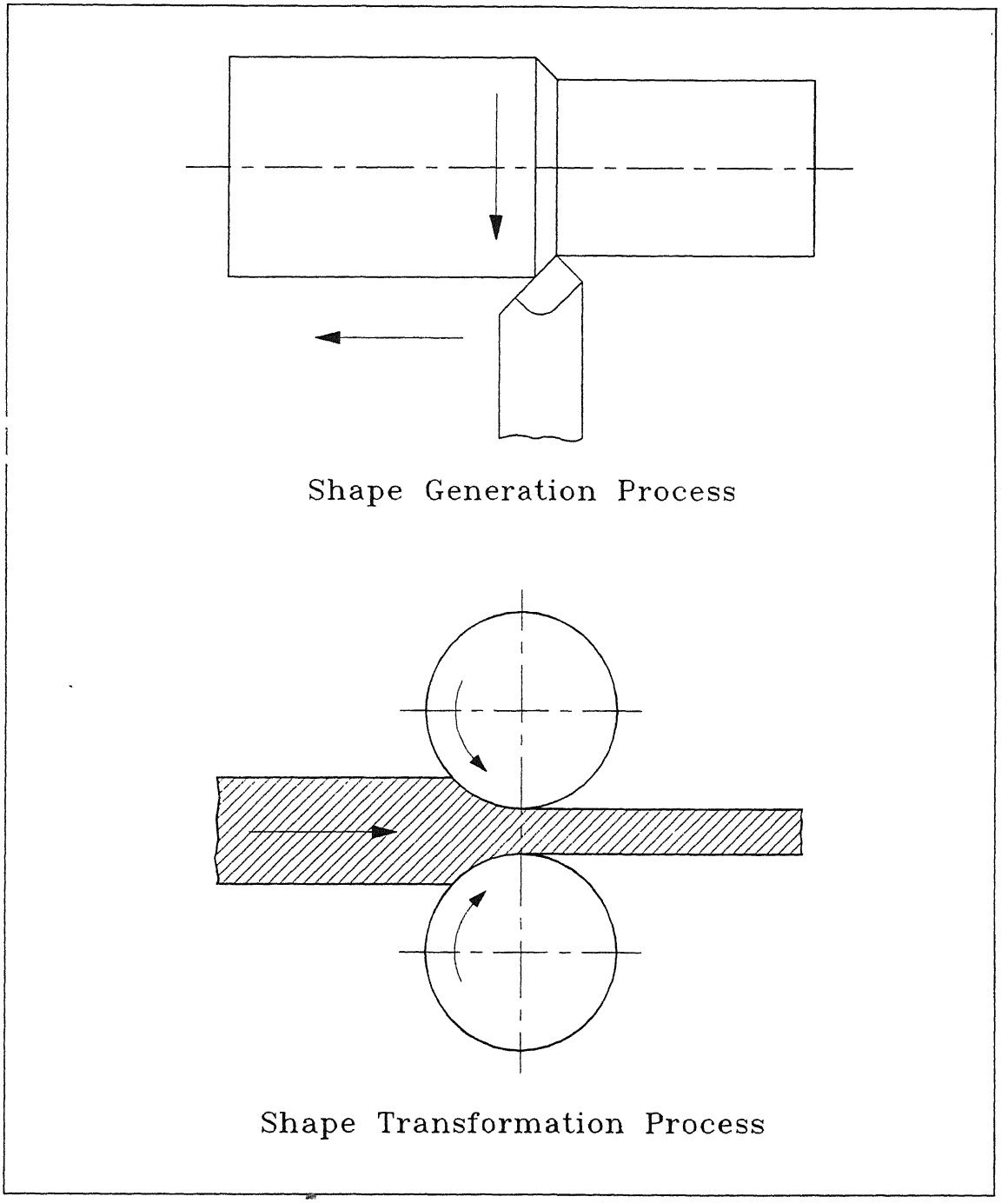

Figure 1.2. Shape Realization Processes.

1.3). Neglecting the springback associated with the deformation, the shape of the product or a component realized in these processes is completely defined by the shape of a tool used.

A majority of the composite fabrication processes can be classified as shape conforming processes (ASM Handbook, 1988; Mallick and Newman, 1990; Bader et. al, 1990; Potter, 1989). In layup, one of the primary composite fabrication processes, the multiple layers of fiber and resin are placed either by hand or a machine into a preshaped mold until the desired thickness is reached. This is often followed by the application of pressure and heat to cause the part to consolidate and cure. The shape of the product obtained here is dictated by the mold shape (Fig. 1.4). Similarly, in one of the versions of compression molding process, the mixture of resin and fiber in the form of a sheet of ready-to-mold composite material known as sheet molding compound(SMC) is placed into one half of the mold cavity mounted in a platen press and is closed with the other half. Under the applied pressure and elevated temperature, the material deforms to conform to the mold surfaces when it is allowed to cure. The shape of the product obtained in the process is defined by mold surfaces to which the sheet molding compound is made to conform (Fig. 1.5).

In a resin transfer molding (RTM) or liquid composite molding (LCM) process, the shape of the product is defined at the stage of preforming. A preform is an assembly of fibrous reinforcement and other inserts that are pre-oriented and formed to near or near-net shape serving as a skeleton of the actual structure. In the common preforming techniques such as cut-and-place preforming, directed-fiber preforming and stamping of thermoformeable materials, the reinforcement material is given a shape of a preform using the predefined mold surfaces. In this manner, it is similar to layup process and the shape realization is conceptually same as any of the shape conforming processes discussed above (Carley et. al, 1989; Steenkamer et. al, 1993).

Manufacture of fiber reinforced thermoplastic composites using preforms made of commingled fabrics is another example in the category of shape conforming processes. Commingled fabric is composed of yarns containing both the reinforcement and matrix in fiber form. A quality of the commingled fabric is its drapability allowing it to con-

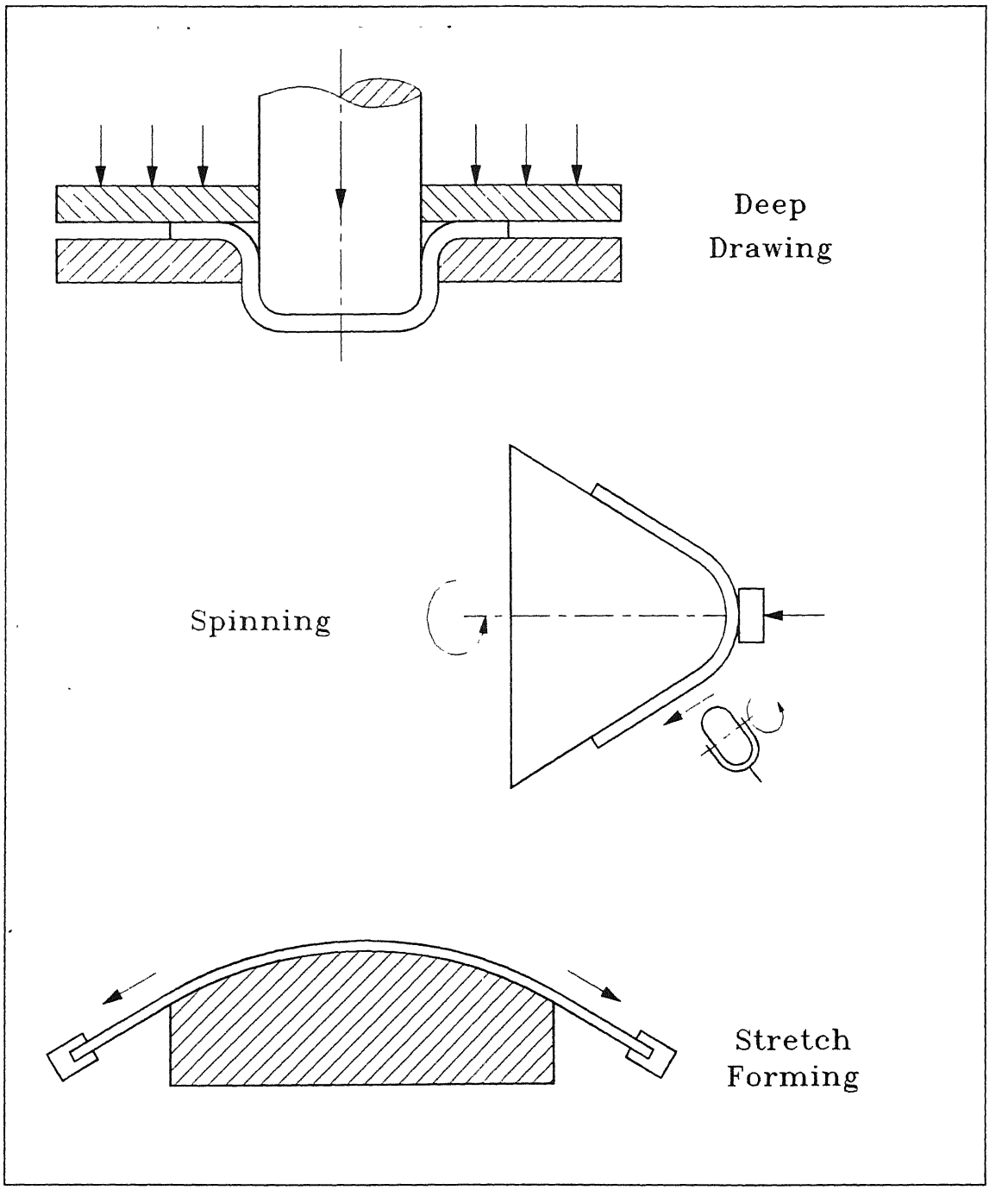

Figure 1.3. Shape Conforming Processes I.

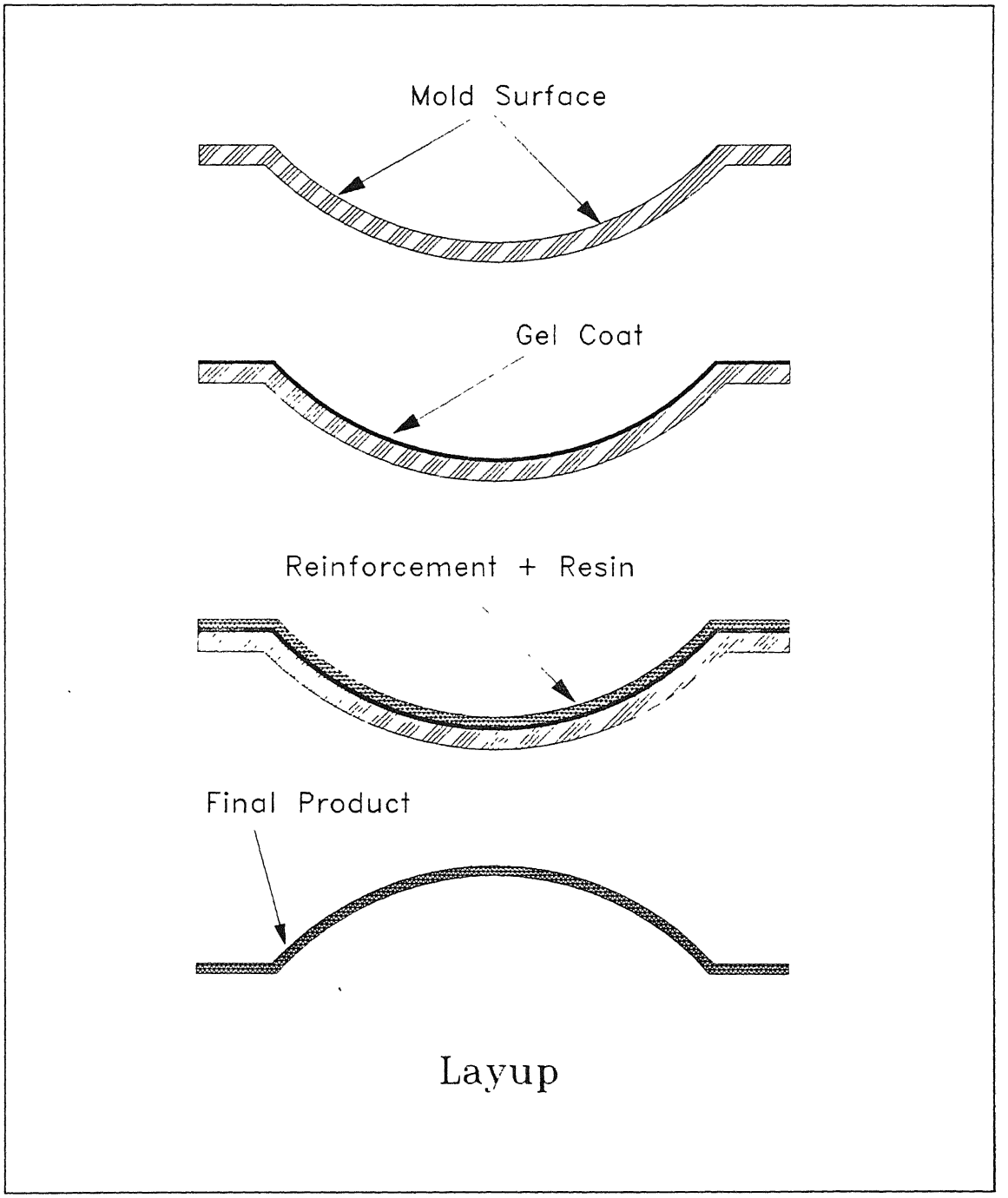

Figure 1.4. Shape Conforming Processes II.

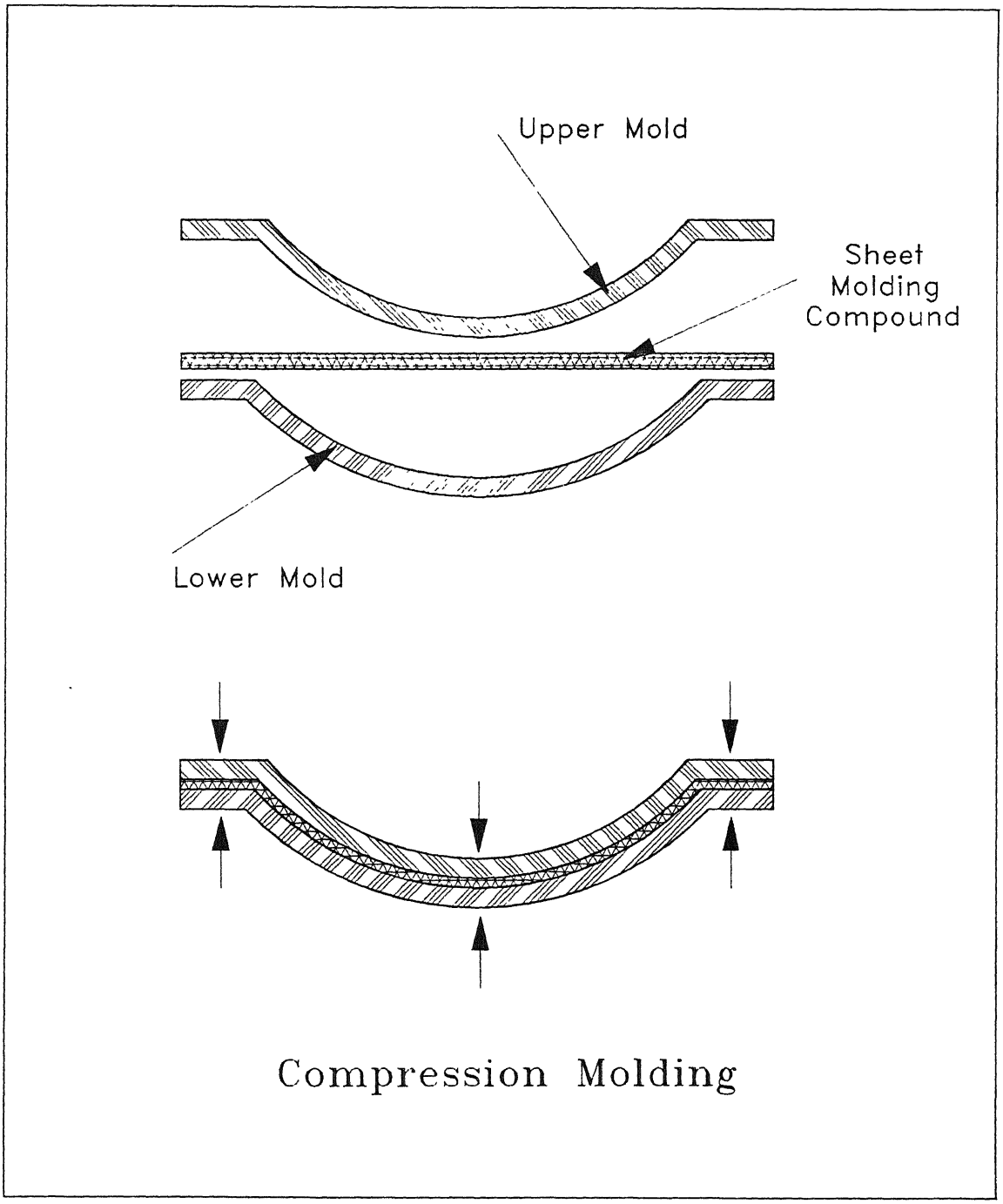

Figure 1.5. Shape Conforming Processes III.

form to mold surfaces having a compound curvature prior to being consolidated into a rigid structure (Shukla, 1989; Van West, 1990). The process of draping here involves mainly two modes of deformation, namely, bending and in-plane shear.

Another example of shape conforming process is thermoforming. The process starts with heating of a thermoplastic sheet to its softening or sag temperature. The hot thermoplastic sheet in rubbery state is placed over a mold and is drawn by vacuum or pressure into or over the mold (Fig. 1.6). The material is held in the mold until it cools and takes the shape of the mold (Farnham, 1972).

1.3 Tooling for Shape Conforming Processes

Tooling is an important aspect in all shape conforming processes. Tooling in the form of molds and dies provide a single or multiple base surfaces required for shaping the metallic sheet or the combination of reinforcing and matrix materials. In other words, tool is a precursor for fabrication of every simple or complex shape. If we neglect the the shape variations due to springback and thermal effects, the shape of the product obtained in these processes is completely defined by the shape of the mold or die used. It can be said that, in an ideal situation, the realizability of a shape in all shape conforming processes is mainly governed by the tool used and is independent of the process. This reduces the problem of shape realization in these processes to that of realization of a tool surface.

The tool design and fabrication for shape conforming processes is a time consuming and often a costly affair. This is true even when the number of components required is small or the environment is that of prototyping. This is because, many of the processes require tools and equipment similar to those used in the actual process to accurately simulate the physical properties achievable in the production level components. Typically, one spends more time on the design and fabrication of a tooling than that involved in the fabrication of component itself. For example, the design and fabrication of a die for a free-form sheet metal component is a costly and often experimentally iterative process. A number of forming experiments with improved die shapes at each stage are

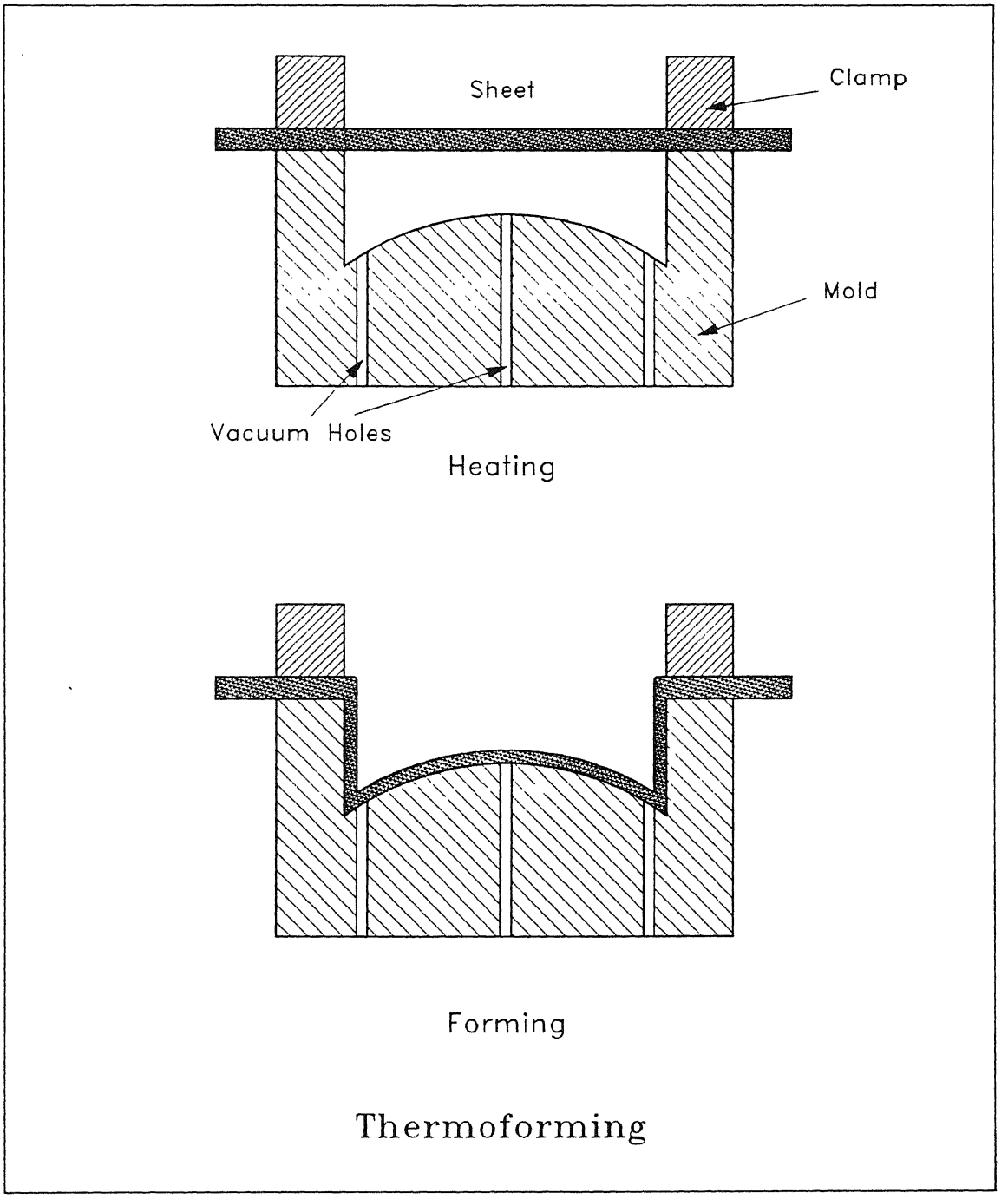

Figure 1.6. Shape Conforming Processes IV.

required to converge to a final die shape which can be used for realizing the desired component shapes (Hardt and Webb, 1982; Hardt, 1992). The computer aided design of dies for such surface shapes calls for the solution of frictional contact problems by numerical methods such as FEM in order to compensate for springback. In a prototyping environment, where the number of components required is often limited, such numerical simulations or forming experiments are both costly and time consuming.

1.4 Tooling for Composites

In the case of composites, the mold design and fabrication is often a slow, labour intensive and a costly affair. Moreover, the choice of tooling for composites is a complicated decision that must take into account many factors. In fact, their design requires the consideration of as many factors as are studied in the design of part itself. Presently, there are three approaches to the fabrication sequence of the a mold for composites (Ham and Molitor, 1989; Strong, 1993).

In the first approach, which is also a traditional composite tool building process, molds are generally made of composite materials such as Glass-Epoxy, Graphite-Epoxy and Fiberglass. This approach consists of two stages (Fig. 1.7). First stage involves the transfer of tool geometry data to a physical working model. Models are made from plaster, Epoxy-faced plaster, Fiberglass-Epoxy, wood and other materials. In a typical scheme, full size mylars are used to layout templates. These templates are then used to create lofting lines for the splining of either plaster or other materials. In the second stage, the master model thus fabricated is used as a base surface for producing a female composite mold by wet or prepreg layup process. The availability of room temperature curable tooling prepreg systems allow the construction of high quality composite tools to be built directly from the master model.

The above method of master fabrication is a slow and labour intensive process. Moreover, due to involvement of human element and thermal expansions, the transformation of geometric data to a master model is not accurate. In the second approach, the masters are produced directly by using common metal working techniques and can

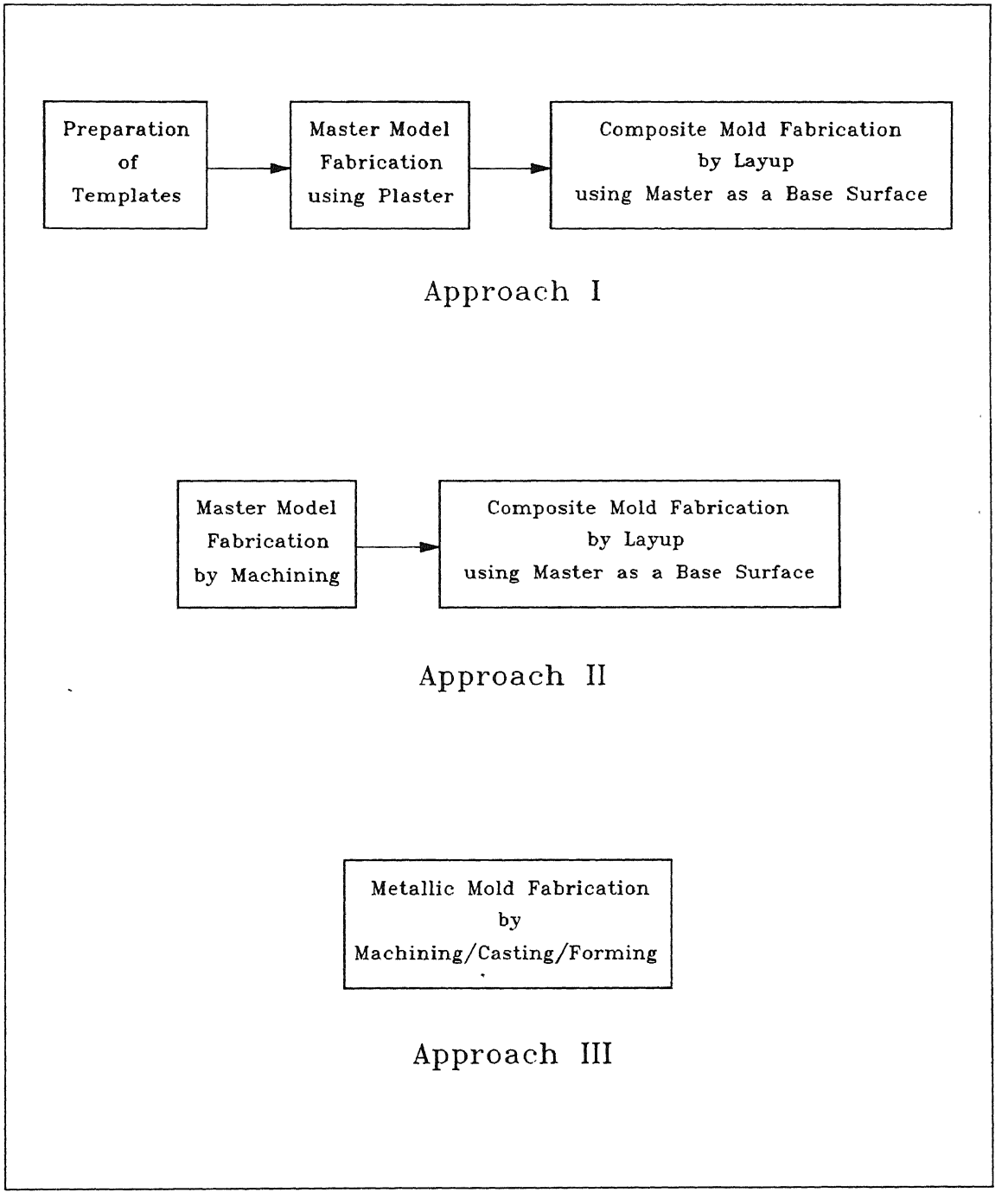

Figure 1.7. Fabrication Sequence of a Mold for Composites.

subsequently be used for the production of female composite molds (Fig. 1.7). By incorporating computer aided design and computer aided manufacturing techniques, it is possible to replace an inherently inaccurate hand built model with a master that is machined directly from the geometric model.

In the third approach, the time consuming phase of master preparation is totally eliminated by producing the female molds directly by machining or casting (Fig. 1.7). When high volumes or complex multipiece tools are required, molds can be machined directly using a CNC machine. In this case, the molds are generally made of Aluminium, Steel or Electroformed Nickel. This shortened tooling sequence provides a substantial reduction in lead time. However, for short production runs or prototyping work this approach is not economical. Moreover, in many cases it is easier to machine the male part of the shape than the female counterpart.

When the quantity of parts to be produced and the production rate are small, the tooling costs would normally be small, unless very high accuracy is required and paid for. The machinery for making the parts would also be lower in cost with relatively more human craftsmanship involved. For a low volume production, the first approach of tool fabrication is still followed in many cases when the molds are made of composites. But, this approach of prototyping composite products by preparation of hand-built masters, and subsequent composite tooling, followed by layup is a time consuming one and hence not productive. There is a need for faster and economical prototyping methods to reduce the time involved in marketing a composite product.

1.5 Flexible Surface Tooling

All shape conforming processes suffer from a limitation of, requirement of tool as a precursor for manufacturing an object. For trial production runs and prototyping work, when the shape changes are frequent, a considerable time and money is spent on the development of a tooling. Moreover, in a typical prototyping environment, the accuracy requirements of the product shapes are not very critical. In such cases, the hard tooling is generally expensive and can be substituted by a flexible tooling for

a class of component shapes. One such tooling which has been proposed for shape conforming processes is *discrete surface tooling.*

The discrete surface tooling is based on the concept of discrete approximation to a continuous surface of a mold or a die. It consists of, a number of closely spaced multiple rigid surface tool elements, each of which is a surface element of an expected contour. The heights of the tool elements can be adjusted to approximate the desired surface shapes (Fig. 1.8). The positioning of each surface tool element can be carried out either manually or using a computer control. The discrete nature of the tool can be overcome by placing a deformable elastomeric sheet over the surface tool elements. The flexible sheet draped over the discrete surface provides with a continuous surface required for the tooling applications. The advantage of such a tooling is that it is adjustable. A variety of surface shapes can be realized by properly adjusting the heights of surface tool elements. The total time involved in the tool setup is considerably less compared to that involved in the development of a hard tool.

Based on the above concept, a reconfigurable tooling system has been proposed for those processes in which two finished surfaces can be obtained such as deep drawing and compression molding (Nakajima, 1969; Hardt and Gossard, 1980). Here, one set of surface tool elements form one half of the mold surface which is held in a press and the other set of tool elements form a second half of the mold whose motion is controlled by the a ram (Fig. 1.9). As the surfaces formed by the surface tool elements will not be smooth, two flexible sheets of rubber-like material are placed between the the component to be formed and each of the mold surfaces respectively.

A variation of the above scheme of tooling has been proposed here and is meant for those processes which can provide a single finished surface of the product, such as layup. It consists of a rubber-like sheet constrained partially or fully along its edges and lifted by a set of surface tool elements deforming the flexible sheet to the required shape (Fig. 1.10). One side of the deformed flexible sheet conforms to discrete surface formed by the surface tool elements and the other side of the sheet can be used for tooling applications. The tooling in this case is known as *flexible surface tool* and the surface tool elements here are referred as *indentors.* A relatively small number of

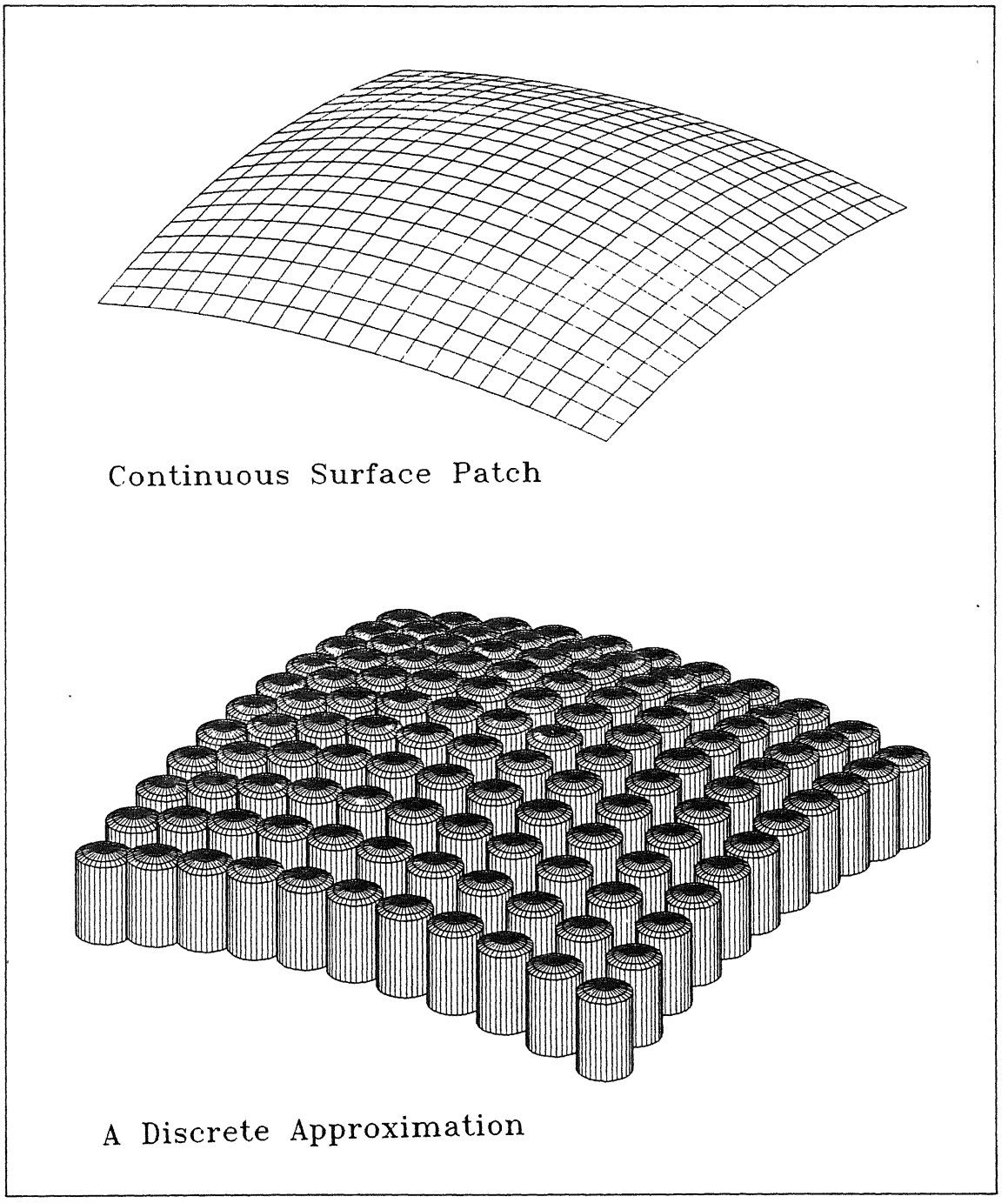

Figure 1.8. A Discrete Approximation to a Continuous Surface.

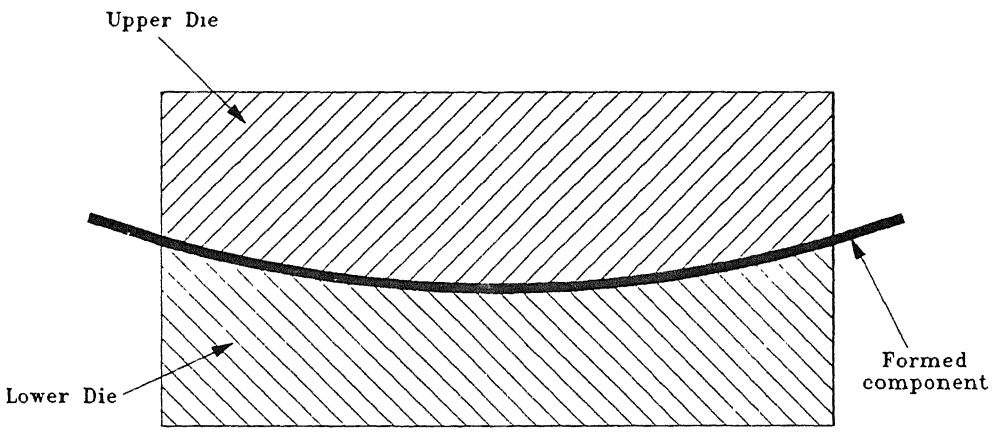

Forming with Continuous Dies

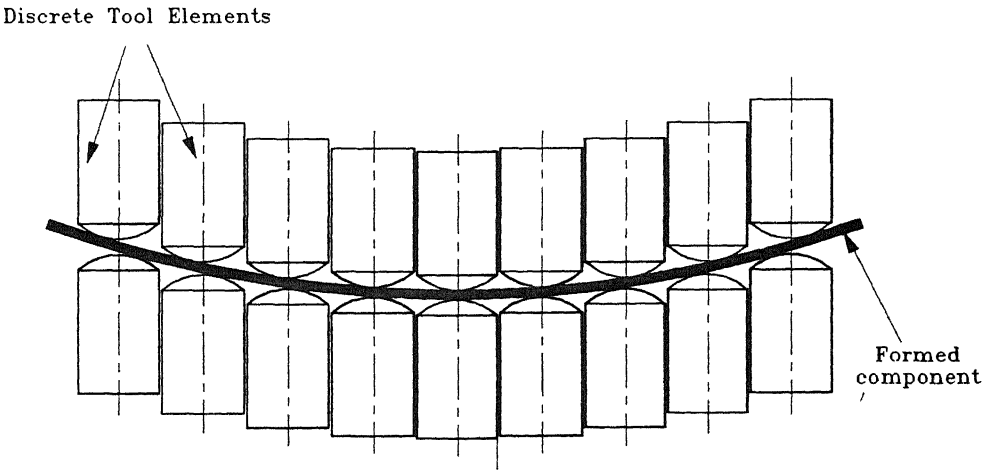

Forming with Discrete Dies

Figure 1.9. A Discrete Surface Tooling.

indentors are used here and the tooling is meant for those processes where the forming forces are considerably less.

One of the limitations of this scheme of tooling is that component shapes having only synclastic regions can be realized. This limitation can be over come by modifying the proposed tooling to include the shapes having anticlastic regions. In the modified version, the tooling consists of a rubber-like sheet with some or all the indentors bonded to it. The indentors can be attached to the flexible sheet by mechanical means or, in another version, the flexible sheet is held by a set of hollow indentors which act as suction cups. However, the nature of tooling restricts the realizable shapes to those having small curvature values in this case.

The two schemes of tooling discussed above namely, the reconfigurable tooling system of Nakajima and the flexible surface tooling system proposed here conceptually differ in terms of realization of the tool surface. In the first scheme of tooling, the mold surfaces are primarily defined by the surface tool elements and the flexible sheet only acts as a smoothing material. In this case, the thickness of the sheet is relatively small, of the order of 1 to 2 mm and it is subjected to high compressive forces due to sandwiching between the component formed and the discrete die surface. On the other hand, in the second scheme of tooling the flexible sheet is subjected to tensile forces due to indentation by surface tool elements. There is a significant change in the effective die shape due to draping of a relatively thick flexible sheet over the discrete surface. In this case the mold surface is primarily defined by the deformed configuration of the flexible sheet.

1.6 Motivation of the Present Work

The present research is motivated by the need to explore the possibilities of using the proposed flexible surface tooling for shape conforming processes in general, and for composite layup in particular. The successful development of a flexible surface tooling will result in considerable reduction of the time involved in prototyping certain class of shapes. Moreover, automated nature of the process may relegate the need of some of

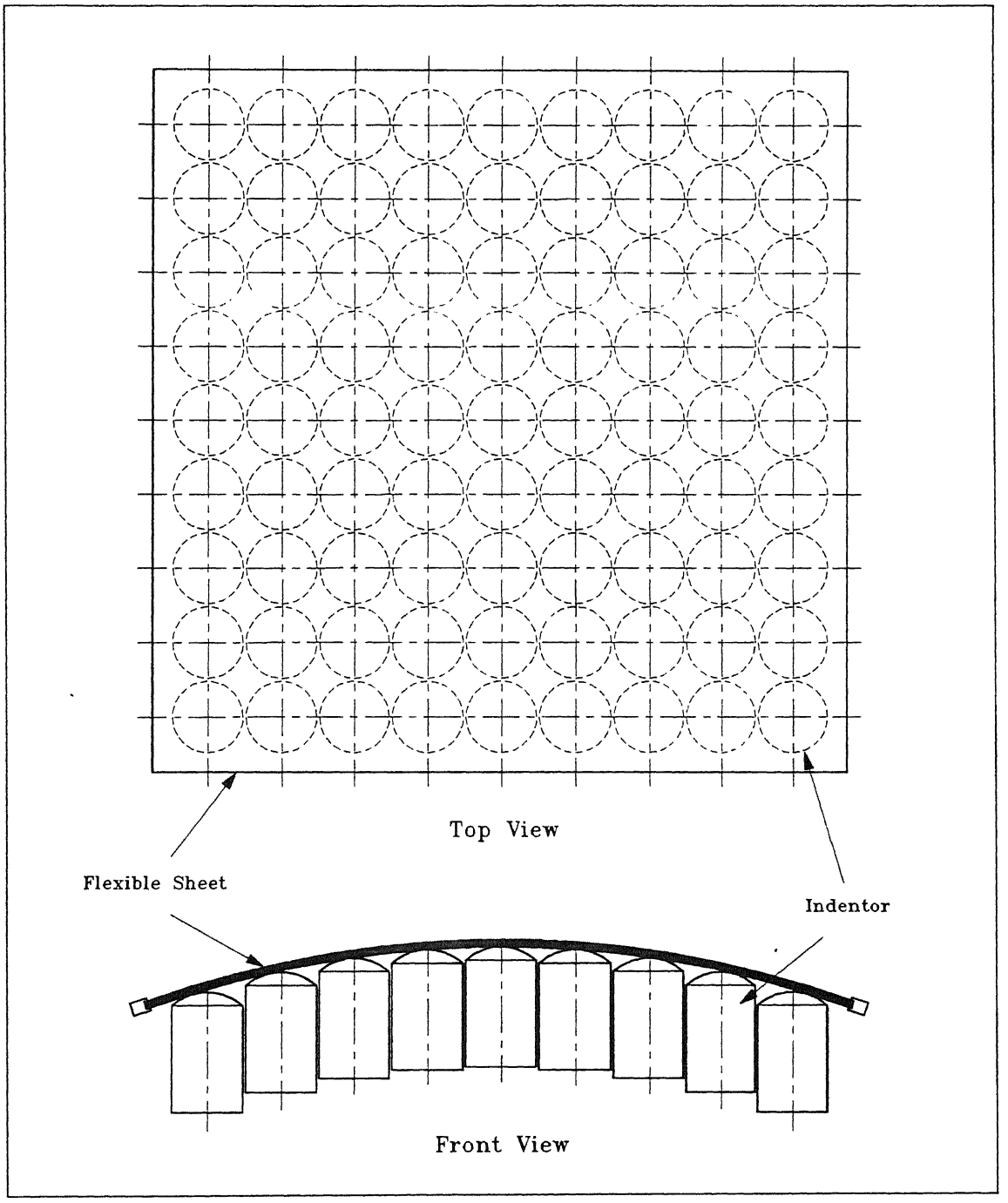

Figure 1.10. Flexible Surface Tooling.

the experts/skilled labours involved in tool design and development. Experiments with new shapes and incorporating design changes will be much easier once such a tooling is made available.

Before a flexible surface tooling machine based on the proposed concept is built, it is necessary to evaluate such an idea computationally. This will help in identifying the the class of shapes which can be realized. The shape accuracies which can be obtained with such a tooling is another important aspect. The computational simulation of the proposed concept also forms a basis for the successful design and the fabrication of the flexible surface tooling machine.

The successful realization of the desired shapes by a flexible surface tooling depends on many tooling parameters. These include the size, the thickness, and the material of the flexible elastomeric sheet, the layout of indentors, the contact and the section geometries of the indentors etc. The study of these tooling parameters and their effect on the shapes obtainable is necessary. An experimental study of these parameters is a time consuming and also not cost effective. A theoretical study and computational simulation based on finite element analysis is now possible and is recommended.

1.7 Overview of Previous Research

The concept of surface discretization for tooling requirements is not an entirely new concept. The rigid sectional templates often used for forming large curved surface structures also belong to the class of discrete surface tooling. Figure 1.11 shows one such tooling for forming stiffened panels used in an aerospace application. However, such a discrete tooling is not adjustable and can not be used for shapes other than the one for which it is built.

The concept of adjustable discrete surface tooling was first given by Nakajima (Nakajima, 1969). The concept was used to fabricate complicated dies for press work and electrodes for electrochemical machining. It consisted of number of thin wires bound together by a retainer into a bundle and the surface composed of each wire end was

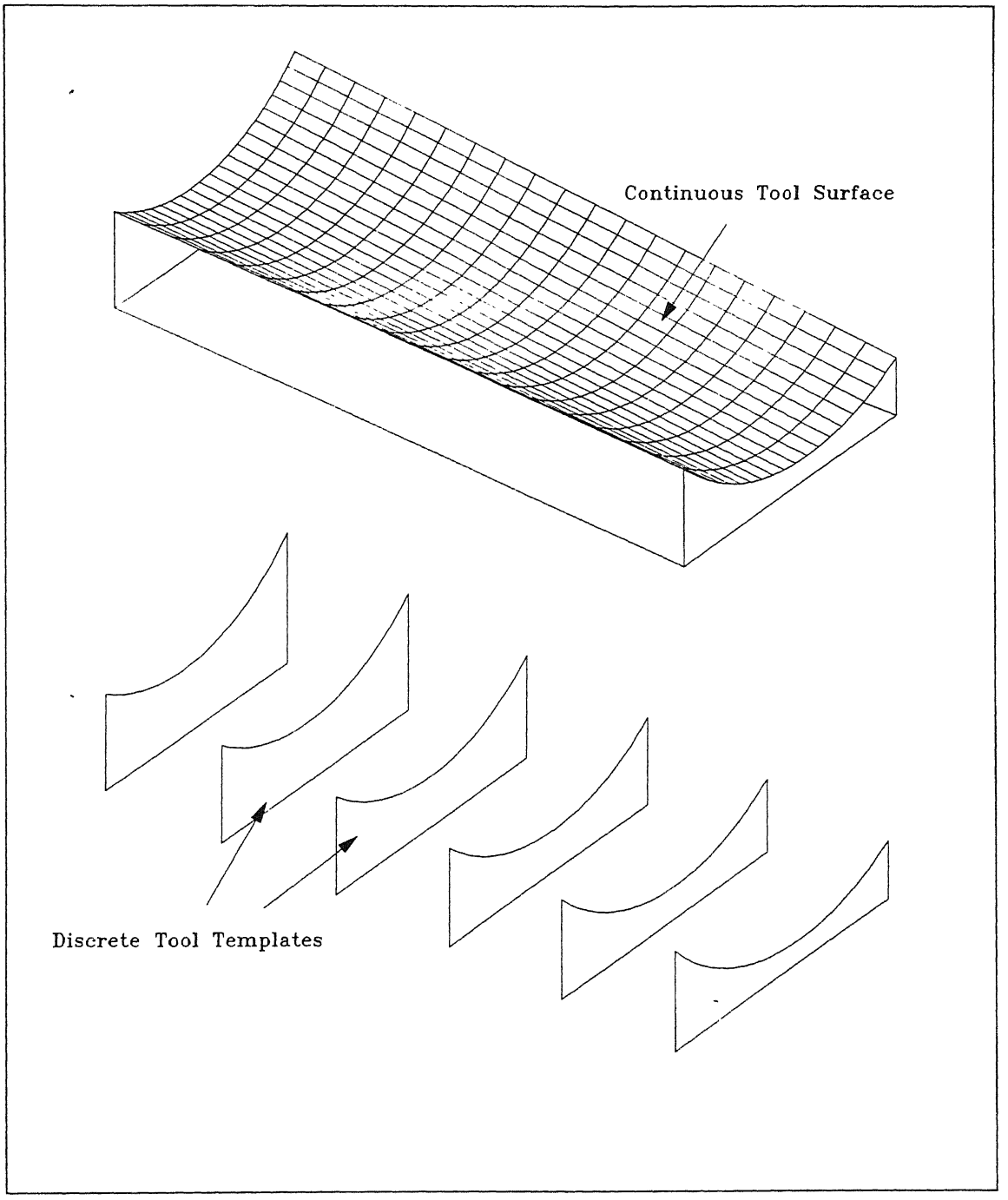

Figure 1.11. Shape Forming with Discrete Tool Templates.

used to simulate and replace the desired die surface (Fig. 1.12). Each of the wire is a surface element of an expected contour which can be pushed in the longitudinal direction to a desired position by an ultrasonic vibrator. The positioning of each wire was carried out manually using a master model of the curved surface or by computer aided numerical control. Experiments were also carried out with a rubber sheet inserted between the blank and the die to avoid the scratching of the blank by wire elements. Constant diameter circular wires were used and the locking of wires was done with an external force applied perpendicular to longitudinal direction of the wires. The tooling is meant for small lot production or trial production and can be extended to die casting, compression molding and vacuum forming of plastics with appropriate modifications.

Nakajima's work successfully demonstrates the use of discrete surface tooling for manufacture of sheet metal and plastic components. However, it does not deal with the detail study of tooling parameters in relation to the accuracy of the product shapes obtained. Once the pins forming the discrete die are positioned using a master model or numerical control, it is quite unlikely that the product with a desired shape can be obtained in the first trial of experiment. This is because the springback in terms of elastic recovery of the sheet after unloading manifests in all sheet metal forming processes. Moreover, the deformation of rubber sheet placed between the discrete die and the product being formed is likely to change the effective die shape at the time of forming. It requires a number of attempts by trial and error method in order to obtain products with a desired surface shape.

An extensive research work on the concept of discrete surface tooling has been carried out by Hardt et. al at the Laboratory for Manufacturing and Productivity at Massachusetts institute of technology (Hardt and Gossard, 1980; Hardt and Webb, 1982; Webb, 1987; Webb and Hardt, 1991; Ousterhout, 1991; Hardt, 1992; Hardt et. al, 1993). They propose the use of a variable configuration discrete element die, which is similar to Nakajima's flexible die. Unlike the forming system proposed by Nakajima, they propose the use of discrete element die in a closed loop shape control system. The system forms a workpiece by an iterative procedure involving forming, measuring and die shape change until the shape convergence occurs. Figure 1.13 shows the conceptual

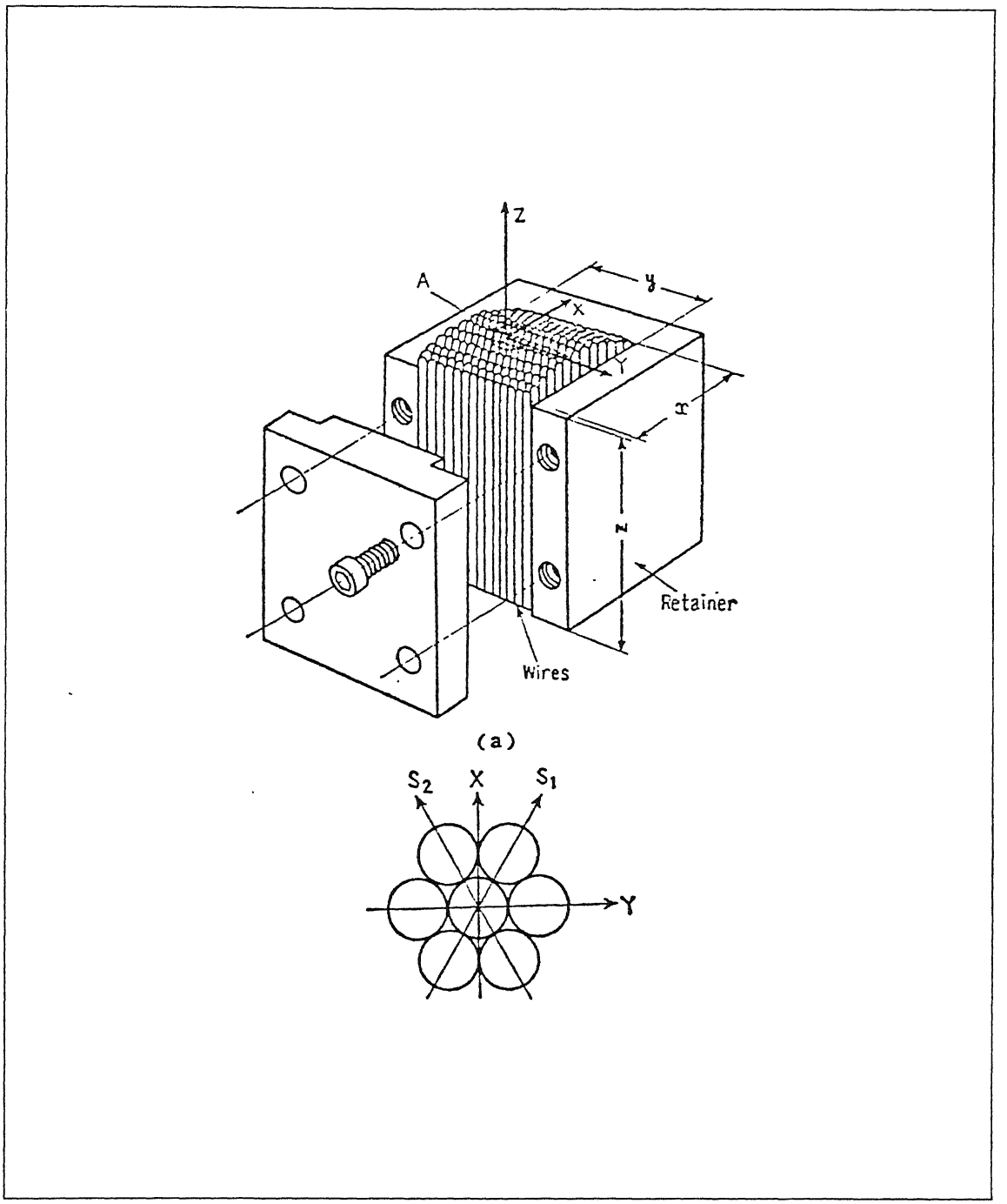

Figure 1.12. Nakajima's Discrete Surface Tooling.

sketch of their flexible sheet forming system.

A rapidly reconfigurable discretized forming machine tool was developed on a large scale for this purpose. The machine tool consists of arrays of square pins with spherical ends, clamped in a housing by a hydraulic actuator with a force of 270 kN. The die shape can be programmed by a series of position servos that adjust a single die element at a time. The deformed shape of the part is measured after forming. The measured shape is compared with the desired shape to generate the shape error. The error is processed by a shape control algorithm to command a new geometry. The new die is then used to deform the workpiece to reduce the shape error. This forming cycle continues until an acceptably low shape error results.

The reconfigurable discrete element die proposed by Nakajima and improved by Hardt el. al is primarily meant for forming sheet metal components. The work carried out by both these groups is based on the forming experiments using such a die, either in an open-loop or a closed-loop control system. Another approach to study the realizability of shapes by a discrete element die is using numerical methods such as FEM. A computational study will be helpful in reducing the number of forming experiments required to arrive at the correct die shape. However, in the case of sheet metal forming processes a numerical study accounting for large strains, material properties of the sheet, springback and the tribological aspects associated with the process is difficult. In fact, the numerical simulation of sheet metal forming processes with continuous forming surfaces provided by the conventional dies is still an active area of research (Cho, 1993; Hasan, 1993; Zhou, 1993).

In the case of composite fabrication processes such as layup, the complexities associated with the sheet metal forming are absent. In this case the forming forces are also considerably less. However, the thermal effects are likely to be present in all composite fabrication processes. But, in the case of wet or prepreg layup with room temperature curing these effects can be neglected. This means that, once the tool surface in terms of deformed flexible sheet is realized, the realization of the part is ensured. It implies that the product shape here is completely defined by the mold shape and the realizability of the shape is independent of the process. These simplifications make the numerical

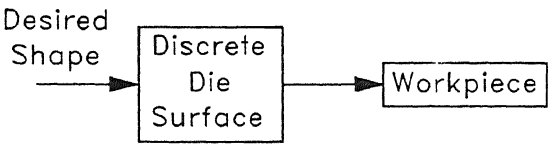

Open Loop Sheet Forming System (Nakajima)

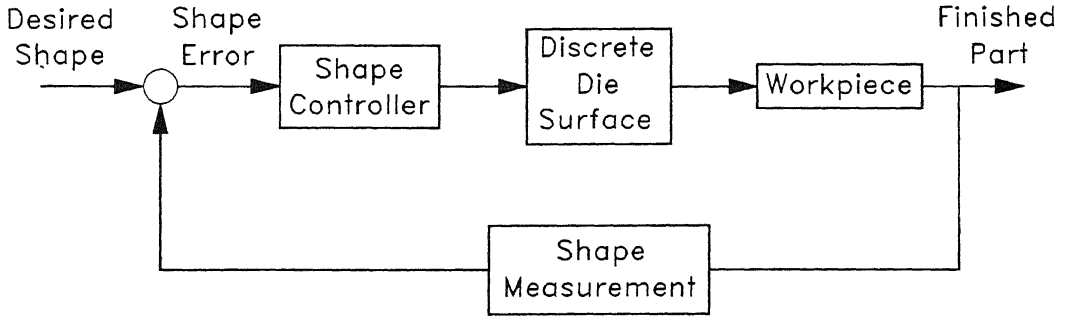

Closed Loop Sheet Forming System (Hardt et al.)

Figure 1.13. Open and Closed Loop Shape Control Systems for Sheet Metal Forming with Variable Configuration Die.

study of the flexible surface tooling feasible for applications like composite layup.

1.8 Objectives and Scope of Work

The overall objective of the present work is to carry out the numerical study of the flexible surface tooling concept in order to evaluate its applicability to composite layup process in a prototyping environment. The specific objective of this research can be stated as follows:

- To identify the shape conforming processes.

A class of manufacturing processes have been identified where the shape realization is due to geometric transformation from an original shape to a tool shape.

- To propose the discrete surface tooling concept to various shape conforming processes.

A discrete surface tooling which is based on the concept of discrete approximation to a continuous surface, has been extended for shape conforming processes in general and composite manufacturing processes in particular.

- To study the realizability of shapes by flexible surface tooling.

A numerical study of the realizability of simple and complex shapes by the proposed flexible surface tool has been carried out. A computer program which deals with the deformation analysis of nonlinear elastic membranes in multiple contact has been written and used for this purpose.

- To study the effect of tooling parameters on the surface shape accuracies.

The effect geometric and material properties of the flexible sheet on the shape accuracies has been studied with an objective to identify the range of these parameter for a given application.

- To identify and study the parameters associated with discrete approximation to a continuous surface.

The tooling parameters related to surface discretization such as the number and the layout of indentors, the section and the contact geometries of the indentors play a major role in obtaining accurate surface shapes. The effect of these parameters on the accuracy of surface shapes has been studied with an objective to identify the suitable range of theses values for fabricating a flexible surface tooling machine.

- To study the static shape optimization of the flexible sheet in the proposed tooling.

The static shape of the deformed flexible sheet in the proposed tooling is used as a base surface for tooling applications. Apart from the other parameters associated with the tooling, the deformed shape of the flexible sheet depends on the heights by which indentors are raised. The sensitivity of the static shape to the indentor heights is an important aspect. This has been dealt with an objective to improve the shape accuracies obtainable.

- To study the realizability of shapes having negative Gaussian curvature.

The proposed scheme of tooling has been modified for realizing the shapes having negative Gaussian curvature. A numerical study of this scheme of tooling has been carried out in order to evaluate the realizability of shapes.

The concept of discrete surface tooling has been extended to some of the shape conforming processes as a part of the present work. However, the present numerical study of the proposed tooling is restricted to only those processes where a single finished surface can be obtained. Another assumption of the present work is that the realizability of a component shape is assumed to be dependent on the the realization of tool surface and is assumed to be independent of the process. Such an assumption is valid only when the forming forces are considerably less and the thermal effects are insignificant. This is true with processes like composite layup with room temperature curing.

1.9 Organization of the Work

A computational study of the proposed flexible surface tooling, for realizing shapes having positive and non-positive Gaussian curvature is the main aim of the present research work. This will help in knowing the shapes realizable, identifying the tooling and discretization parameters for obtaining products with improved shape accuracies.

In the proposed tooling system, deformed configuration of the flexible elastomeric sheet is used as the mold surface. Hence, the deformation analysis of the flexible sheet forms the central idea of the present work. This involves solving a finite elasto-static contact problem with multiple contacts. Chapter 2 presents the formulation and the numerical scheme used for solving this problem. The chapter describes the modeling of the flexible elastomeric sheet for the purpose of analysis, finite element formulation of the problem, the computational procedure and the contact searching scheme. The chapter also presents the validation of the computer code developed for the purpose of analysis.

Chapter 3 starts with the description of the steps involved in the shape realization procedure followed here. This consists of a preprocessor to determine the indentor heights, the deformation analysis and the post processing for the evaluation of error between the desired and realized surface. The chapter presents the results of the numerical experiments in terms of realization of singly and doubly curved surface shapes. The results of the study of various parameters associated with the flexible sheet such as geometric and material properties of the sheet, sheet dimensions etc. on the accuracy of shapes realized are presented. The effect of external loading on the realized shapes is also dealt as a part of this study.

A discrete approximation to a continuous surface is an important ingredient in the proposed tooling. Chapter 4 is concerned with the study of parameters associated with the surface discretization. These include the number of indentors, the layout of indentors, the section and contact geometries of the indentors etc. The objective of this study is twofold. The main purpose of this study is to know the effect of discretization parameters in order to improve the accuracy of realizable shapes. The secondary objective of such a study is to identify the range of discretization parameters

for a surface tooling machine to be fabricated.

Chapter 5 of the thesis deals with the static shape optimization of the flexible sheet for the indentor heights. In the absence of the flexible elastomeric sheet between the mold surface and the part, the problem of discrete approximation to a given continuous surface turns out to be a trivial one. But the presence of flexible sheet on the discrete surface of the mold changes the effective mold shape. This change is significant for higher values of the thickness of the flexible sheet. In such cases, the sensitivity of the static shape of the flexible sheet for indentor heights forms an important and interesting aspect of the present study. This aspect has been investigated with an objective to minimize the error between the desired and realized surface.

A flexible surface tool in which the flexible sheet is constrained by some or all the indentors bonded to it has been proposed as another version of the tooling. This version of the tooling can be used for realizing shapes having both synclastic and anticlastic regions. A numerical study of this version of tooling forms the contents of Chapter 6. The main objective of this study is to evaluate the realizability of shapes having negative Gaussian curvature. A secondary objective of this study is to compare this version of tooling with the earlier version dealt as a part of Chapter 3.

The conclusions of this work are presented in Chapter 7. The future scope of the work in terms of analysis, design and fabrication of the proposed tooling are discussed in detail. The possibility of extending the concepts and results which are the outcome of the present work to applications in other areas of engineering is also discussed.

Chapter 2

DEFORMATION ANALYSIS OF FLEXIBLE SURFACE TOOL

2.1 Introduction

A flexible surface tooling system has been proposed in the previous chapter for shape conforming processes. In the proposed tooling system, the deformed configuration of the flexible elastomeric sheet is used as a base surface for the tooling requirements. The elastomeric sheet undergoes deformation due to indentation by a matrix of indentors. Knowing the deformed configuration of the flexible sheet for a given configuration of the indentors is an important aspect in the above mentioned tooling. If the thickness of the flexible sheet is small, and if the change in sheet thickness due to indentation is uniform, and also if the sheet is in contact with all the indentors then the deformed configuration of the flexible sheet can be known by geometric methods. But, this is not true in most of the cases. The complexities associated with the deformation of rubber-like materials make this problem a non trivial-one.

A mechanics-based approach accounting for the large deformations of rubber-like materials and the contact boundary conditions is essential to solve the above problem. The

presence of contact constraints together with nonlinear elastic nature of the flexible sheet makes the solution of this problem possible only by numerical methods such as FEM. This chapter describes the formulation of the above elasto-static contact problem and the numerical scheme used for solving it.

2.2 Scope of the Analysis

The flexible sheet used in the proposed tooling is subjected to a considerable stretching due to indentation. The sheet is made of rubber-like material and can be modeled as an isotropic hyperelastic medium for the purpose of analysis (Oden, 1972). Further, most of the rubber-like materials are treated as incompressible because of their capability of sustaining severe deformations without an appreciable change in volume. The flexible sheet here is of uniform thickness before deformation and it's thickness is small compared to it's other dimensions (less than 1%). As the state of stress in the sheet is essentially two dimensional in this case, the sheet can be idealized as a thin membrane with no bending effects. Thus, in the present analysis the flexible sheet is treated as a thin incompressible isotropic hyperelastic membrane.

The present computational analysis of the flexible sheet is limited to calculation of displacements only, and no attempt has been made to evaluate the stresses. It is assumed that the flexible sheet is capable of taking the applied strains without any failure. The contact friction between the flexible sheet and the indentors is not considered as a part of the present analysis. The flexible sheet is subjected to indentation on one side and the other side is acted upon by some external forces due to material processing. These external forces are small in magnitude for processes like layup. Secondly, the surface finish of the indentors is high. These factors contribute in reducing the contact friction between the sheet and the indentors.

2.3 Material Description

The deformation process involving hyperelastic materials is reversible and isothermal in nature. These materials are characterized by the presence of an elastic potential, w known as strain energy density which represents the strain energy per unit volume of the undeformed body. For rubber-like materials which can be considered as isotropic, the strain energy density is of the following form (Oden, 1972).

$$w = w(I_1, I_2, I_3) \tag{2.1}$$

where I_1, I_2 and I_3 are the three strain invariants. The incompressibility condition can be imposed by treating the third strain invariant I_3 as unity. Accordingly the strain energy function for incompressible material reduces to following form.

$$w = w(I_1, I_2); \qquad I_3 = 1. \tag{2.2}$$

Various approximations of w for specific materials have been proposed. A general form of these expressions is given by,

$$w = \sum_{i=0}^{\infty} \sum_{j=0}^{\infty} C_{ij}(I_1 - 3)^i (I_2 - 3)^j; \qquad I_3 = 1. \tag{2.3}$$

The most widely used special case of (1.3) is the Mooney-Rivlin material description (Mooney, 1940; Rivlin, 1948). It is used for characterizing rubber-like materials undergoing large strains. It is given by,

$$w = C_1(I_1 - 3) + C_2(I_2 - 3); \qquad I_3 = 1. \tag{2.4}$$

where C_1, and C_2 are the material constants. For $C_2 = 0$, the strain energy function w, reduces to a standard neo-Hookean form given by,

$$w = C(I_1 - 3) \tag{2.5}$$

2.4 Earlier Work

The first significant theoretical study of the large deformations of rubber-like materials was carried out by Adkins and Rivlin (1952) using the neo-Hookean and Mooney forms of strain energy function. More details of this work can be found in the book by Greens and Adkins (1960). Subsequent contributions in this direction in terms of analytical studies were made by Klingbeil and Shield (1964), Hart-Smith (1966), Foster (1967) and Hart-smith and Crisp (1967) etc. Finite element methods for the analysis of finite deformations of elastic bodies were first developed by Becker (1966) and Oden (Oden, 1966; Oden, 1967; Oden and Sato, 1967) independently. They attempted the plane stress problem involving large deformations of rubber-like materials. Subsequently, the problems of finite plane strain, axisymmetric and three dimensional cases were solved by finite element method (Oden, 1968; Oden and Key, 1970; Oden and Key, 1971). Much of this early work in this direction can be found in the books of Oden (1972, 1984).

Contact problems involving elastic bodies have attracted considerable attention since the work of Hertz (1882) in the last century. Problems of solid and structural mechanics with contact constraints have in recent years been the subject of a number of both theoretical and numerical investigations. There is enough literature, now available on contact problems and the more details of which can be found in the texts/monographs by Gladwell (1980), Kikuchi & Oden (1988) and Zhong (1993). As the present work deals with a contact problem involving hyperelastic membrane, only those references which are of direct relevance to the present problem are discussed in more detail.

One of the first contact problems involving elastic membranes was attempted by Yang and Hsu (1971). They solved the problem of axisymmetric indentation of a circular membrane by a rigid sphere. The problem was solved by dividing the deformed membrane into two regions: a region of contact with the sphere and a region which is free of external load except boundaries. The common boundary between the two regions is not known a priori. The nonlinear membrane equations are applied specifically to each of the regions satisfying the continuity of stress and deformation at the common

boundary.

The inflation analysis of highly elastic membranes in the presence of rigid constraints has been carried out by Feng et al. (Feng and Yang, 1973; Feng, 1974; Feng, 1975). The coordinate functions that describe the deformed configurations of the membrane are assumed to be represented by a series of geometrically admissible functions with unknown coefficients. The shape and the boundary of the contact region and the configuration of the deformed membrane under both inflation and indentation were found by minimizing the potential energy. The optimization process is carried out by using the Fletcher-Powell iterative descent method subjected to inequality constraint conditions.

The confined axisymmetric inflation of a hyperelastic cylindrical membrane with fixed ends is examined by Khayat et al. (1993). Assuming a Mooney-Rivlin constitutive model the problem is formulated to account single and multiple contacts. The tangency conditions between elastic membrane and solid boundary is respected but the formulation does not account for large deflections.

In the context of thermoforming process, the finite element analysis of rubber-like membranes with contact constraint has been dealt by a few investigators (Charrier et al., 1987; deLorenzi and Nied, 1987; Charrier et al., 1989). Thermoforming process consist of inflating or pressing a heated polymer membrane against a relatively cold mold. In these works the hot polymer is modeled as a nonlinear elastic incompressible membrane. The contact between polymer and the mold is treated as frictionless and non-slipping. The work of Charrier and associates deals with the deformation analysis of axisymmetric and non-axisymmetric shapes using one dimensional and three noded triangular finite elements respectively (Charrier et al., 1987; Charrier et al., 1989). De Lorenzi and Nied (1987) use finite element program ADINA for modeling thermoforming and blow molding. More details of the application of finite elements in the thermoforming process can be found in Zamani et al. (1989).

Ogden's strain energy function based on principal stretches has been used by Gruttman and Taylor (1992) for finite element formulation of contact problem involving elastic

membranes. Inflation analysis of a torus constrained between two plates has been carried out by them using Newton's algorithm and penalty based contact constraint.

In the contact problems discussed above the rubber-like bodies are in the membrane or plane state of stress. The contact problems of hyperelastic materials in the state of finite plane strain, finite axisymmetric deformations and the three dimensional state of stress have been attempted by many investigators. The notable among them are the works of Kikuchi & Song (1980), Endo et al. (1984), Batra (1985), Sussman & Bathe (1987), Bass (1987), Haggblad & Nordgren (1989) etc.

2.5 The Present Methodology

Most of the problems dealing with rubber-like materials in contact have been attempted by finite element method. The incremental-iterative strategies based on total or updated Lagrangian concepts are commonly used to solve this nonlinear problem. The material incompressibility and contact constraints are dealt either by mixed formulation or penalty based approach (Gadala, 1986). However, when the problem involves frictionless contacts and plane or membrane state of stress it can also be attempted by a mathematical programming approach. This approach, is commonly known as *energy search*, and consists of searching for the equilibrium configuration of the body which corresponds to a state when the potential energy is minimum. Such an approach is widely used for solving linear elasto-static contact problems (Chand et al., 1976; Hung and Saxce, 1980; Kamat and Hayduk, 1980; Westbrook, 1982; Sayegh and Tso, 1986; Johnson and Quigley, 1989; Lee and Kwak, 1989). The mathematical programming approach has been followed by a number of investigators for the deformation analysis of rubber-like membranes with or without contact constraints (Levinson, 1965; Becker, 1966; Feng and Yang, 1973; Feng et al., 1974; Tielking and Feng, 1974; Feng and Huang, 1974; Feng and Huang, 1975; Rigbi and Hiram, 1981). While, Becker uses the finite element discretization together with the energy search, other investigators follow Rayleigh-Ritz type of procedure with continuous trial functions.

In the present work the problem of deformation analysis of flexible sheet has been

attempted by finite element discretization and potential energy minimization in the presence of contact constraints. The approach is same as that of Becker (1966) except for the contact constraints. Three noded triangular elements are used for the finite element discretization. Mooney-Rivlin model is used for the strain energy calculations with incompressibility condition. The incompressibility condition has been dealt by analytical treatment which is possible in the case of plane or membrane state of stress (Gadala, 1986; Oden and Sato, 1967). The conjugate gradient method with Polak-Ribiere correction is used for energy minimization. The contact constraints are treated using a penalty approach.

2.6 Theoretical Development

In this section, kinematics of thin membrane geometry, membrane strain tensor and potential energy expressions are presented. Lagrangian description of motion referred to a set of convected coordinates is used to describe the membrane kinematics. The theoretical formulation used here is similar to that of Oden & Sato (1967). As the analysis is restricted to calculation of displacements only, an explicit computation of hydrostatic pressure is not necessary. Because, in an incompressible deformation process the hydrostatic pressure component affects only the stresses but not strains or displacements.

Consider the geometry of deformation of a thin homogeneous elastic membrane of uniform thickness h_0. The undeformed and deformed configurations are represented by $\mathbf{\Omega}_0$ and $\mathbf{\Omega}$ respectively (Fig. 2.1). The region $\mathbf{\Omega}_0$ is bounded by the planes $X_3 \pm h_0/2$, the middle surface being $X_3 = 0$. The position vectors $\mathbf{x} = x_1\mathbf{i_1} + x_2\mathbf{i_2} + x_3\mathbf{i_3}$ and $\mathbf{X} = X_1\mathbf{i_1} + X_2\mathbf{i_2} + X_3\mathbf{i_3}$ of the deformed and initial configurations respectively, are related through expression given by,

$$\mathbf{x} = \mathbf{X} + \mathbf{u} \tag{2.6}$$

where $\mathbf{u}$ is the displacement vector.

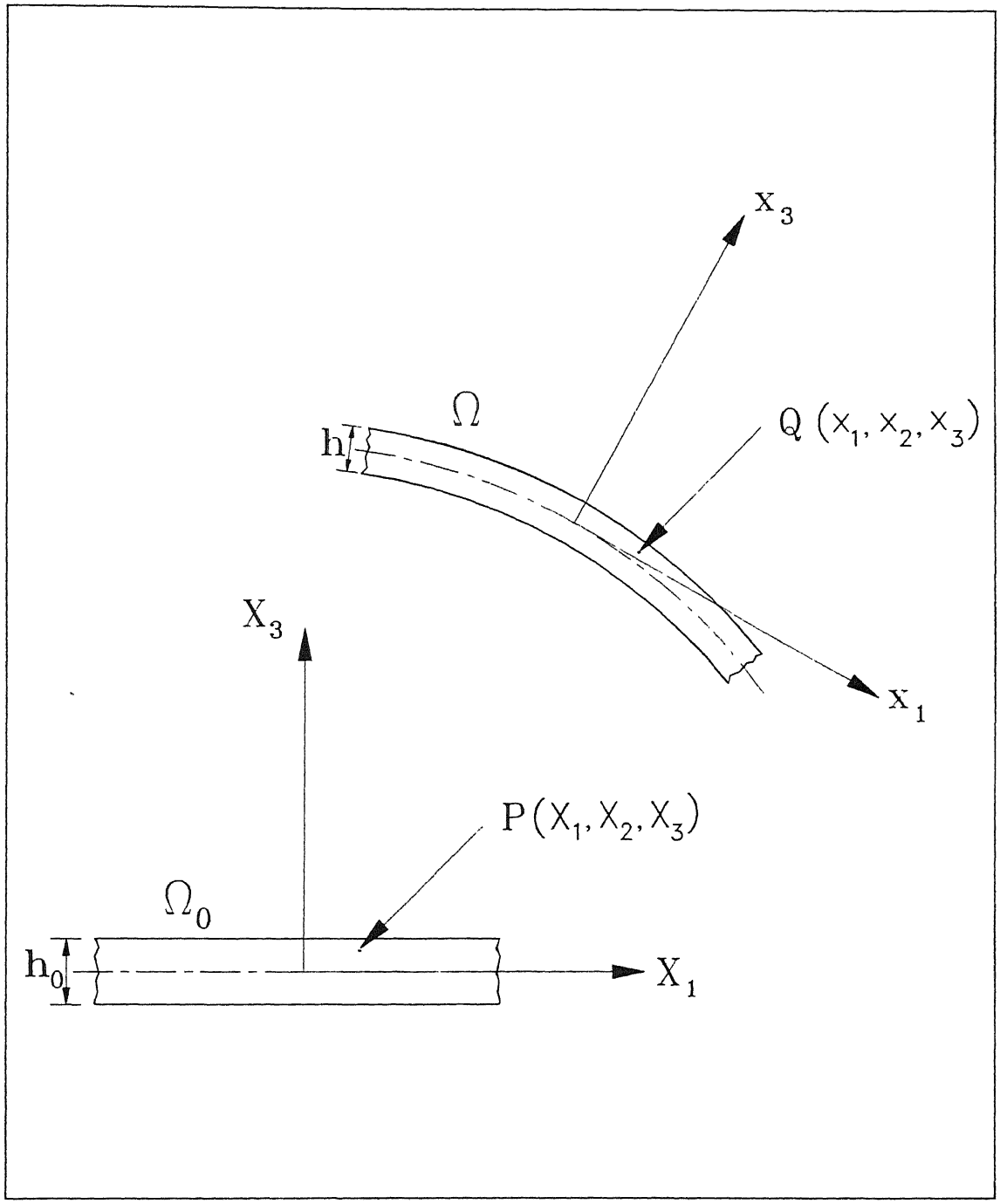

Figure 2.1. The Geometry of Deformation of a Membrane.

The Lagrangian strain tensor is now given by the relation

$$\gamma_{ij} = \frac{1}{2}\left(\frac{\partial x_k}{\partial X_i}\frac{\partial x_k}{\partial X_j} - \delta_{ij}\right) \tag{2.7}$$

where δ_{ij} is the Kronecker delta. Thickness of the membrane after deformation, h, is given by

$$h = \lambda h_0 \tag{2.8}$$

where λ is the extension ratio at the middle surface in a direction normal to the middle surface. Assuming the membrane to be thin, strain tensor can be written as

$$\gamma_{\alpha\beta} = \frac{1}{2}\left(\frac{\partial u_\alpha}{\partial X_\beta} + \frac{\partial u_\beta}{\partial X_\alpha} + \frac{\partial u_i}{\partial X_\alpha}\frac{\partial u_i}{\partial X_\beta}\right)$$

$$\gamma_{13} = 0 \quad \gamma_{23} = 0 \quad \gamma_{33} = \frac{1}{2}\left(\lambda^2 - 1\right) \tag{2.9}$$

where $\alpha, \beta = 1, 2$ and $i = 1, 2, 3$. The three strain invariants I_1, I_2, I_3 are given by

$$\begin{aligned} I_1 &= \lambda^2 + 2(1 + \gamma_{\alpha\alpha}) \\ I_2 &= -\lambda^4 + \lambda^2 I_1 + \frac{1}{\lambda^2} I_3 \\ I_3 &= \lambda^2 (1 + 2\gamma_{\alpha\alpha} + 2e_{\alpha\beta}e_{\lambda\mu}\gamma_{\alpha\lambda}\gamma_{\beta\mu}) \end{aligned} \tag{2.10}$$

where α, β, γ, $\mu = 1, 2$ and $e_{\alpha\beta}$ and $e_{\lambda\mu}$ are the two dimensional permutational symbols ($e_{12} = 1$, $e_{21} = -1$, $e_{11} = e_{22} = 0$). Imposing the incompressibility constraint $I_3 = 1$, the above expressions can be written as,

$$\begin{aligned} I_1 &= \lambda^2 + 2(1 + \gamma_{\alpha\alpha}) \\ I_2 &= -\lambda^4 + \lambda^2 I_1 + \frac{1}{\lambda^2} I_3 \\ \lambda^2 &= (1 + 2\gamma_{\alpha\alpha} + 2e_{\alpha\beta}e_{\lambda\mu}\gamma_{\alpha\lambda}\gamma_{\beta\mu})^{-1} \end{aligned} \tag{2.11}$$

The potential energy for the deformed membrane, Π is given by

$$\Pi = U - W = \int_v w\,(I_1, I_2)\,dv - \int_s \mathbf{t} \cdot \mathbf{v} ds \tag{2.12}$$

where U is the strain energy of the deformed membrane and W the virtual work of external traction forces, $\mathbf{t}$. $\mathbf{v}$ is the kinematically admissible displacement field and s is the part of boundary on which tractions are specified.

2.7 Finite Element Formulation

The finite element idealization used here consists of replacing the middle surface of the membrane by a patchwork of plane triangular elements and loading it with equivalent concentrated loads at the nodes. Local state of stress here is considered to be that of plane stress ($\sigma_3 = 0$). The analysis further assumes that the principal stresses are tensile everywhere ($\sigma_1 \geq 0$, $\sigma_2 \geq 0$). This is the central idea on which the works of Oden and Sato (1967) and Charrier et al. (1989) are based.

Consider a triangular element $\Omega_0{}^e$ with nodes A, B and C in a coordinate space, defined by a triad of unit vectors $\langle \mathbf{i_1}\ \mathbf{i_2}\ \mathbf{i_3} \rangle$. The element undergoes deformation to take a new shape Ω^e with nodes a, b and c (Fig. 2.2). In order to calculate the strain energy due to stretching of the membrane, it is convenient to compare the two configurations in a common plane. For this purpose, undeformed element is placed in the plane of deformed one. Such a transformation does not affect the strain energy calculations as it involves only rigid body translations and rotations.

We define a local coordinate system for the undeformed element by a triad of unit vectors $\{\mathbf{E}\}^T = \langle \mathbf{E_1}\ \mathbf{E_2}\ \mathbf{E_3} \rangle$. The unit vector $\mathbf{E_1}$ is directed from node A to B. The unit vector $\mathbf{E_3}$ is perpendicular to the plane of the element and $\mathbf{E_2}$ is the cross product of $\mathbf{E_3}$ and $\mathbf{E_1}$. Similarly, we attach a local coordinate system for the deformed element which is defined by the triad of vectors $\{\mathbf{e}\}^T = \langle \mathbf{e_1}\ \mathbf{e_2}\ \mathbf{e_3} \rangle$. The two local coordinate systems are related to global coordinate system $\{\mathbf{i}\}^T = \langle \mathbf{i_1}\ \mathbf{i_2}\ \mathbf{i_3} \rangle$ by transformation matrices $[R]$ and $[r]$ given by,

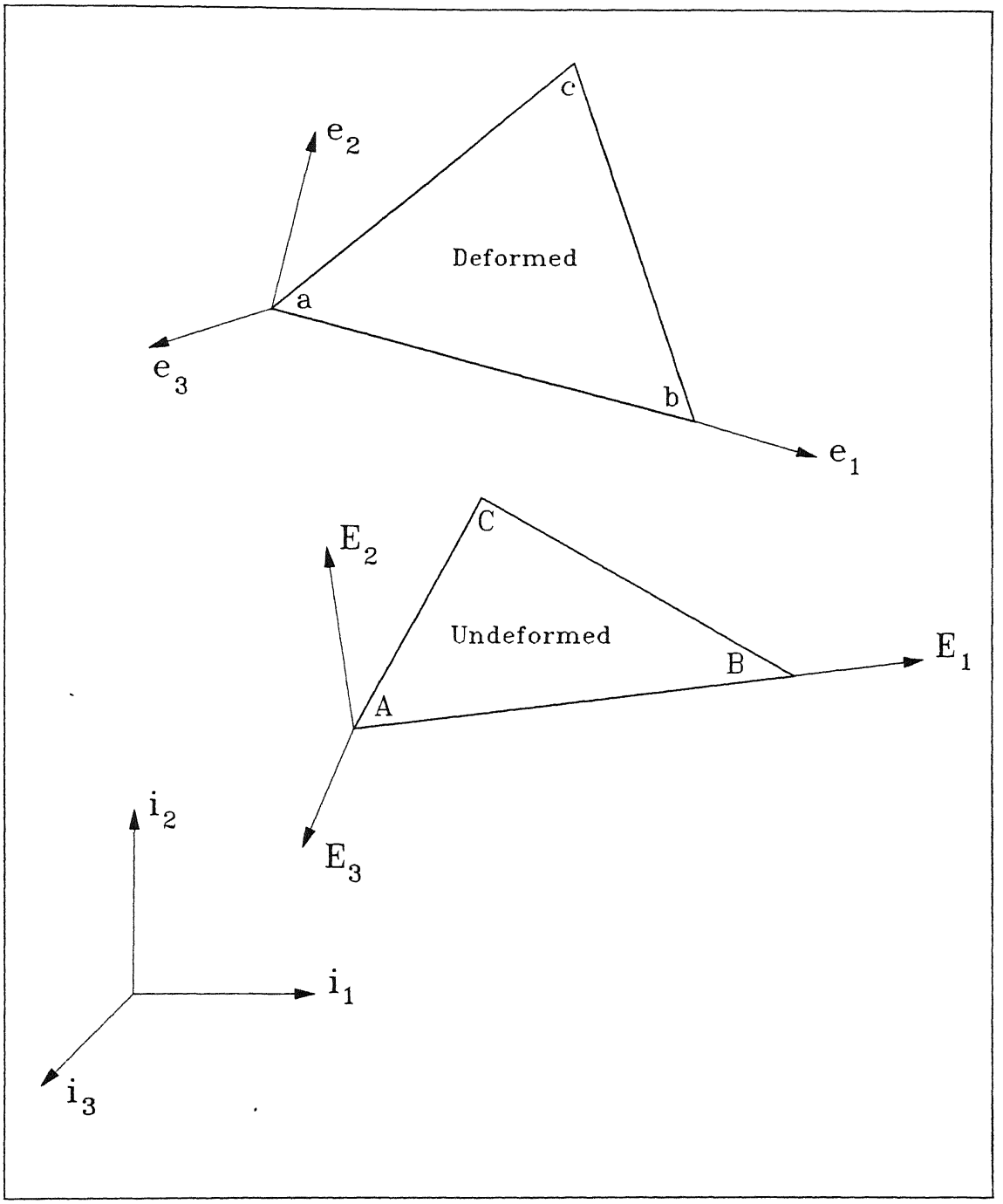

Figure 2.2. Deformation of a Triangular Membrane Element in Space.

$$[R] = \{\mathbf{E}\}\{\mathbf{i}\}^T \qquad [r] = \{\mathbf{e}\}\{\mathbf{i}\}^T \tag{2.13}$$

Figure 2.3 shows the undeformed element (after transformation) and the deformed element in the local coordinate system of the latter. Let $\{u\}^T = \{u_A\ u_B\ u_C\}$ and $\{v\}^T = \{v_A\ v_B\ v_C\}$ are respectively the nodal displacements of the triangular element in $\mathbf{e}_1$ and $\mathbf{e}_2$ directions respectively. The displacements u and v of a point within the element, using a linear variation is given by,

$$\begin{aligned} u &= N_A u_A + N_B u_B + N_C u_C = \{u\}^T [N] \\ v &= N_A v_A + N_B v_B + N_C v_C = \{v\}^T [N] \end{aligned} \tag{2.14}$$

where N_A, N_B and N_C are shape functions given by,

$$\begin{aligned} N_A(x,y) &= \frac{1}{2\Delta}\left[(y_C - y_B)(x_B - x) - (x_C - x_B)(y_B - y)\right] \\ N_B(x,y) &= \frac{1}{2\Delta}\left[(y_A - y_C)(x_C - x) - (x_A - x_C)(y_C - y)\right] \\ N_C(x,y) &= \frac{1}{2\Delta}\left[(y_B - y_A)(x_A - x) - (x_B - x_A)(y_A - y)\right] \end{aligned} \tag{2.15}$$

$$2\Delta = (x_C - x_B)(y_A - y_C) - (x_A - x_B)(y_C - y_B)$$

Using Equation (1.15), one can derive the the following.

$$\begin{aligned} \frac{\partial u}{\partial x} &= \frac{1}{2\Delta}\left[(y_B - y_C)u_A + (y_C - y_A)u_B + (y_A - y_B)u_C\right] \\ \frac{\partial v}{\partial x} &= \frac{1}{2\Delta}\left[(y_B - y_C)v_A + (y_C - y_A)v_B + (y_A - y_B)v_C\right] \\ \frac{\partial u}{\partial y} &= \frac{1}{2\Delta}\left[(x_C - x_B)u_A + (x_A - x_C)u_B + (x_B - x_A)u_C\right] \\ \frac{\partial v}{\partial y} &= \frac{1}{2\Delta}\left[(x_C - x_B)v_A + (x_A - x_C)v_B + (x_B - x_A)v_C\right] \end{aligned} \tag{2.16}$$

the strain energy, U can now be evaluated by substituting the results of (1.16) in the

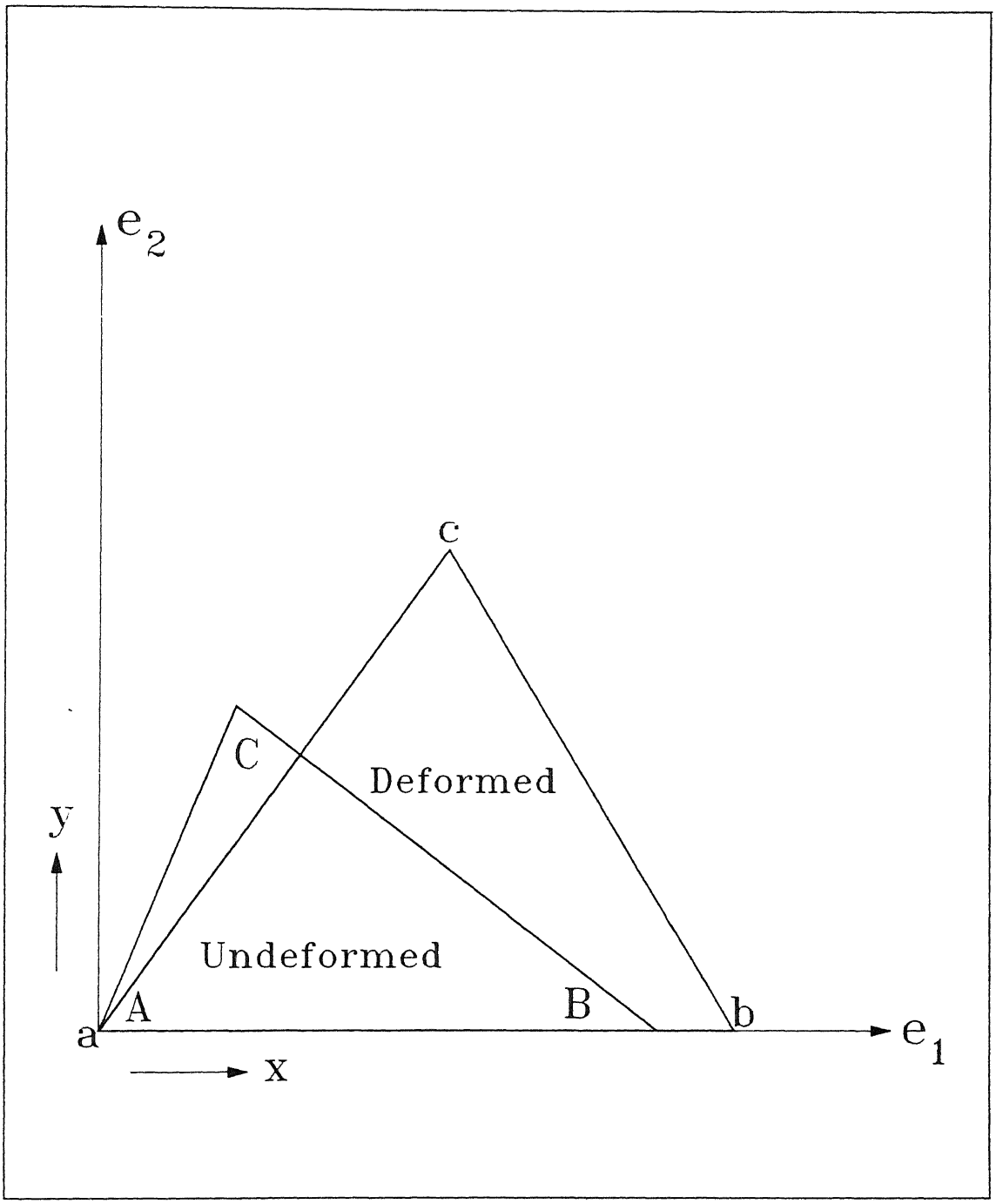

Figure 2.3. Comparison of Deformed and Undeformed Elements in the Plane of Deformed Element.

expressions of membrane strain tensor given by Equation (1.9) and using Equations (1.11) and (1.12).

The external forces in this problem are in the form of pressure loads acting on the surface element. As the membrane deforms not only does the direction of this pressure change but also the area on which it acts changes. To account this, it is first assumed that the dimensions of each element are sufficiently small that the pressure is essentially unform over the surface of individual elements. It can be shown that consistent with the linear variation of displacement assumed within an element and the positive sense of pressure, the equivalent out of plane forces at the element nodes are

$$F_{zA}{}^{L} = F_{zB}{}^{L} = F_{zC}{}^{L} = -\frac{p\Delta_d}{3} \tag{2.17}$$

where p is the applied pressure and Δ_d is the deformed element area. The global components of the nodal forces can now be obtained by the following transformation.

$$\left[F^G\right] = [R]\left[F^L\right] \tag{2.18}$$

2.8 Contact Constraints

The deformed configuration of the flexible sheet due to indentation is such that the geometric constraints are not violated. In other words any solution to the equilibrium configuration of the membrane is such that no interpenetration of the indentor and membrane materials is allowed. This condition on the kinematically admissible displacement field of the flexible sheet can be imposed by penalty approach. The penalty being proportional to the amount of violation.

The above contact conditions which are not known a priori needs to be evaluated by contact searching. The two models which are often used for evaluation of contacts are node-to-node interface model and node-to-segment interface model (Zhong, 1993). The node-to-segment contact searching scheme is generally used for bodies undergoing large displacements and rotations which consist of discretizing the contacting body in

terms of finite elements and also discretizing the target body in terms of polygons. Then, each of the potential contacting nodes of the contacting body are checked with each of the segments of the target body.

A slightly modified version of the node-to-segment algorithm has been used here which consists of, checking for each of the potential contacting nodes of the contacting body with the surface of the target body without any discretization. The target bodies here, namely, the indentors are rigid and axisymmetric. They can be defined in terms of surface equations and this definition of surface is directly used for contact evaluation. A number of minimax tests are used to identify potential contacting nodes and to avoid any unnecessary computation involved.

2.9 Computational Procedure

The computational procedure used here consists of, minimizing the total potential energy of the system subjected to given geometric constraints. For this purpose, the domain Ω_0 is discretized into three noded triangular finite elements. The total number of nodes and elements being N and E respectively. The number of variables in the minimization problem are $3N'$; N' being the total number of unconstrained nodes. The objective function is the total potential energy of the system summed over E elements. Potential energy of the individual element consists of the strain energy due to deformation obtained from undeformed and deformed configurations of the element after transformation and the potential of loads, if any, on the element.

To solve this constrained optimization problem efficiently, the sequential unconstrained minimization technique (SUMT) has been used. SUMT transforms the constrained optimization problem to an unconstrained one by penalizing the constraint violation if any. The conjugate gradient algorithm with Polak-Ribiere correction is adopted as the minimization technique. This technique has been used by other investigators also for a successful solution of contact problems. (May, 1986; Dilintas et al., 1988). The method of multipliers (MOM) type of penalty which is equally effective in both feasible and non-feasible solution domains is used for transforming constrained optimization

problem into an unconstrained one (Schuldt et al., 1977; Reklietis, 1989). The computer program developed for this purpose is written in C and is implemented on DEC-3000 platform.

It is convenient to assume the initial or undeformed configuration as a starting solution to the above optimization problem. A starting solution close to the equilibrium configuration is found to save a lot of computational time. The analysis has been carried out with different starting solutions and in every case the solution converged to the equilibrium configuration. These experiments justify the uniqueness of the solution in this case. The experiments were also carried out with single and multiple load steps. Based on the results of these experiments, it has been found that the convergence of the solution in this case is independent of the load step. This further strengthens the uniqueness of the solution and the smooth convergence of the optimization process in this case.

2.10 Validation

The correctness of the formulation and the numerical scheme used here has been verified by running the computer program developed, for three standard test cases taken from the works of Becker (1966), Feng & Huang (1974) and Feng et al. (1974). The first test case deals with the problem of in-plane stretching of an elastic sheet. A thin square membrane is fixed along one of its edges and the opposite edge is moved to stretch the membrane to twice its original length. The purpose of this example is to verify the correctness of strain energy calculations and the convergence of the solution process. The ratio of first and second Mooney constants, C_1/C_2 is taken as 8.0 for the analysis. Figure 2.4 shows the deformed profile of the stretched membrane. The deformed geometry has been compared with the results of Becker (1966) and the maximum deviation in displacement has been found to be the order of 0.8% (Fig. 2.5).

The second test case is concerned with the inflation of a square membrane for various applied pressures. The results are compared with the work of Feng & Huang (1974). Figure 2.6 shows the deformed configuration of the membrane at various inflation

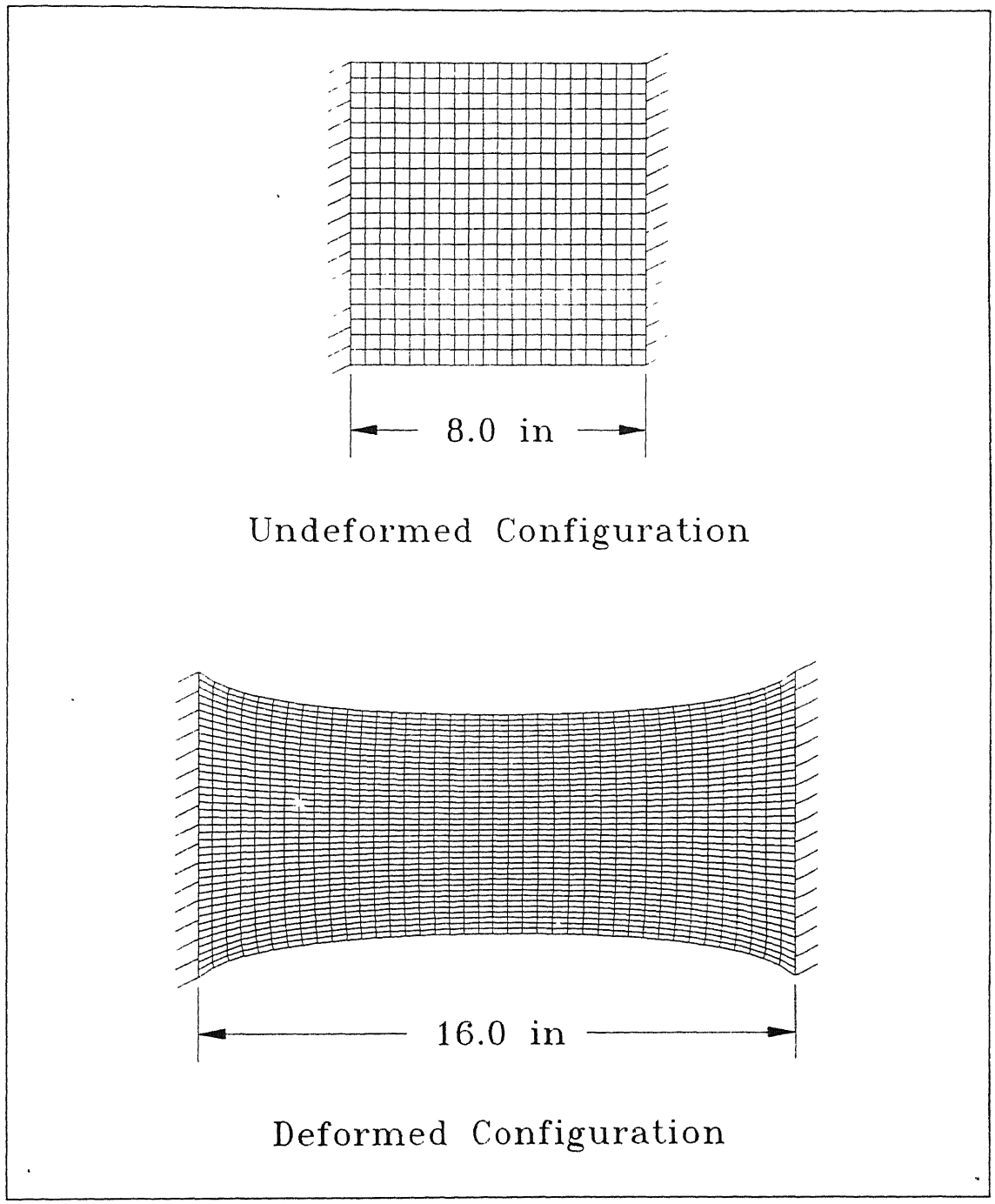

Figure 2.4. In-plane Stretching of a Thin Elastic Membrane.

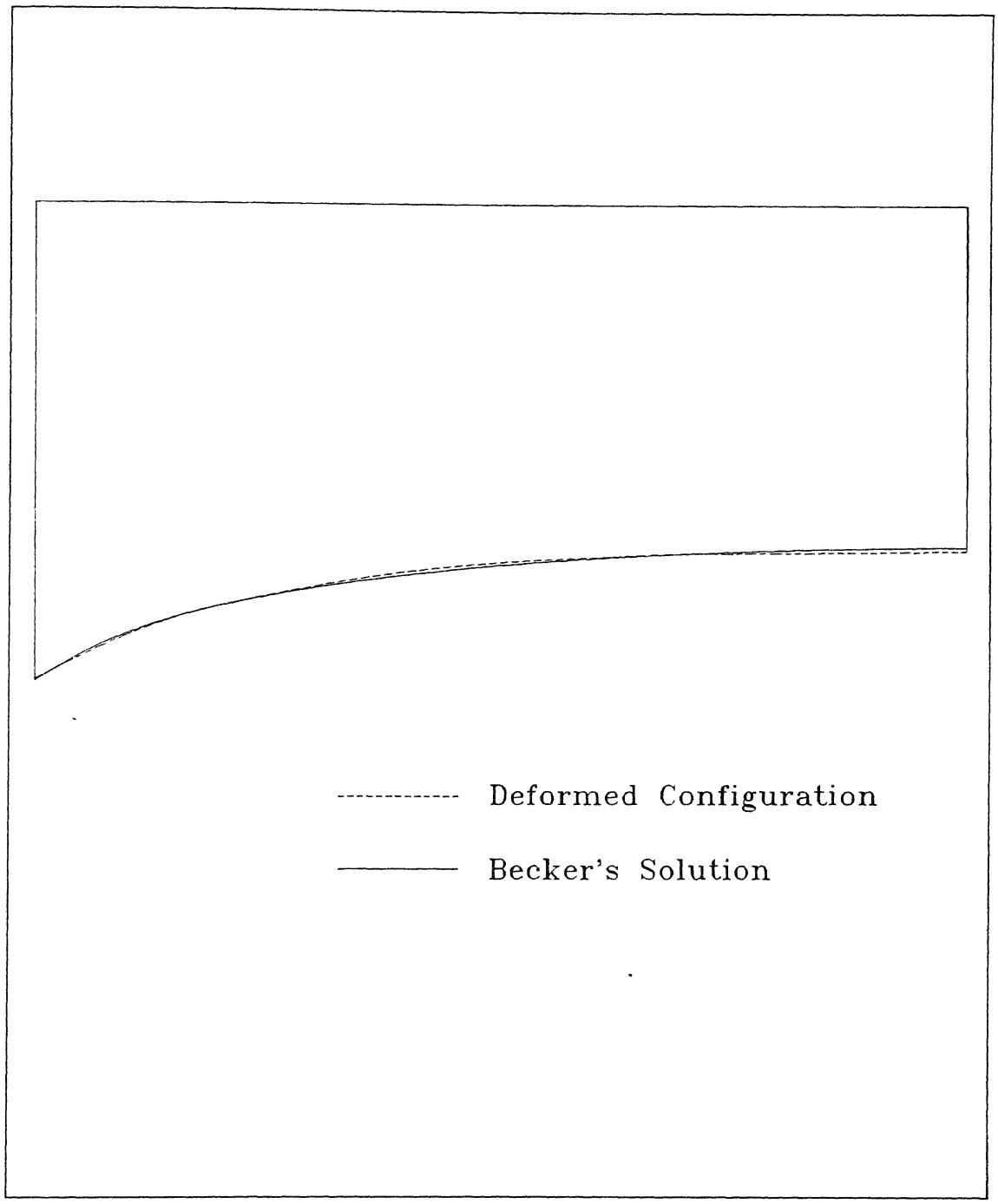

Figure 2.5. In-plane Stretching of a Thin Elastic Membrane: A comparison with Becker's Solution.

pressures. The inflation pressure values are measured in terms of non-dimensional pressure value P^* given by,

$$P^* = \frac{pa}{2C_1 h} \tag{2.19}$$

where p, C_1 and h are the applied pressure, the non-dimensional Mooney constant and the thickness of the membrane respectively as defined in the Feng & Huang (1974). The square membrane is of the size $2a$. The ratio of first and second Mooney constants, C_1/C_2 is taken as 5.0. Figure 2.7 shows the variation of the non-dimensional height of the middle point of the membrane, $Y1$ for different non-dimensional pressure value, P^*. The results of the work carried out by Feng & Huang are also shown in the figure by means of small circles.

The first two test cases conform the correctness of strain energy calculations and the potential of loads. The third test case is an extension of the second one where the inflation of a square membrane is carried out in the presence of a rigid geometric constraint. The ratio of first and second Mooney constants, C_1/C_2 is taken as 10.0 here. The geometric constraint is in the form of a rigid flat surface placed above the membrane. As the applied inflation pressure increases, the membrane comes in contact with the flat constraint which acts as a barrier. The deformed profile of the center-line of the membrane is plotted in Figure 2.8. The results are compared with that of Feng and associates (1974). The deformed profile of Feng et al. are indicated by small circles.

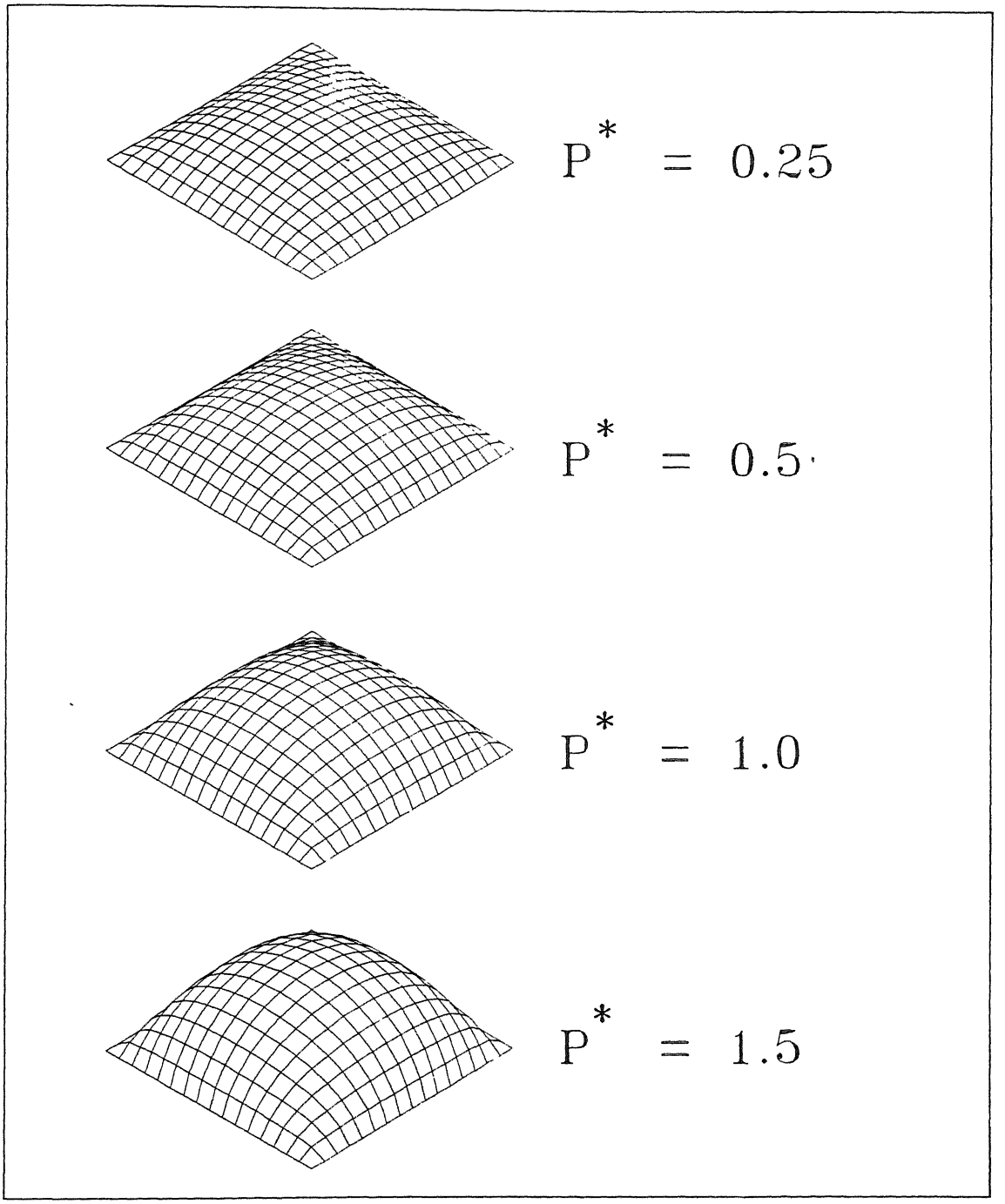

Figure 2.6. Inflation of a Square Membrane.

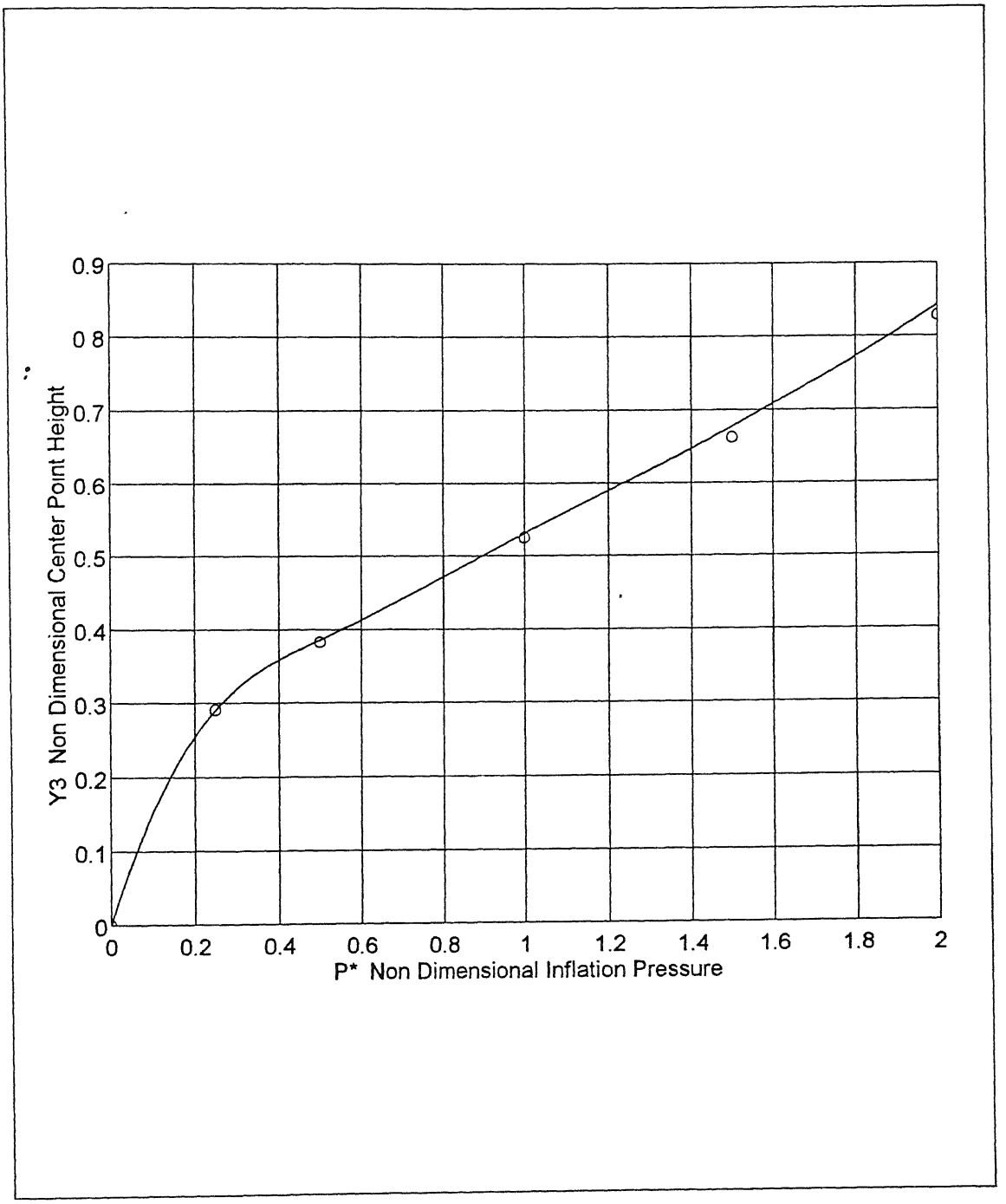

Figure 2.7. Inflation of a Square Membrane for Various Applied Pressures.

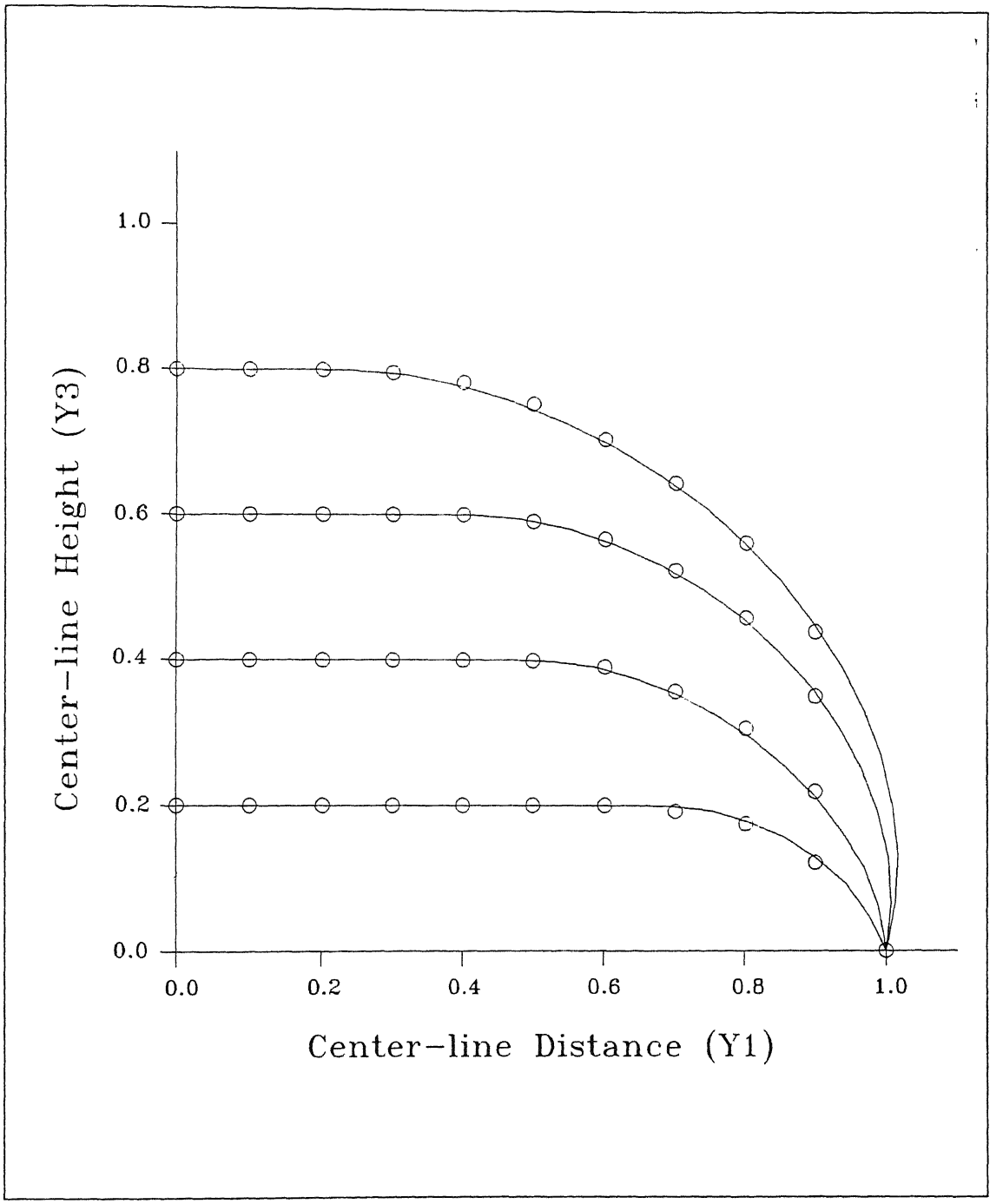

Figure 2.8. Inflation of a Square Membrane with a Geometric Constraint.

for the indentors is assumed which is also a datum for measuring the heights of the individual indentors. In their base position the indentors do not make any contact with the flexible sheet. As the indentors are raised above their base position they come in contact with the flexible sheet and deform it.

The main objective in the proposed tooling system is to deform the flexible sheet to a desired shape. This involves, knowing the heights by which the individual indentors are to be raised in order to deform the flexible sheet to a required shape. There can be two approaches to attempt this problem. In the first approach, the heights by which the indentors are to be raised to realize a given surface are known in advance. This is an *open loop approach.* Using a matrix of indentors a discrete approximation to a given continuous surface can be built by simple geometric methods. The relative heights of the indentors which form such an approximation can be used to realize the desired surface in the proposed tooling.

In the second approach, the heights by which the indentors are to be raised are not known in advance. The process of shape realization starts with some initial assumed heights of the indentors. The deformed shape of the flexible sheet is measured for this set of heights and the error between the desired and realized surfaces is fed to some shape control algorithm which suggests new positions of the indentors. This procedure is repeated until the shape error ceases to improve beyond certain limit. Such an approach is known as *closed loop approach.* The numerical experiments carried out as a part of this chapter are based on the first approach. Some of the results obtained by following the closed loop approach are presented in the subsequent chapters.

3.2 Shape Realization Software

In order to study the shape realization by the proposed tooling, a set of computer programs have been written. The software developed for this purpose is in three modules: a preprocessor, a deformation analysis program and a post-processor. The input to the shape realization software consist of the following.

- The shape to be realized or the desired surface shape
- Dimensions of the flexible sheet
- Sheet thickness
- Material properties of the sheet
- Geometry of the individual indentors
- Layout or the arrangement of indentors

Knowing the heights by which indentors are to be raised to approximate a given continuous surface, is the first step in the process of shape realization. The preprocessor part of the software deals with this aspect. For this purpose, a common coordinate system is used to define the desired shape and the indentor positions. Each of the indentors is now raised incrementally till it makes a contact with the desired surface. After all the indentors are raised in a similar manner, it forms a discrete approximation to the given continuous surface.

The heights of the indentors decided as part of the preprocessor together with various tooling parameters mentioned above, form the input to analysis module. The deformation analysis program is based on the theoretical formulation and the computational procedure described in the previous chapter. The analysis program uses the middle surface of the flexible sheet as a reference surface, whereas, the upper surface of the flexible sheet is the desired one. This offset can be easily accounted using Equation (2.8) as the deformation of the flexible sheet proceeds.

As a part of the post-processor, the deformed configuration of the flexible sheet obtained as a result of analysis is compared with the desired surface shape to evaluate the shape error. The realizability of a given shape here is measured in terms of the root mean square (RMS) error and the average absolute (AVAB) error between the desired and realized surface shapes. Before such a comparison is made, one of the surface shapes needs to be localized with respect to the other. Localization refers to the problem of determining the optimum position of one surface with respect to other for a minimum distance norm. The localization procedure followed here consists of positioning the deformed surface shape with respect to desired one by exhaustive search.

3.3 Numerical Examples

Five examples of shape realization are presented in this section. Three of which are concerned with the surface patches which are doubly curved. The first example deals with the realization of a simple cylindrical patch. The parametric representation of the patch is given by,

$$\begin{aligned} x &= 2.8625\, cos(u) \\ y &= 1.0 * v - 0.5 \\ z &= 2.8625\, sin(u) - 2.7625 \end{aligned} \tag{3.1}$$

$$\text{where } 1.395 \leq u \leq 1.746 \text{ and } 0.0 \leq v \leq 1.0$$

In order to realize the above surface, a rectangular sheet of size 1.6 m by 1.2 m and thickness 4 mm is indented with a total of 121 indentors. Two of the edges of the flexible sheet of 1.2 m length are constrained. The square indentors of 99 mm side with spherical end (radius=100 mm) are used. The indentors are placed in an area of 1.1 m by 1.1 m forming 11 rows, each row consisting of 11 equally spaced indentors (Fig. 3.1). The ratio of first and second Mooney constants, C_1/C_2 is taken as 4.0. The analysis has been carried out with a total of 3072 triangular elements (Fig. 3.2).

Figure 3.3 shows the desired and deformed surface patches. The figure shows only that region of the deformed surface which is in contact with the indentors. Figure also depicts the error between the desired and deformed surface patches at higher magnification.

In order to realize the above surface patch, the analysis is also carried using a square sheet of size 1.6 m with all the four sides constrained. The average absolute (AVAB) error and the root mean square (RMS) error between the desired and deformed surfaces for the two cases are indicated in Table 3.1.

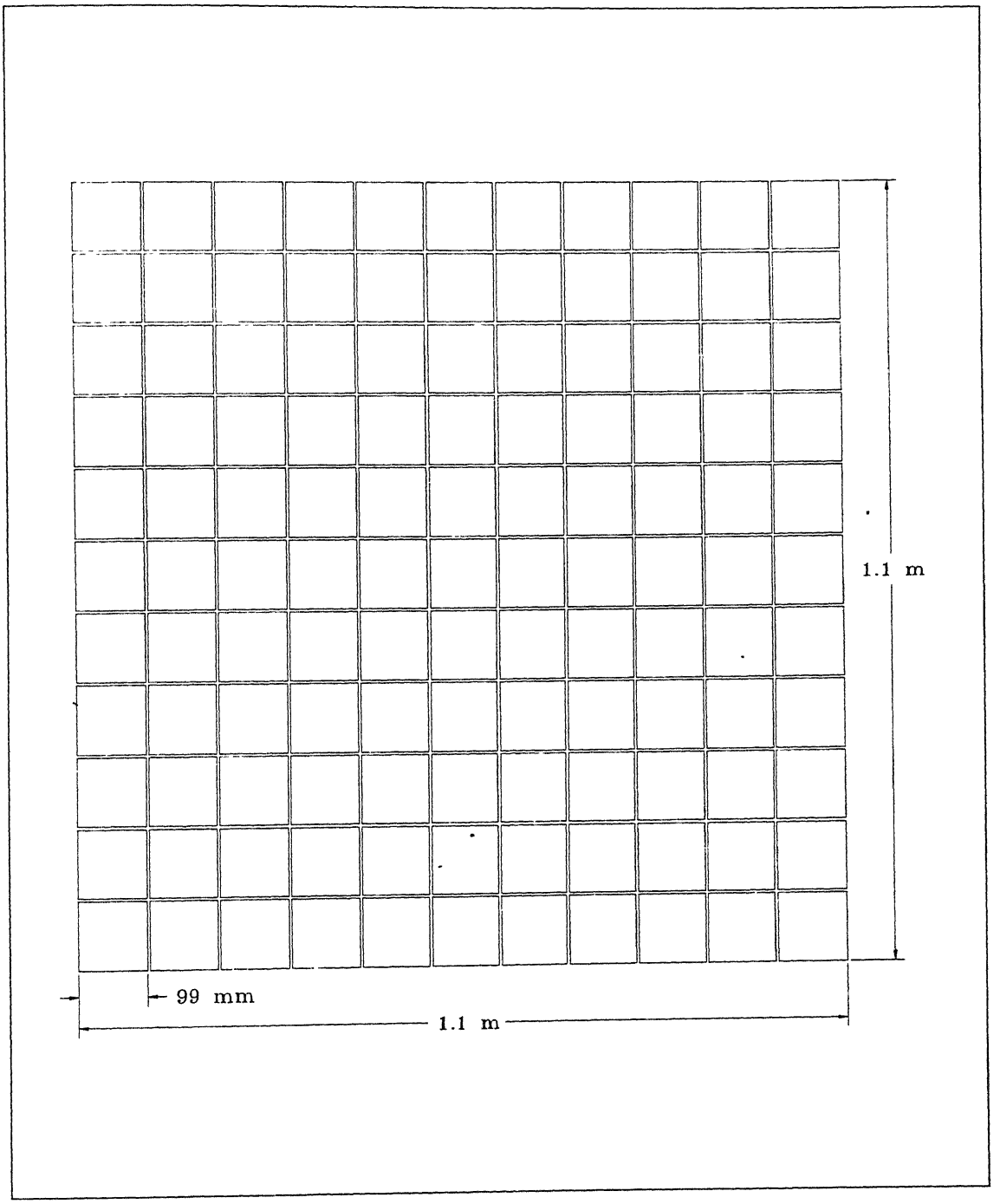

Figure 3.1. Indentor Layout (Numerical Example I).

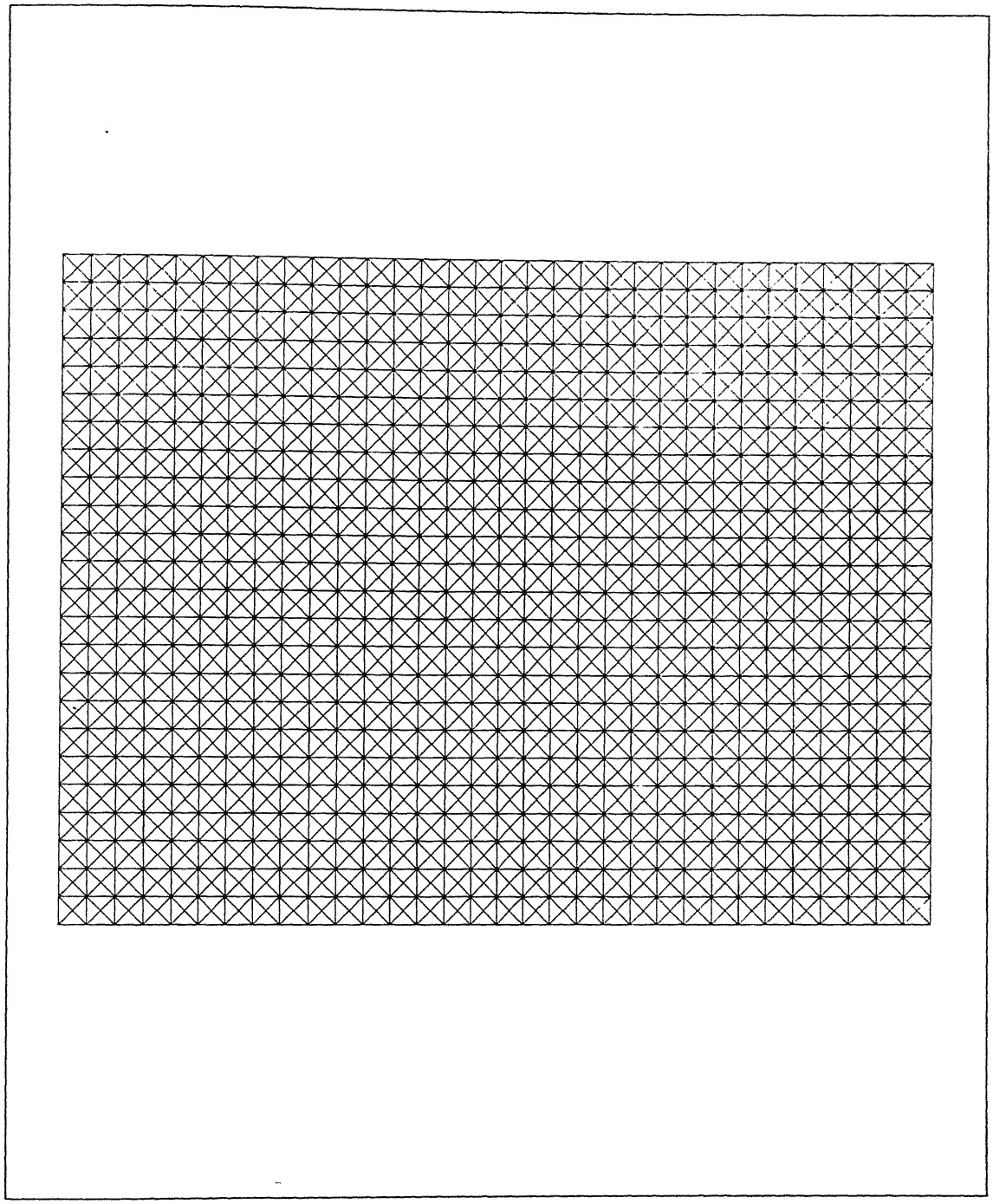

Figure 3.2. Finite Element Discretization of the Membrane (Numerical Example I).

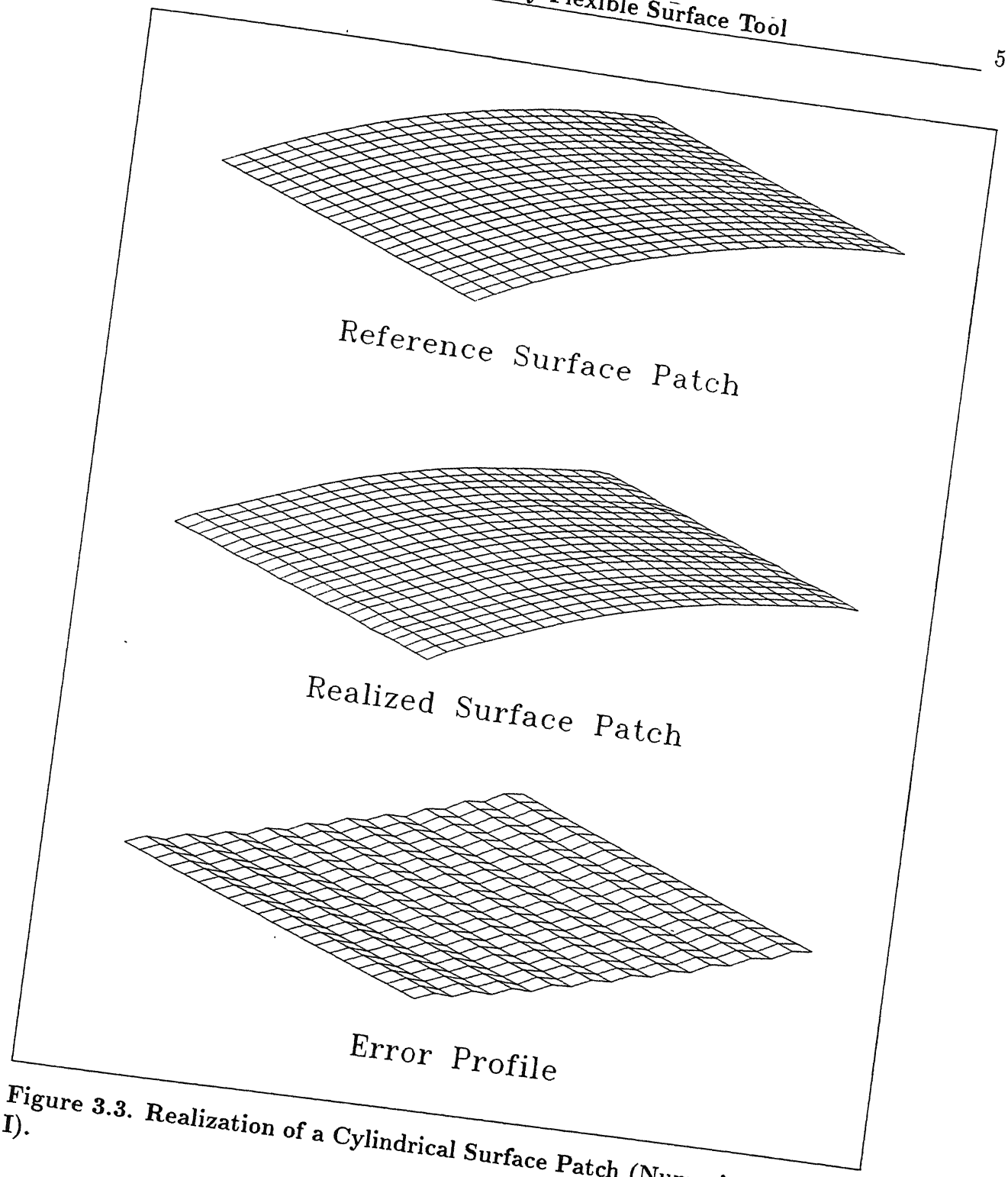

Figure 3.3. Realization of a Cylindrical Surface Patch (Numerical Example I).

Boundary Condition	Average Absolute Error	Root Mean Square Error
Two Sides Constrained	0.2595 mm	0.3248 mm
Four Sides Constrained	0.3261 mm	0.3931 mm

Table 3.1 AVAB and RMS Errors (Numerical Example I).

In the second example a rectangular membrane of thickness 5.0 mm is indented with multiple indentors to simulate an elliptic cylindrical surface patch. Circular indentors of radius 49.5 mm are used (Fig 3.4). The other tooling parameters being same as that of previous example. The parametric equation of the desired surface is given as follows.

$$\begin{aligned} x &= 1.51625\ cos(u) \\ y &= 1.0 * v - 0.5 \\ z &= 0.758125\ sin(u) - 0.658125 \end{aligned} \tag{3.2}$$

$$\text{where } 1.0534 \leq u \leq 2.0882 \text{ and } 0.0 \leq v \leq 1.0$$

The desired and deformed configurations of the membrane are shown in Figure 3.5. The AVAB error and the RMS error between the desired and deformed surfaces are given in Table 3.2.

Boundary Condition	Average Absolute Error	Root Mean Square Error
Two Sides Constrained	0.6936 mm	0.8611 mm
Four Sides Constrained	0.7591 mm	0.9350 mm

Table 3.2 AVAB and RMS Errors (Numerical Example II).

The third numerical example deals with the realization of a doubly curved surface patch. The equation of the surface patch expressed in an explicit form is given as,

$$z = 0.08 \left[(4x/3)^2 - 1\right]^2 \left[(4y/3)^2 - 1\right]^2 \tag{3.3}$$

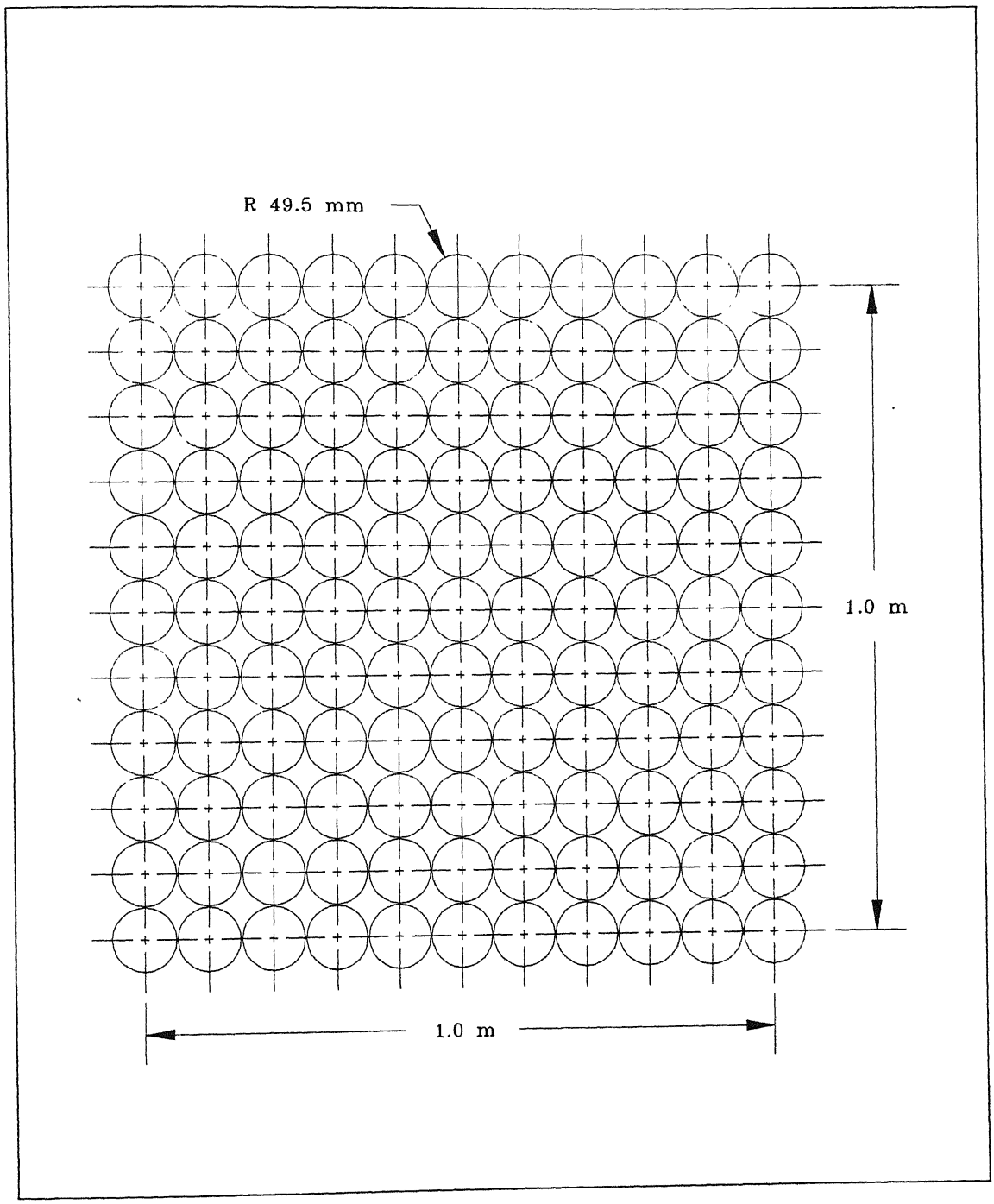

Figure 3.4. Indentor Layout (Numerical Example II).

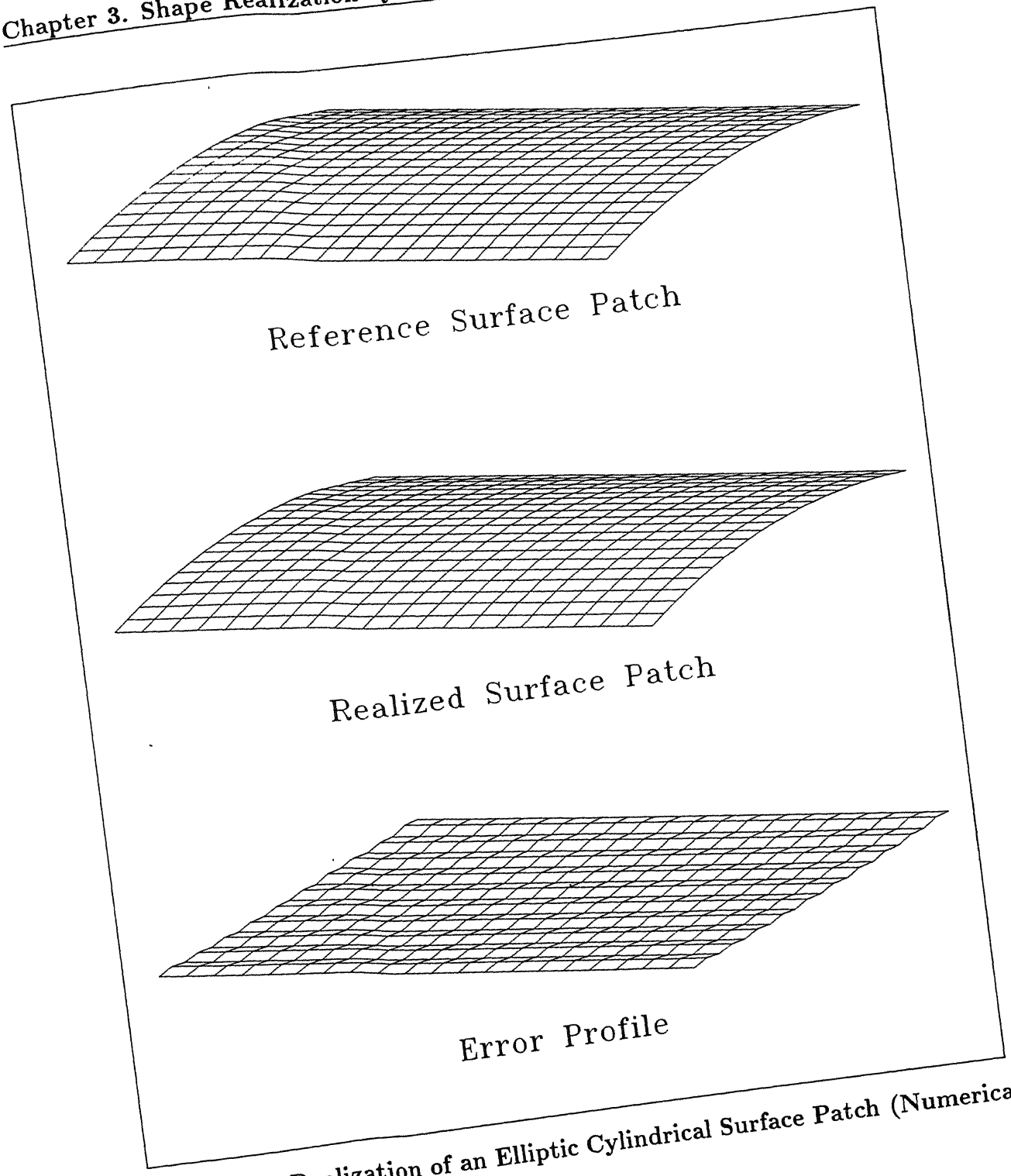

Figure 3.5. Realization of an Elliptic Cylindrical Surface Patch (Numerical Example II).

$$\text{where } -0.5 \leq x \leq 0.5 \text{ and } -0.5 \leq y \leq 0.5$$

In order to realize this surface patch, a square membrane of size 1.6 m by 1.6 m and thickness 5 mm is constrained at all the four edges and indented with a total of 121 indentors. Other input data is same as that of example I. The desired surface, deformed configuration and the error profile are shown in Figure 3.6. The AVAB and RMS errors are given in Table 3.3.

Average Absolute Error	Root Mean Square Error
0.3187 mm	0.3975 mm

Table 3.3 AVAB and RMS Errors (Numerical Example III).

In the next numerical example, an asymmetrical bicubic Bezier patch has been realized. The characteristic polyhedron which defines the Bezier patch is given in Table 3.4.

$$\begin{bmatrix} \begin{Bmatrix} -0.9 \\ 0.9 \\ 0.0 \end{Bmatrix} & \begin{Bmatrix} -0.3 \\ 0.9 \\ 0.0 \end{Bmatrix} & \begin{Bmatrix} 0.3 \\ 0.9 \\ 0.0 \end{Bmatrix} & \begin{Bmatrix} 0.9 \\ 0.9 \\ 0.0 \end{Bmatrix} \\ \begin{Bmatrix} -0.9 \\ 0.3 \\ 0.0 \end{Bmatrix} & \begin{Bmatrix} -0.3 \\ 0.3 \\ 0.2 \end{Bmatrix} & \begin{Bmatrix} 0.3 \\ 0.3 \\ 0.25 \end{Bmatrix} & \begin{Bmatrix} 0.9 \\ 0.3 \\ 0.0 \end{Bmatrix} \\ \begin{Bmatrix} -0.9 \\ -0.3 \\ 0.0 \end{Bmatrix} & \begin{Bmatrix} -0.3 \\ -0.3 \\ 0.1 \end{Bmatrix} & \begin{Bmatrix} 0.3 \\ -0.3 \\ 0.15 \end{Bmatrix} & \begin{Bmatrix} 0.9 \\ -0.3 \\ 0.0 \end{Bmatrix} \\ \begin{Bmatrix} -0.9 \\ -0.9 \\ 0.0 \end{Bmatrix} & \begin{Bmatrix} -0.3 \\ -0.9 \\ 0.0 \end{Bmatrix} & \begin{Bmatrix} 0.3 \\ -0.9 \\ 0.0 \end{Bmatrix} & \begin{Bmatrix} 0.9 \\ -0.9 \\ 0.0 \end{Bmatrix} \end{bmatrix}$$

Table 3.4 Bezier Characteristic Polyhedron (Numerical Example IV).

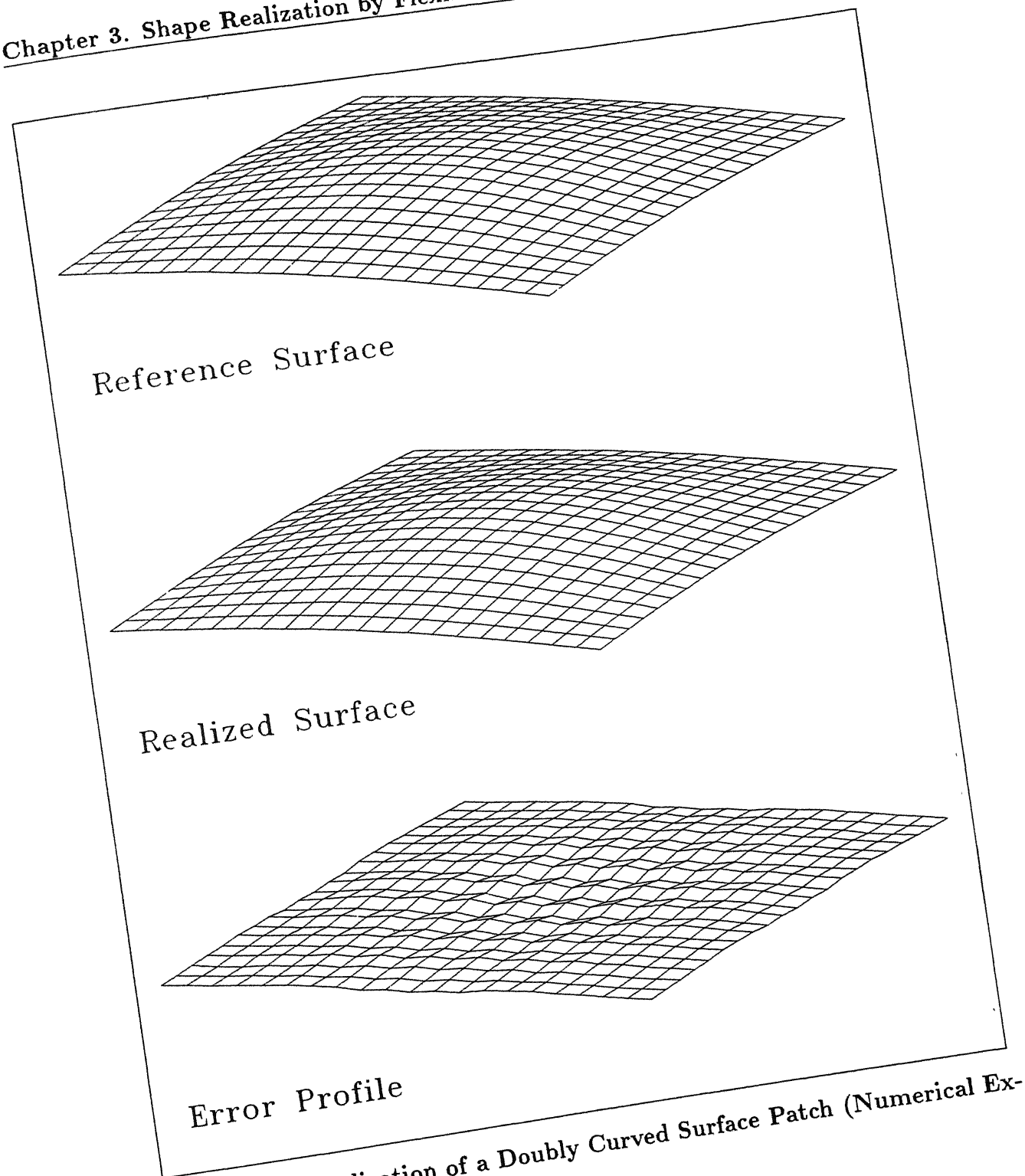

Figure 3.6. Realization of a Doubly Curved Surface Patch (Numerical Example III).

A square membrane with side 1.8 m has been used for the realization of this patch and the indentors are placed in an area of 1.1 m by 1.1 m. The results are presented in Figure 3.7 and the AVAB and RMS errors are given in Table 3.5.

Average Absolute Error	Root Mean Square Error
0.2041 mm	0.2531 mm

Table 3.5 AVAB and RMS Errors (Numerical Example IV).

Lastly, the results of realization of another doubly curved surface patch are presented in Figure 3.8. The curvatures of the surface patch here are much higher than those of the previous examples. The equation of the surface patch expressed in an explicit form is given as,

$$z = 0.25 \left[1 - (5x/4)^2\right] \left[1 - (5y/4)^2\right] \tag{3.4}$$

$$\text{where } -0.5 \leq x \leq 0.5 \text{ and } -0.5 \leq y \leq 0.5$$

The AVAB and RMS errors between the desired and the realized surface patches after localization are given in Table 3.6.

Average Absolute Error	Root Mean Square Error
1.1949 mm	1.4755 mm

Table 3.6 AVAB and RMS Errors (Numerical Example V).

The values of the average absolute and root mean square errors presented above are only typical values and not necessarily the best values obtainable. The error between the desired and deformed surface patches can be further reduced by selecting the optimum

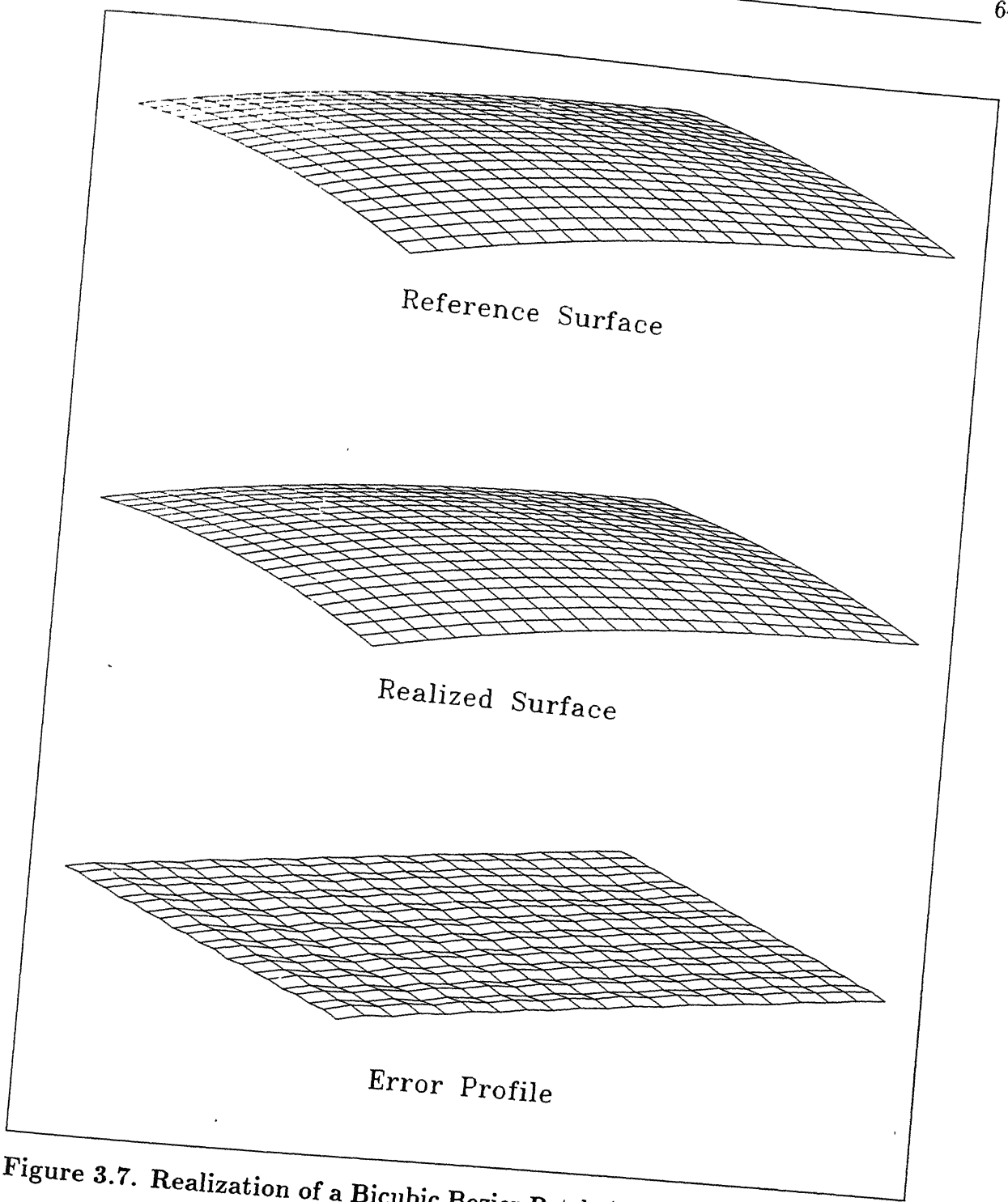

Figure 3.7. Realization of a Bicubic Bezier Patch (Numerical Example IV).

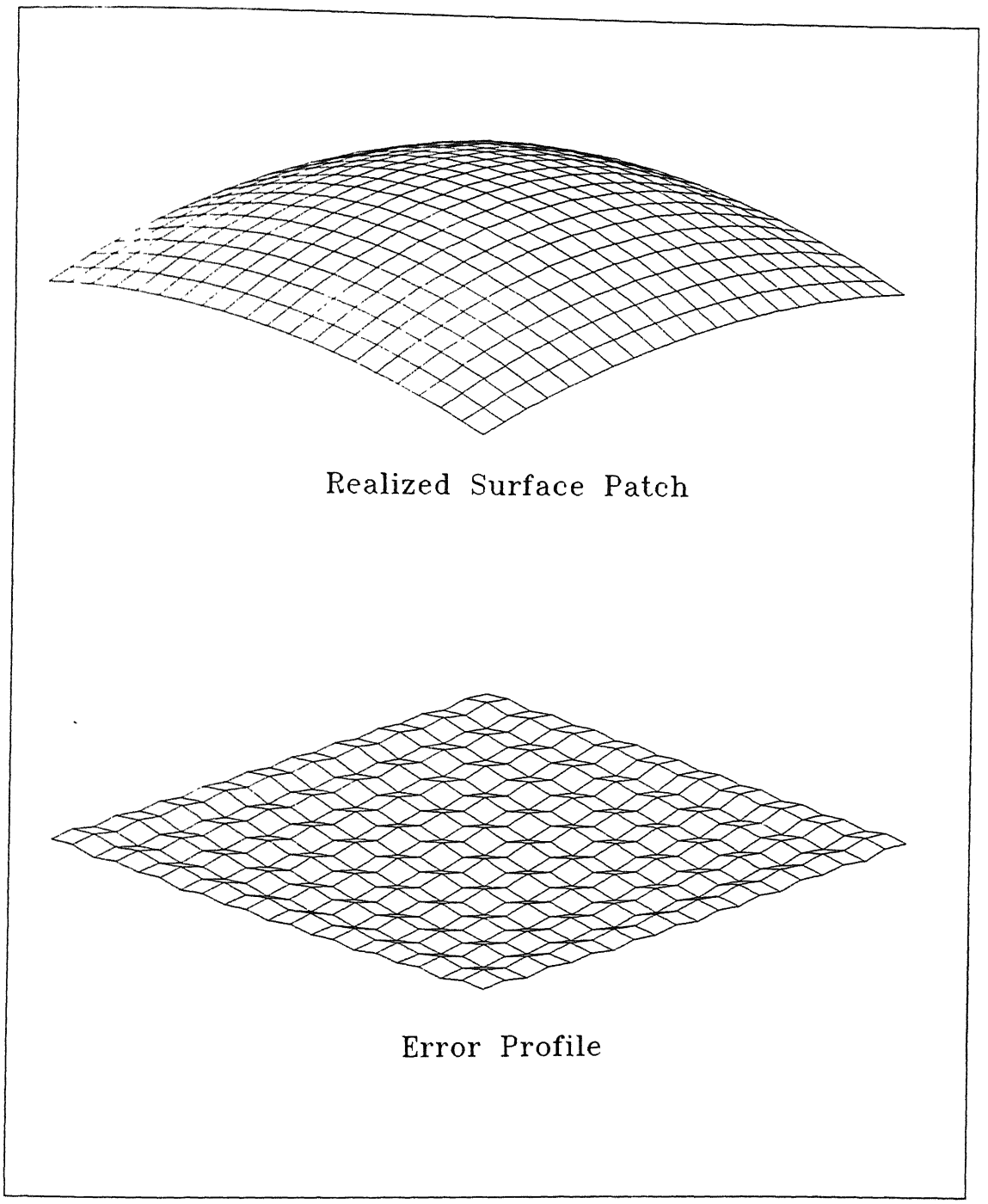

Figure 3.8. Realization of a Doubly Curved Surface Patch (Numerical Example V).

values of the tooling parameters. The subsequent sections and chapters deal with this aspect in detail.

3.4 Effect of External Loading on the Shape Accuracy

The numerical examples presented in the previous section assume that there is no external loading on the flexible sheet. The deformation of the flexible sheet in these cases is only due to indentation. In practice, some form of an external loading on the flexible sheet can be expected. This may be due to loads encountered as a result of the material processing. The shape realization in the presence of external loading then becomes an important aspect. This aspect has been dealt as a part of the present section.

The numerical experiments were carried out for two forms of loading acting on the flexible sheet. These are uniformly distributed and dead loading. With the uniformly distributed loading (UDL), the direction of the loading changes with the deformation of the flexible sheet. The loads are assumed to be acting on the flexible sheet in an area where the indentors are placed. The effect of these two types of loads has been studied for a variety of surface shapes. Figures 3.9 to 3.12 present the results of the same for a typical surface shape. The thickness of the flexible sheet used here is 4 mm.

Figure 3.9 shows the variation of average absolute (AVAB) error with an increasing dead load. As can be seen from the figure, the effect of dead loading is to improve the accuracy of the shapes at small loads. This is because, in the absence of any loading, the flexible sheet does not make a contact with all the indentors. The application of dead loading is to bridge the gaps left between the sheet and indentors, if any. With further increase in dead load the accuracy deteriorates. The effect of dead load on the RMS error is shown in Figure 3.10.

Figures 3.11 and 3.12 present the variation of AVAB and RMS errors with an increasing UDL. The effect of UDL on the surface shape accuracy has been found to be more or

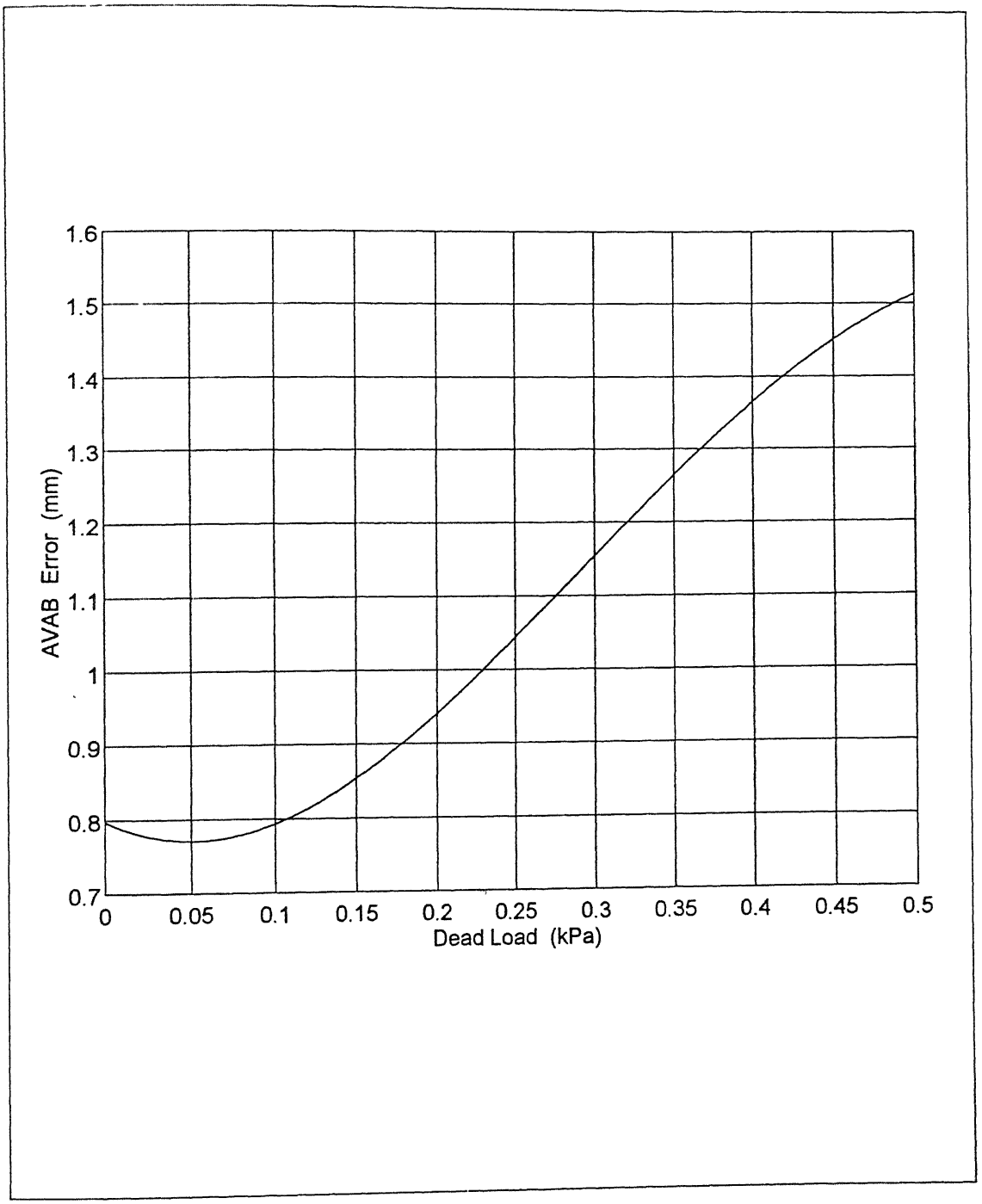

Figure 3.9. Variation of AVAB Error with Dead Loading.

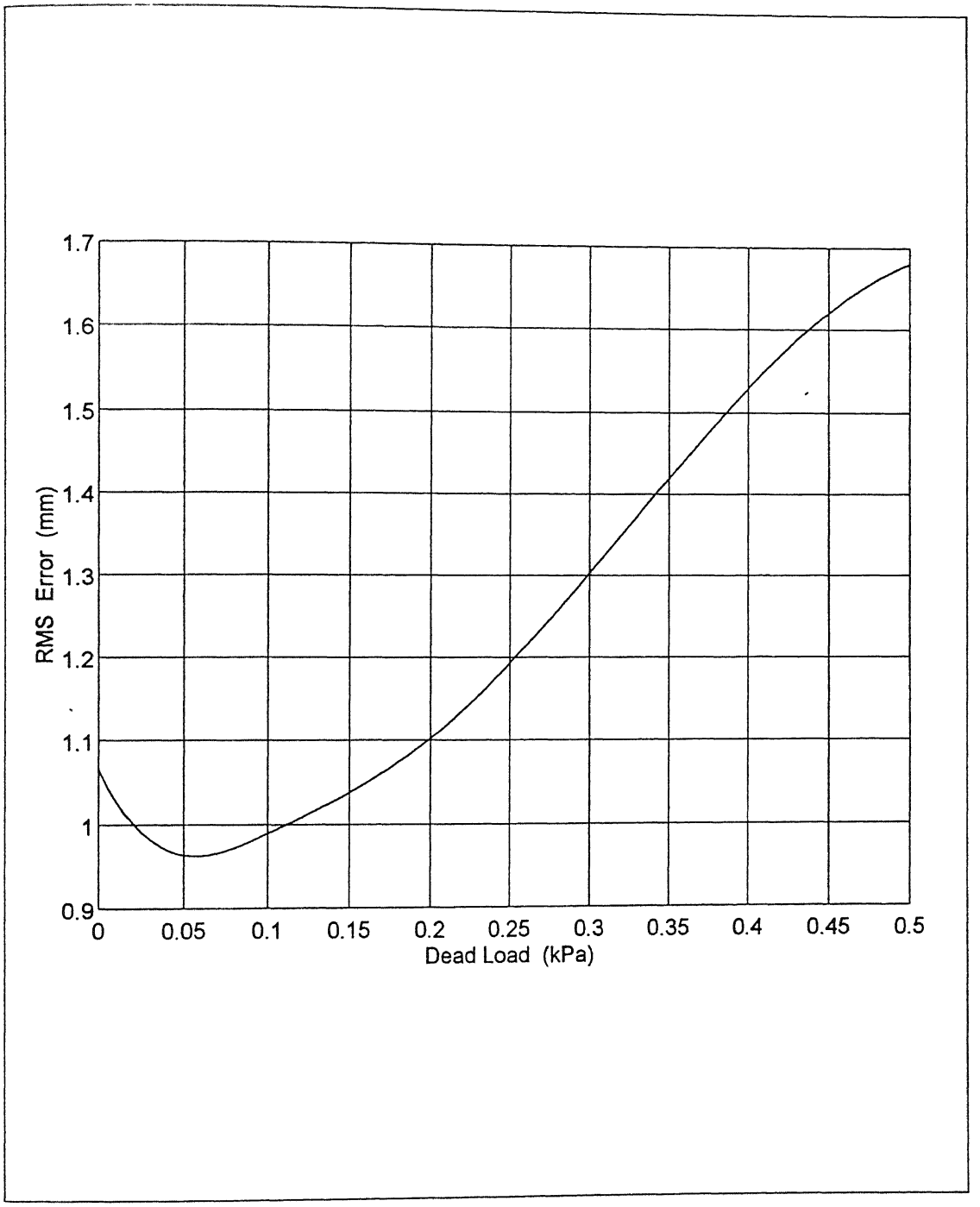

Figure 3.10. Variation of RMS Error with Dead Loading.

less same as that of dead loading. This is evident from Figures 3.11 and 3.12. Based on the similar numerical experiments carried out with other surface shapes, the variation of AVAB and RMS errors with dead loading/UDL has been found to be qualitatively same as here. However, the load values up to which the shape accuracy improves, varied from shape to shape.

3.5 Effect of Sheet Variables on the Surface Shape Accuracy

The dimensions of the flexible sheet, the sheet thickness and the material of the flexible sheet form some of the important variables in the present study of shape realization. The effect of these parameters on the accuracy of realized shapes is important and helps in knowing the optimum values of these parameters for a given application.

The dimensions of the sheet are important as it affects the realizability of a given shape as well as the size of the flexible surface tooling machine. The flexible sheet used here is of rectangular shape. The size of the sheet is larger than the area in which the indentors are placed (Fig. 3.13). The extra area of the sheet which does not come in contact with the indentors is an important variable and can be measured in terms of margins. The effect of sheet margins on the surface shape accuracy for a typical case is given in Table 3.7. The indentors were placed in an area of 1.0 m by 1.0 m in this case.

X and Y Margin	AVAB Error	RMS Error
200.0 mm	0.21750	0.26821
300.0 mm	0.23716	0.27479
400.0 mm	1.70882	2.00238
500.0 mm	4.58881	4.98410

Table 3.7 Effect of Sheet Margins on the Surface Shape Accuracy.

As can be inferred from the table above, better shape accuracies can be obtained at smaller margins of the flexible sheet. This is due to higher tensions of the flexible sheet

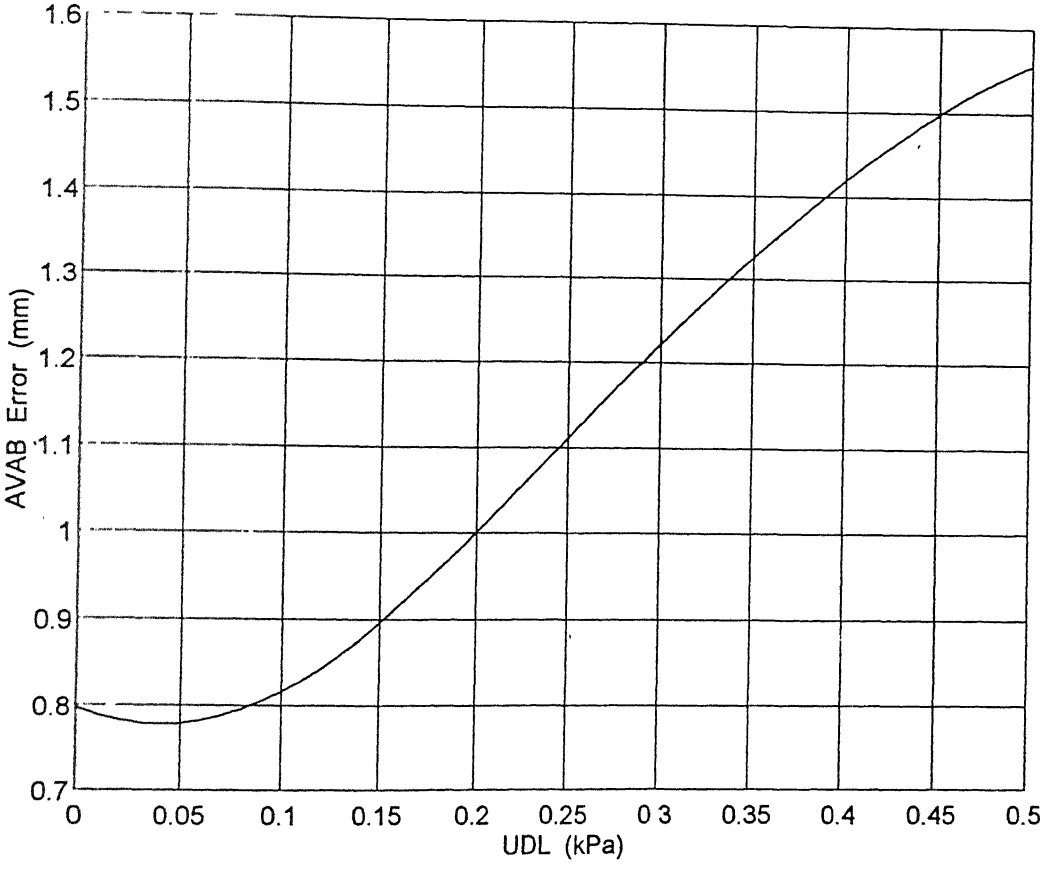

Figure 3.11. Variation of AVAB Error with UDL.

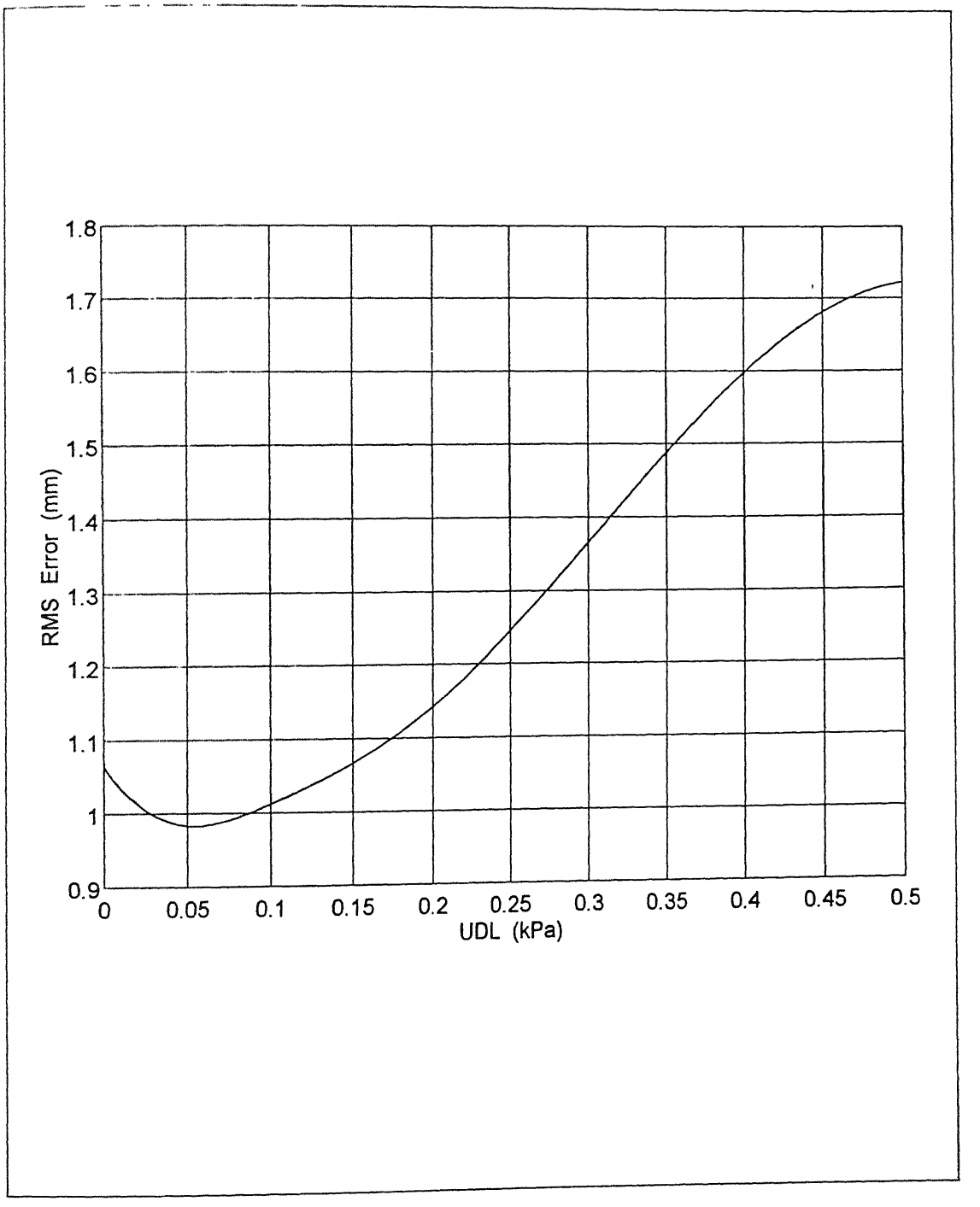

Figure 3.12. Variation of RMS Error with UDL.

associated with smaller margin values. At higher margin values the flexible sheet looses contact with more and more indentors giving rise to poor realized shapes.

Figures 3.14 and 3.15 show the effect of sheet thickness on the surface shape accuracy in terms of AVAB and RMS errors respectively. In the present analysis the flexible sheet is idealized as a membrane. Because of this the the sheet thickness has no effect on the deformed configuration of the membrane when there is no external loading. However, the effect of sheet thickness in the presence of an external loading is significant. This is evident from the above figures which show the variation of shape error with sheet thickness in the presence of an UDL of 0.25 kPa.

The variation of the error between the desired and deformed surface shapes with the change in material properties of the flexible sheet are presented in Figure 3.16. The the ratio of first and second Mooney constants C_1/C_2 is generally used to characterize rubber-like materials. The figure presents the variation of AVAB and RMS errors with increasing values of C_1/C_2. As the material of the flexible sheet tend to be more elastic with increasing values of C_1/C_2 better results were obtained at these values.

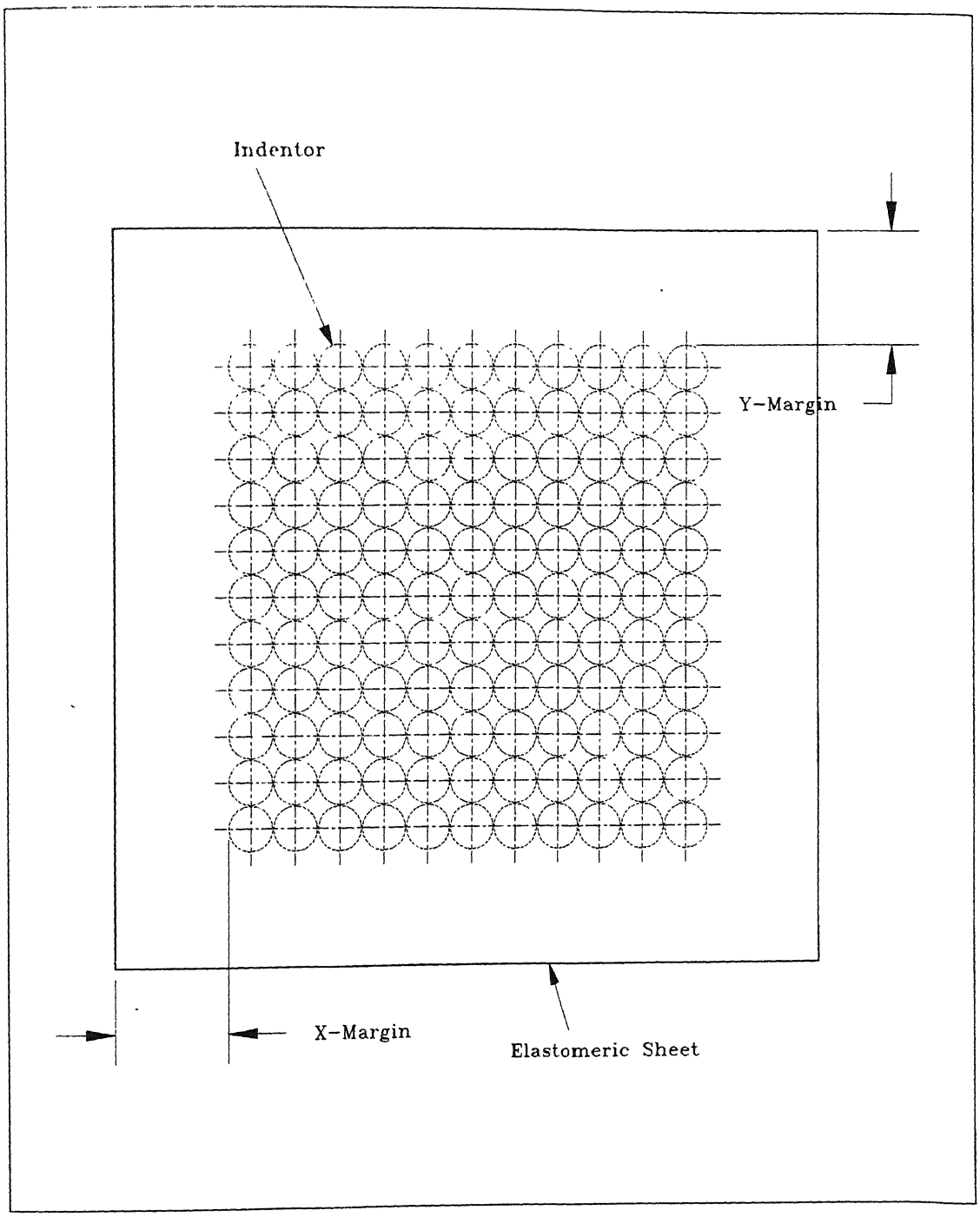

Figure 3.13. Sheet Margins.

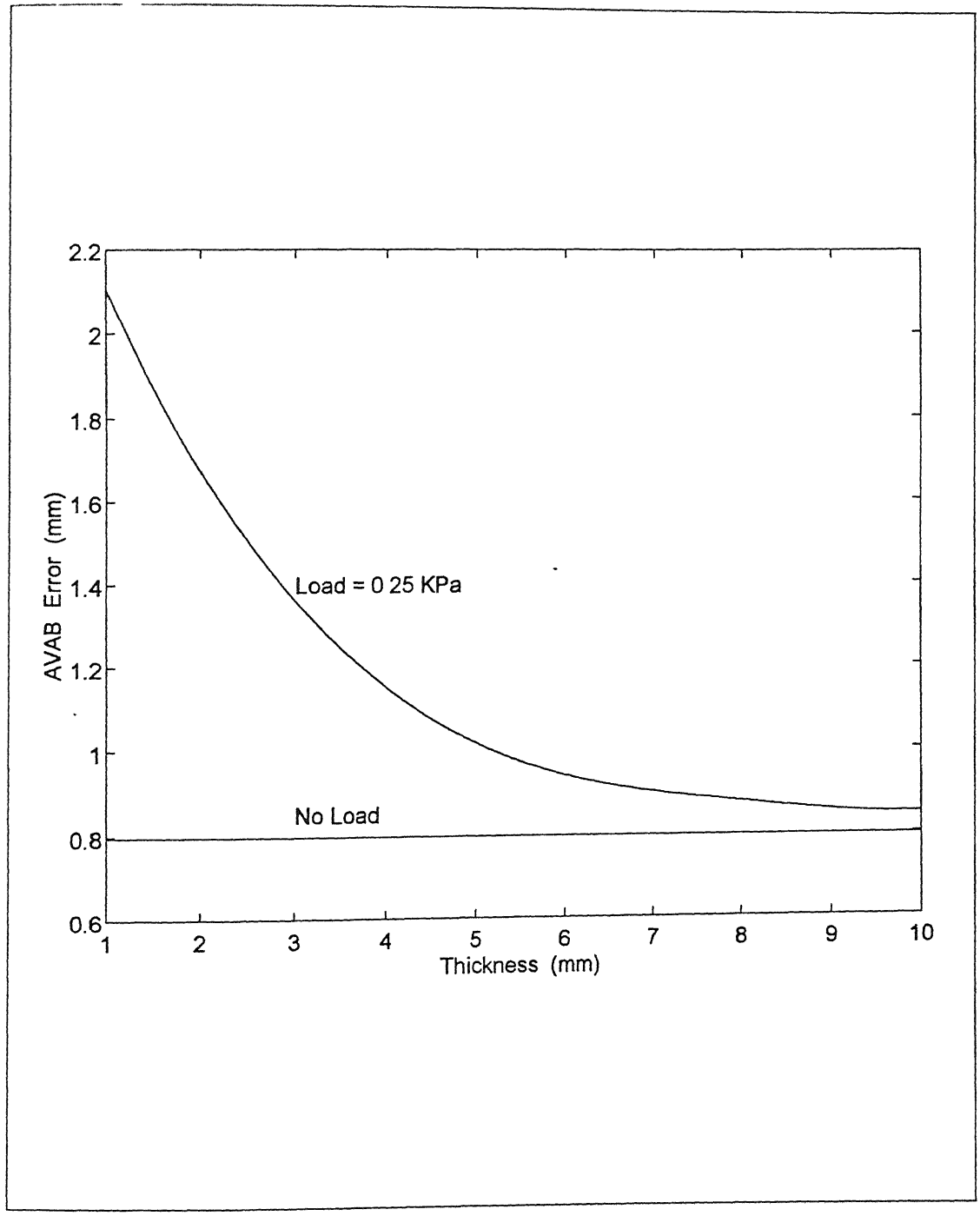

Figure 3.14. Variation of AVAB Error with Sheet Thickness.

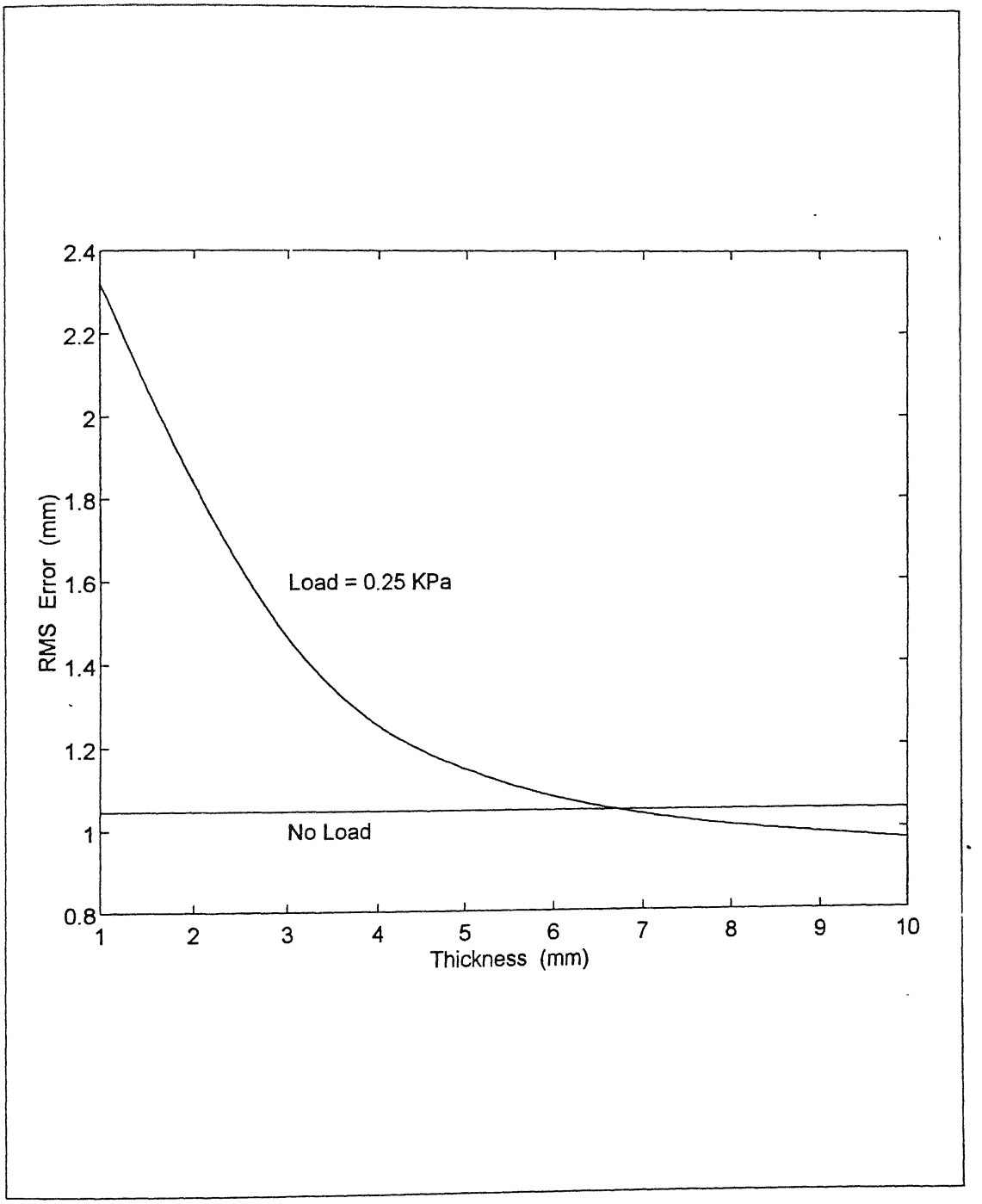

Figure 3.15. Variation of RMS Error with Sheet Thickness.

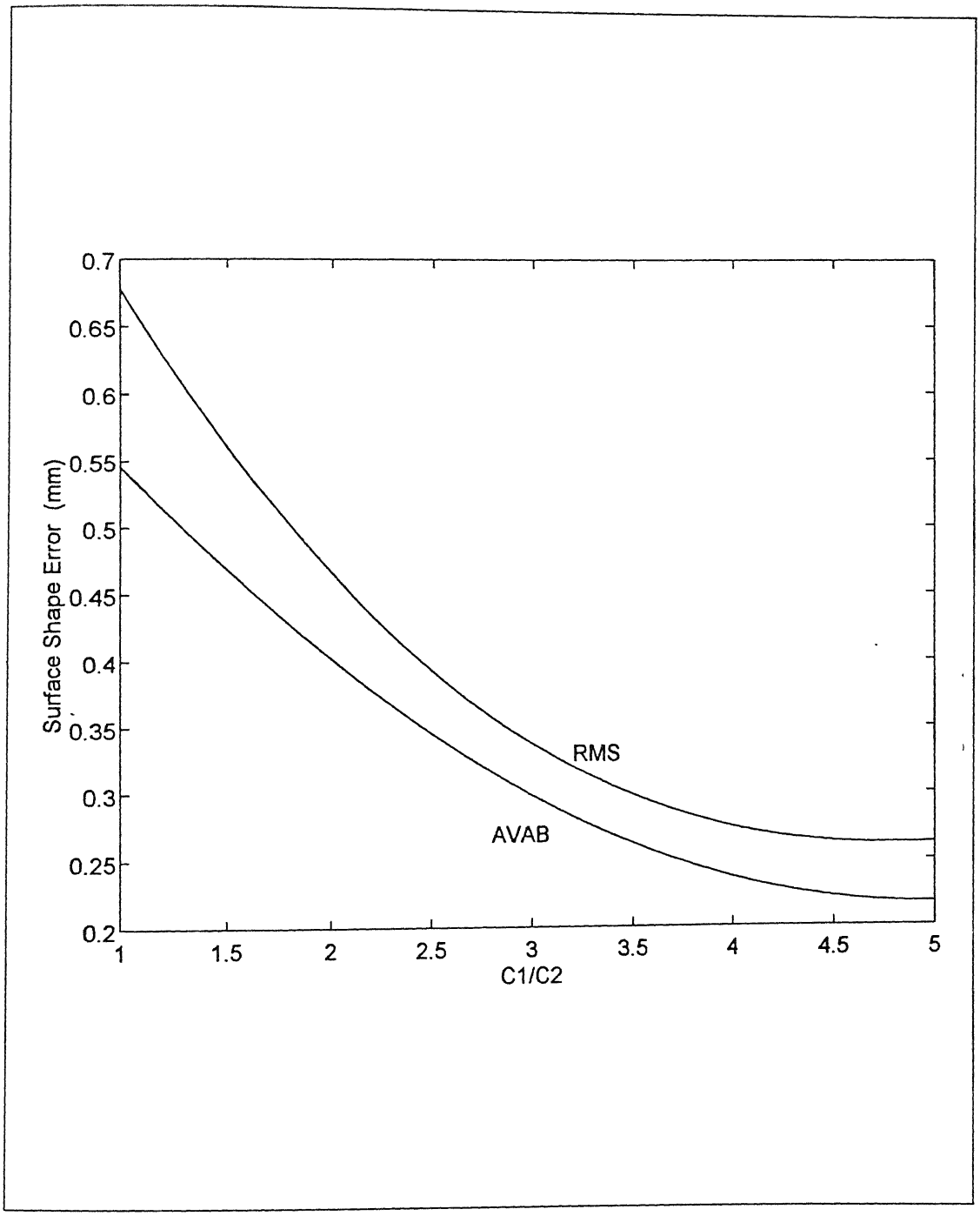

Figure 3.16. Effect of Sheet Material on the Surface Shape Accuracy.

Chapter 4

SURFACE DISCRETIZATION FOR THE FLEXIBLE SURFACE TOOLING

4.1 Introduction

Realizability of a shape by flexible surface tool has been discussed in the previous chapter. The proposed tooling system is based on the concept of approximating a given continuous surface with a discrete one. The discrete surface here is in the form of finite number of closely spaced rigid tool elements known as indentors. The indentors are of square/circular/hexagonal cross-section with spherical ends. They occupy fixed positions in the form of a two dimensional layout, such that, their axes are perpendicular to the middle surface of the flexible sheet in its undeformed position. Each of the indentors can be moved along their axes independently and can be locked in their respective positions. When all the indentors are moved by appropriate heights the spherical ends of all the indentors together constitute a discrete approximation of a given continuous surface.

Given a layout of indentors and the indentor geometry, the heights by which the indentors are to be raised to approximate a given continuous surface can be evaluated trivially. This is done by first localizing the desired continuous surface appropriately with respect to indentors and then raising each of the indentors incrementally till it makes a contact with the desired surface. The open-loop approach to shape realization discussed in the previous chapter is based on deciding the indentor heights in this manner.

In the proposed tooling, the number of indentors used for approximating a continuous surface is finite as well as limited. In this context, the geometry of the individual indentors, the indentor density and the indentor layout are important factors in designing an effective discrete surface. The study of these parameters with an objective to improve the accuracy of realizable shapes is the main subject of this chapter. The specific objectives of this study are as follows.

- A geometric study of the discrete approximation of a continuous mold surface.
- To study the change in effective mold shape due to presence of flexible sheet.
- To study the change in effective mold shape due to external loads on the sheet.

4.2 Indentor Density

One of the important parameters related to discrete approximation of a continuous surface is the number of indentors used or the indentor density. Theoretically, a continuous surface can be approximated by an infinite discrete surface tool elements of infinitesimal size. In practice, the number of surface tool elements or indentors used for approximating a continuous surface is finite. A small number of indentors used for approximation often yields poor results. When the number of indentors used for approximation is too large it is difficult to manipulate and control them individually. In this context, the effect of indentor density on the accuracy of realizable shapes is an important aspect.

The concept of discrete approximation to a continuous surface is made use of, in an

impression toy for recording negative impressions of a complicated curved geometry such as palm of a human hand. The toy consists of a matrix of large number of pins arranged in an area. An individual pin can be pushed and locked in the longitudinal direction. The object whose impression is to be recorded is placed over the matrix of pins and is pressed against them gently until all the pins come in contact with the surface of the desired object. At this stage, the pins are locked in their respective positions and the object is removed. The end points of all the pins together form a discrete negative impression of the desired object. A discrete impression of a spherical object can be seen in Figure 4.1.

In the case of a toy, the number of pins used is very large and the area of individual pins is very small. This can be considered as an example of approximating a continuous surface with discrete points. But, in the case of indentors the area of cross-section is significant and cannot be idealized as points. One way to measure the effectiveness of the discrete surface here is by the fraction of volume under the desired surface patch which is occupied by the indentors. For example, Figure 4.2 demonstrates this aspect for a two dimensional case. Here, a discrete approximation to a curve is built using area templates which are 2D equivalent of indentors. The figure shows the effectiveness of the approximation with increasing number of templates.

This can be extended to a 3D case by considering a typical surface shape of compound curvature. Considering the surface patch given by the equation,

$$z = 0.25 \left[1 - (5x/4)^2\right] \left[1 - (5y/4)^2\right] \tag{4.1}$$

$$\text{where } -0.5 \leq x \leq 0.5 \text{ and } -0.5 \leq y \leq 0.5$$

In order to approximate this surface patch, indentors in the range of 81(9 by 9) to 225(15 by 15) are used. In each case the approximation error is plotted for number of indentors used (Fig. 4.3). The effectiveness of the discretization with increasing number of indentors is evident. The approximation error here is evaluated by the following expression.

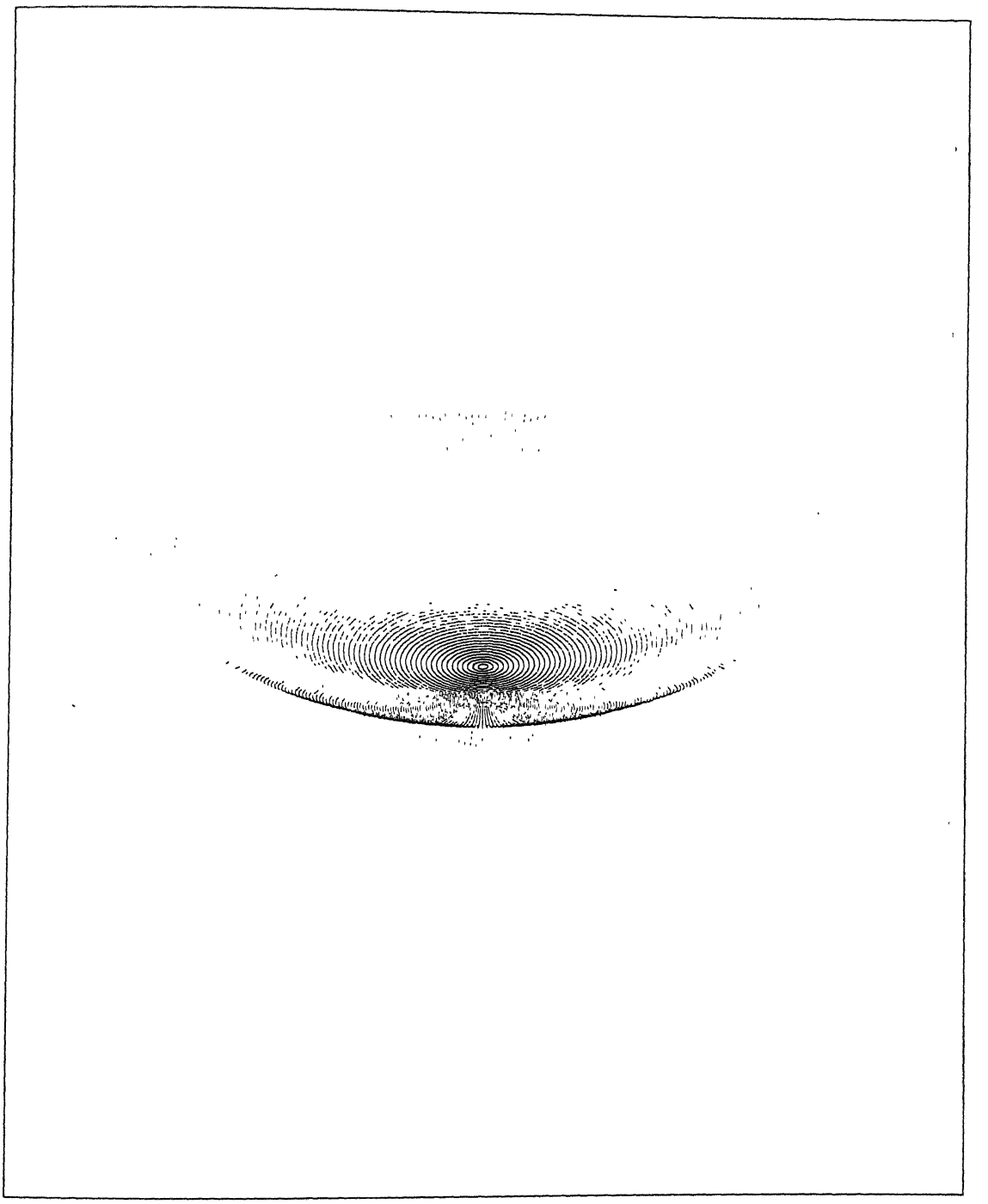

Figure 4.1. Approximating a Continuous Surface with Discrete Points.

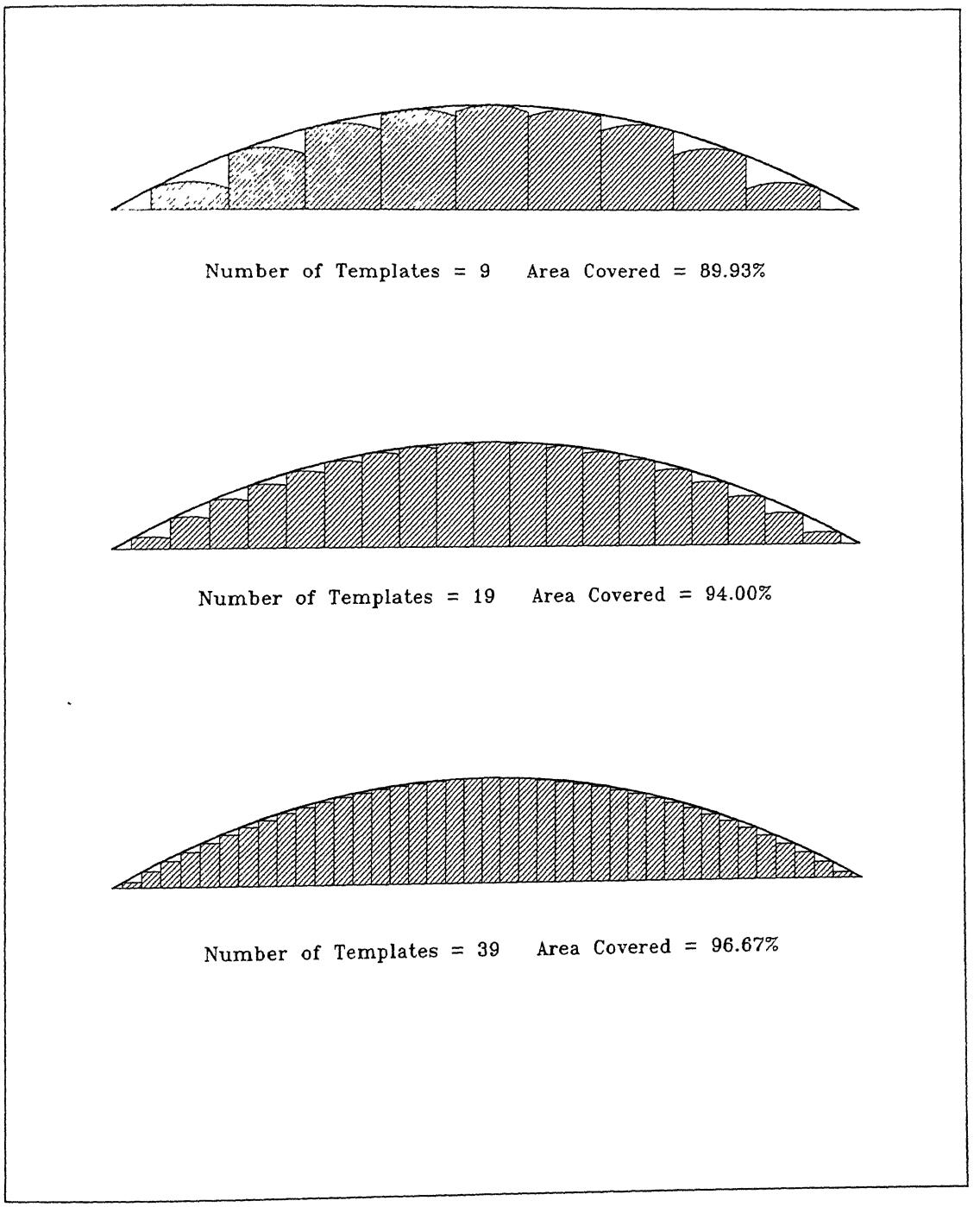

Figure 4.2. A Discrete Approximation of a Curve by Area Templates.

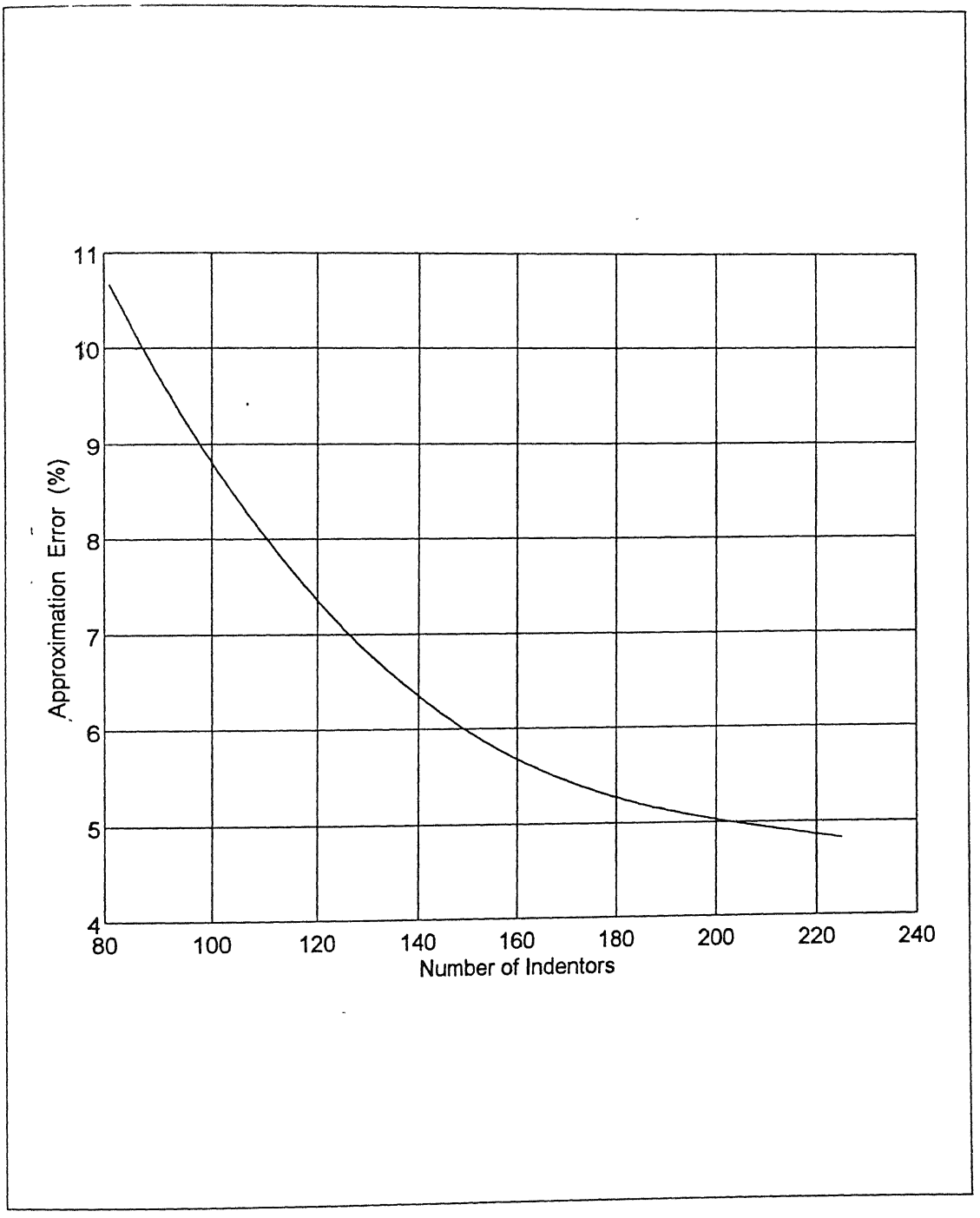

Figure 4.3. Effectiveness of the Discretization with Increasing Number of Indentors.

$$approximation\ error = 1 - \frac{volume\ occupied\ by\ the\ indentors}{volume\ under\ the\ surface\ patch} \tag{4.2}$$

In the proposed tooling, the discrete surface formed by a grid of indentors is not directly used as a mold surface. A flexible sheet is draped over the discrete surface to obtain a continuous surface. The presence of the flexible sheet over the indentors changes the effective mold shape. A physically based analysis accounting for the deformation of the flexible sheet is necessary to know the actual mold shape. Moreover, the presence of external loading on the flexible sheet further changes this shape. It is necessary to know the change in mold shape due to presence of external loading.

Based on the theoretical formulation and the numerical scheme discussed in the second chapter, shape realization experiments were carried out with increasing number of indentors. The detailed procedure of shape realization has been discussed in the previous chapter. The results of one such experiment for the surface patch discussed above are given in Figures 4.4 and 4.5. in terms of AVAB and RMS errors respectively.

In the absence of any external loading on the sheet, the AVAB and RMS errors continuously decrease with the increasing number of indentors. In the presence of an UDL on the sheet, there is a significant improvement in the accuracy of realized shapes in the range of 81(9 by 9) to 196(14 by 14). When the number of indentors are beyond this value the improvement in the accuracy is not much. It was pointed out in the previous chapter that with the application of external loading on the flexible sheet, the accuracy of realized shape first improves and then continuously decreases (Fig. 3.11 & 3.12). It has been found that with the increasing number of indentors this tendency of the realized shapes to improve at smaller loads, decreases.

4.3 Contact Geometry

Contact geometry of the indentors is another important parameter in approximating a continuous surface for the tooling requirements. It refers to spherical end portion of the indentors which comes in contact with the flexible sheet. The contact geometry can be

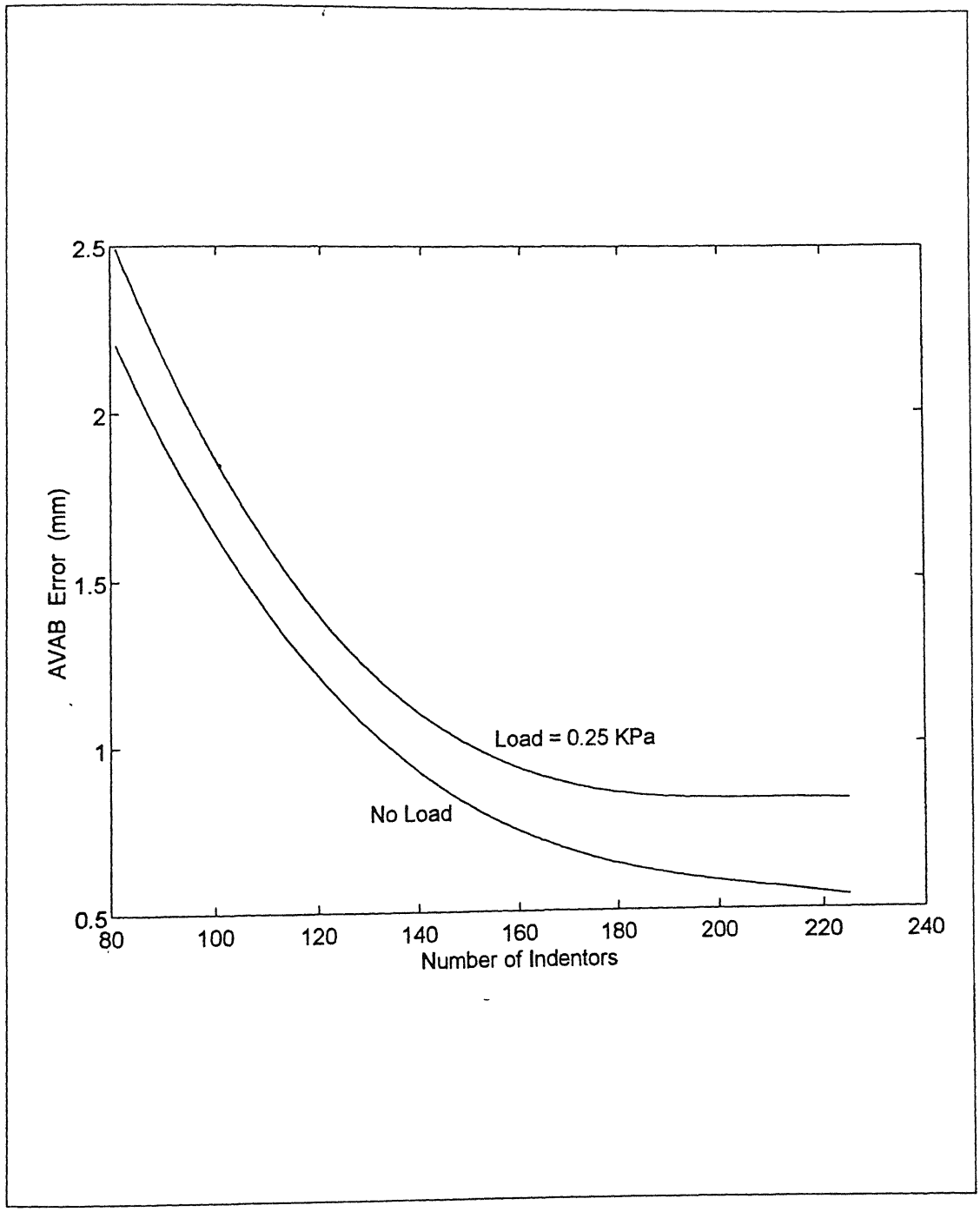

Figure 4.4. Variation of AVAB Error with Increasing Number of Indentors.

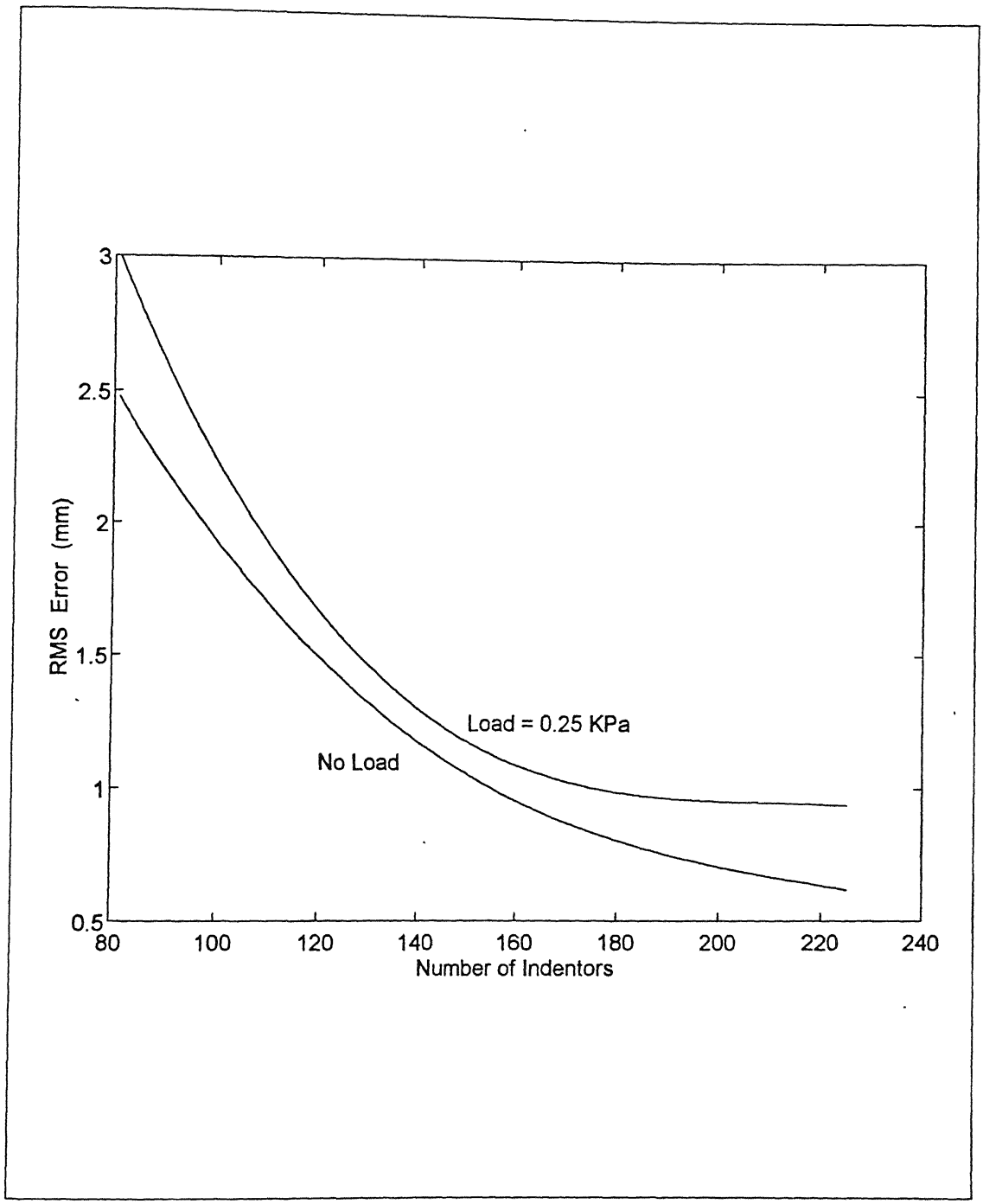

Figure 4.5. Variation of RMS Error with Increasing Number of Indentors.

measured in terms of radius of this spherical segment or contact curvature which refers to reciprocal of the contact radius. If the contact geometry of the indentor matches with the local shape of the surface patch to be realized, a better approximation can be expected. This is difficult to achieve assuming that all the indentors are of identical shape. Moreover, the same set of indentors are used for realizing a class of shapes varying significantly from one another.

Considering the surface patch of previous section given by Equation (4.1), the effect of contact geometry on the realizability of a shape can be demonstrated. In the given parameter range, most of the region of this patch is synclastic. The variation of approximation error for this surface patch with increasing contact radii is shown in Figure 4.6. The approximation error is evaluated using the expression given by Equation (4.2). The results of numerical experiments in terms of AVAB and RMS errors for this surface patch are given in Figures 4.7 and 4.8 respectively. For a given surface shape there exist a range of contact radius/curvature values of the indentors which gives best results. In this range the effect of external loading on the accuracy of realized shape is not much. In the absence of any external loading, best results were obtained with indentors of small curvature. This can be expected as the desired shape too has small values of curvatures.

Similar numerical experiments were performed with other surface shapes of varying curvature values. Based on the results of these experiment it has been found that the same set of indentors cannot give good results for a class of shapes varying considerably in terms of curvature values. In order to improve the range as well as the accuracy of realizable shapes the use of removable indentors having different contact radii is suggested (Fig. 4.9). In this case, the indentors of required contact geometry can be inserted depending on the local shape of the surface to be realized.

4.4 Indentor Layout

In the proposed tooling, the arrangement of indentors or the indentor layout for shape realization forms another interesting topic. The indentor layout is closely related to the

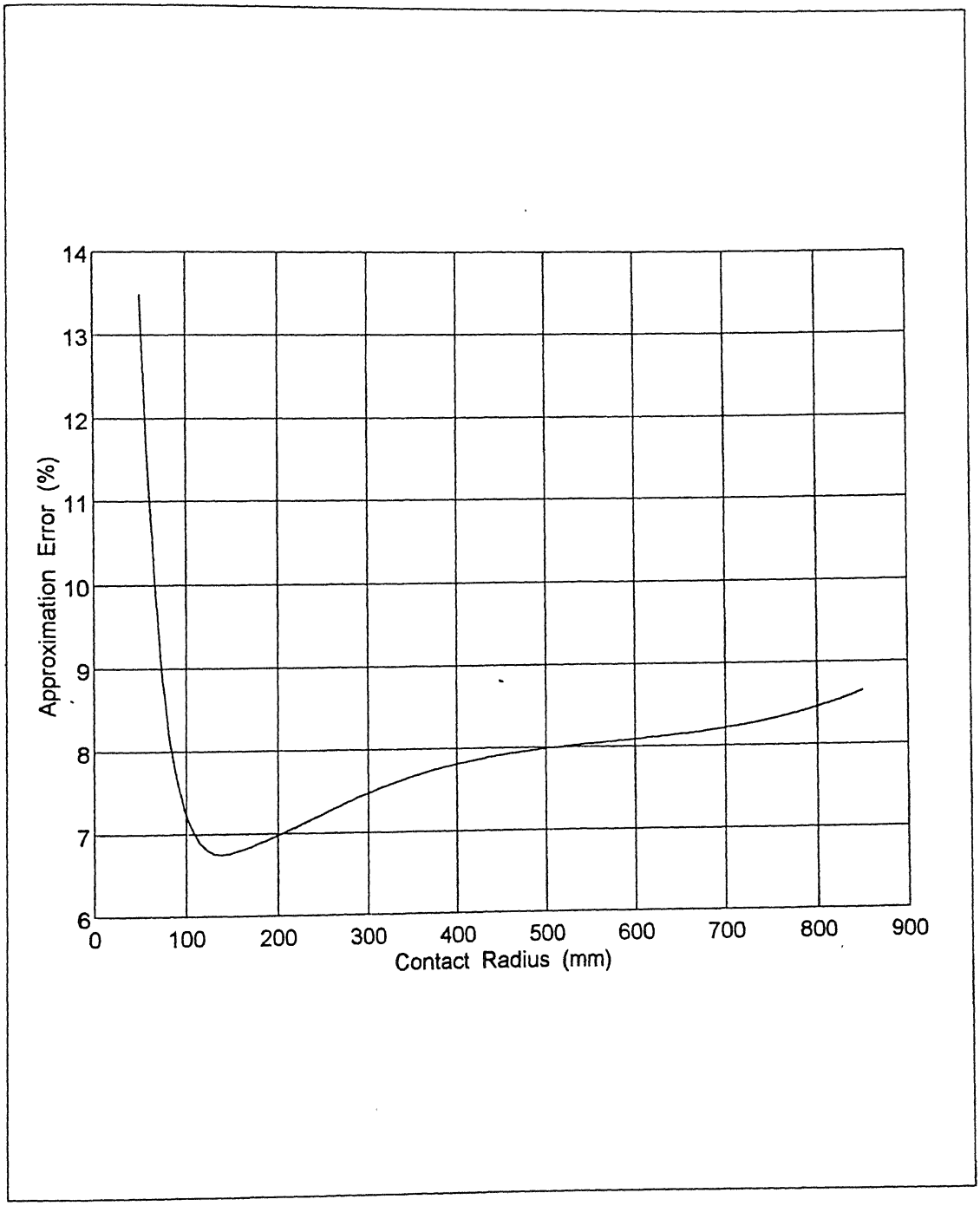

Figure 4.6. Variation of Approximation Error with Contact Radius.

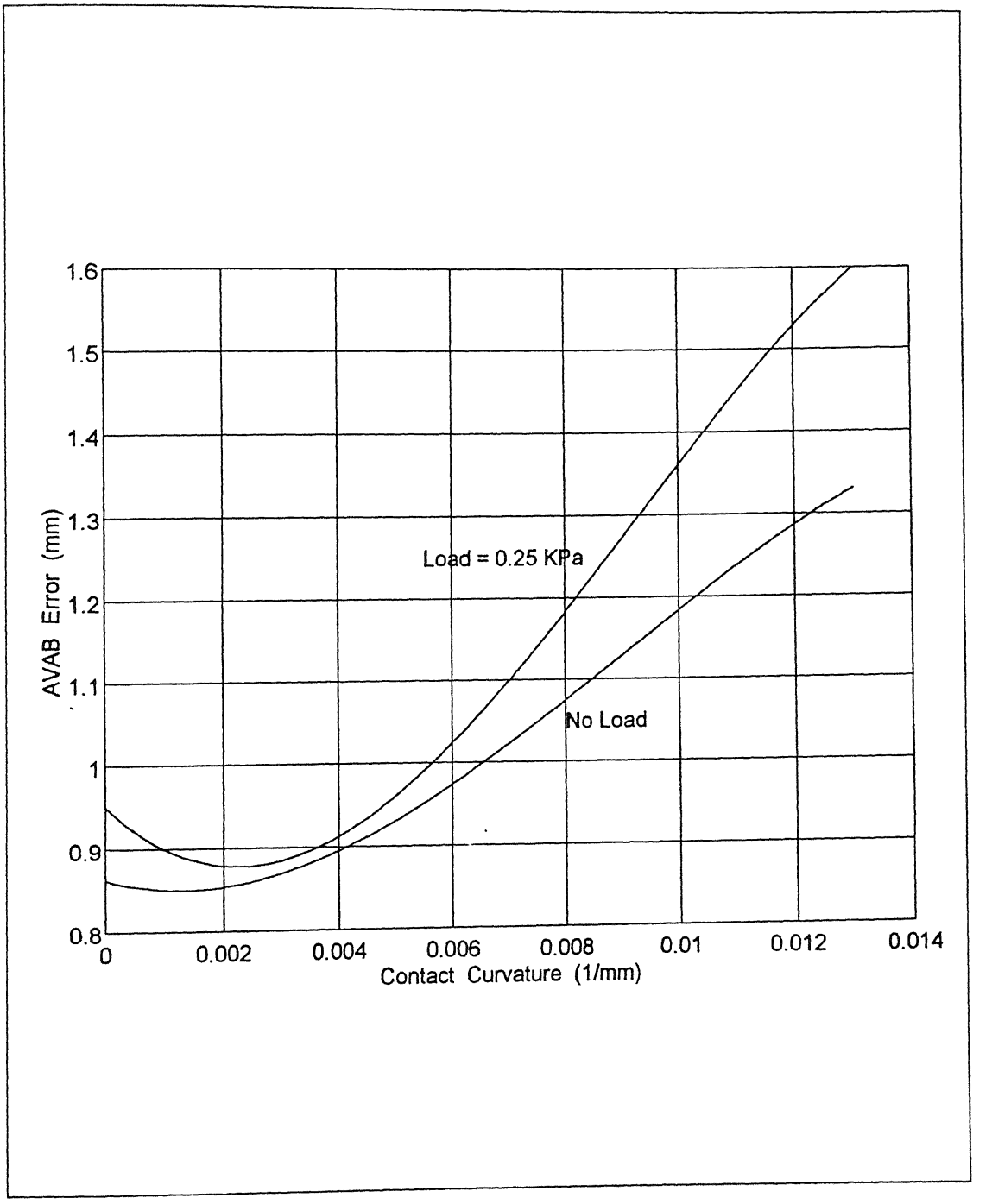

Figure 4.7. Variation of AVAB Error with Contact Curvature.

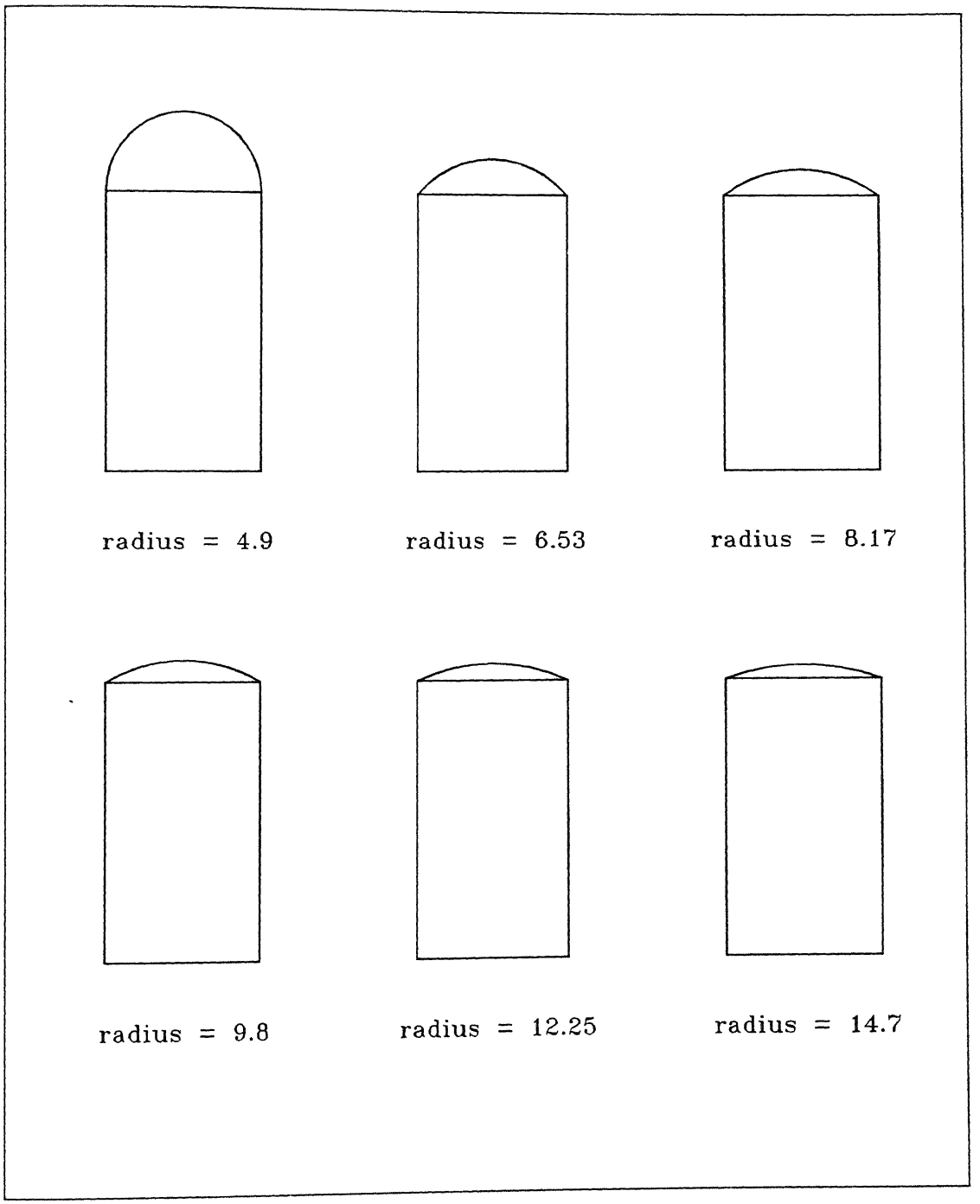

Figure 4.9. Insertable Indentors of Different Contact Radii.

indentor section geometry. Figure 4.10 shows four different combinations of indentor layout and indentor section geometry which are considered as a part of the present study. Due to compact arrangement of indentors, the layouts 'B' and 'D' with square and hexagonal sections respectively can be expected to give better results than layouts 'A' and 'C'.

Table 4.1 presents the results of shape realization using four layouts for a typical shape. The contact geometry of the indentors in all the four cases is same. Based on the numerical experiments which were carried out on some typical shapes of varying curvature, the performance of layouts "B" and "D" was found to be better than layout "C". The layout "C" performed better than "A". The relative performance of the four layouts in the presence of uniformly distributed load of 0.25 kPa was also more or less same. Further, it is noticed that the variation in their performance was more in the case of realizing surface patches of small curvature values.

Indentor Layout	UDL (kPa)	Average Absolute Error	Root Mean Square Error
Layout "A"	0.0	0.9542 mm	1.2977 mm
	0.25	1.1665 mm	1.3132 mm
Layout "B"	0.0	0.7978 mm	1.0551 mm
	0.25	1.0657 mm	1.2047 mm
Layout "C"	0.0	0.8771 mm	1.0826 mm
	0.25	1.0869 mm	1.2351 mm
Layout "D"	0.0	0.7429 mm	0.9500 mm
	0.25	0.9887 mm	1.1354 mm

Table 4.1. Effect of Indentor Layout on the Surface Shape Accuracy

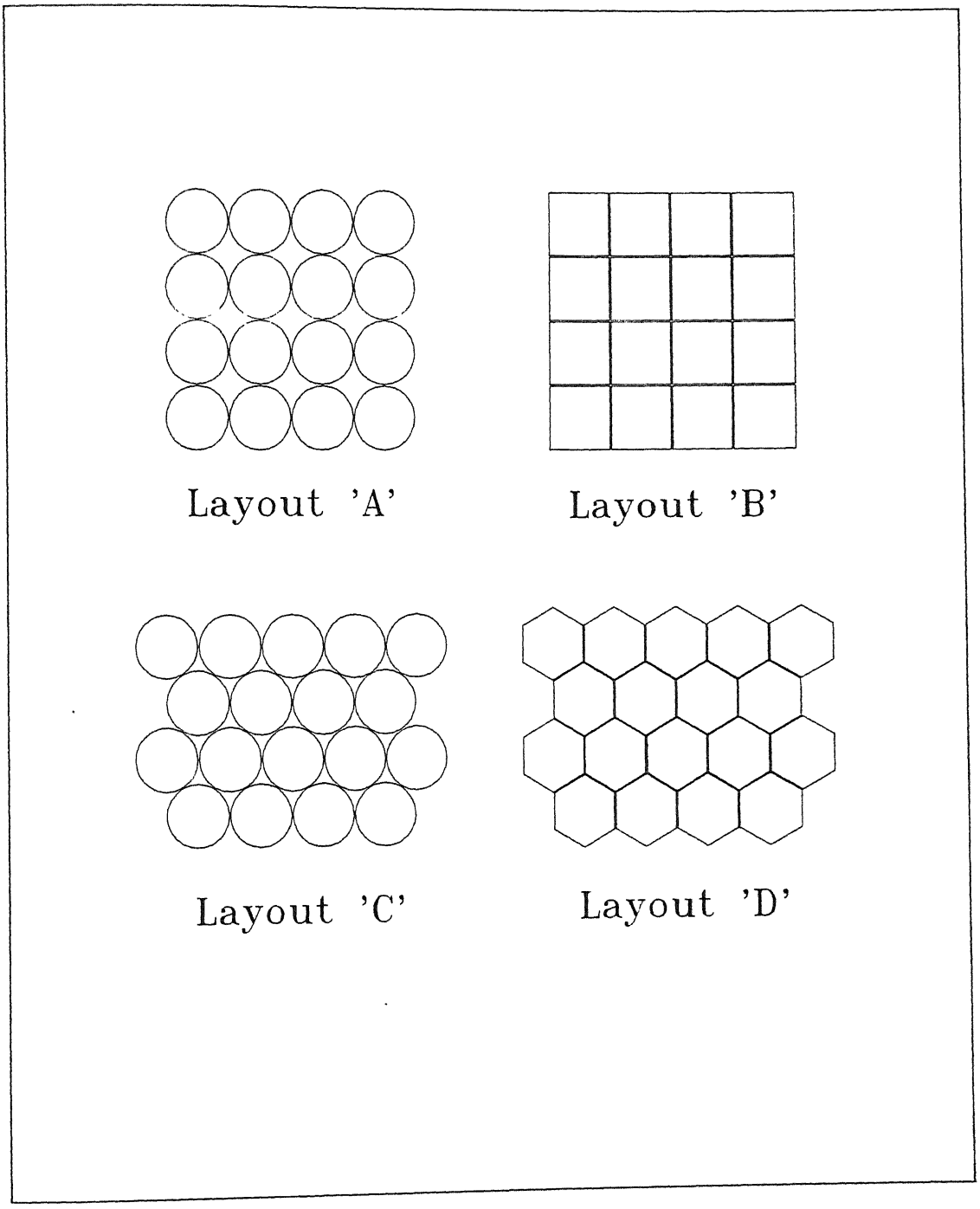

Figure 4.10. Indentor Layout.

Chapter 5

STATIC SHAPE OPTIMIZATION

5.1 Introduction

The results of shape realization experiments using flexible surface tooling were presented in Chapters 3 and 4. In these numerical experiments, the relative positions of the indentors in order to realize a given surface shape were decided off-line. The procedure adopted for deciding the indentor heights has been discussed in the previous chapter. This is an open-loop approach to shape realization in which the error between the desired and realized surface shapes is fixed for a given set of tooling parameters. An alternate approach is to manipulate the heights of the indentors after every deformation analysis run for any possible improvement in the accuracy of the realized shapes. The main objective of this chapter is to investigate this aspect in detail.

The problem of shape realization by closed-loop approach can be formulated as a static shape optimization problem. This involves minimizing the error between the desired and realized surface shapes by treating the indentor heights as design variables. If the indentors are manipulated one at a time, the possible improvement in the accuracy of realizable shapes will be at the expense of high computational cost. Depending on the shape to be realized and the number of indentors used, the number of function

evaluations may be excessively large. Such a scheme is not practical from the operational point of view and is not advisable in most of the cases. However, the number of function evaluations can be reduced by manipulating a group of indentors instead of manipulating a single indentor at a time. This aspect has been discussed in detail in the subsequent sections.

5.2 Previous Work

The problem of optimizing the static shape of a deformable object is often found in the area of design and control of large flexible space structures, such as, large antennas, mirrors, telescopes and interferometers. The shape control of these space structures is of great interest to structural designers (Haftka and Adelman, 1985; Orozco and Ghattas, 1991; Padula et al., 1989). These structures are often mounted on a number of discrete supports, some or all of which are fixed in space and are known as passive supports. If a support can be manipulated to change the static shape of the structure after erection, it is referred to as an active support. One of the main objectives here is to seek ways to minimize the need for active supports or to eliminate them by careful design and construction of the space structure. The studies in this area have shown that in some cases geometrical shape accuracy can be maintained with passive supports by carrying out off-line shape optimization. One of the ways to achieve the desired static shape of the reflecting surface here is to manipulate the supports without changing their respective locations. This is a case of finding the optimum supports for the structure when its topology and shape are predetermined. This problem is similar to the present closed-loop approach to shape realization by flexible surface tooling.

The above problem is usually posed as a nonlinear optimization problem with an objective to minimize the error between the desired and deflected shape of the structure. Conventionally, a structural analysis is first performed for some initial guess of the design variables and using this as a starting point search direction is determined with the aid of a nonlinear optimization algorithm. The search direction is now used to improve the current design and the cycle is repeated until some convergence criteria is

met. This approach is usually called *nested* and several procedures have been proposed to improve its performance (Haftka, 1989; Orozco and Ghattas, 1991).

5.3 Present Methodology

A similar procedure is possible in the present case of static shape optimization of the flexible sheet for optimum indentor heights. The error between the desired and realized surface shapes can be minimized by using a nonlinear optimization technique and treating the indentor heights as design variables. The evaluation of objective function in this case involves the deformation analysis of the flexible elastomeric sheet for a given set of indentor heights. In the worst case, when there is no symmetry in the arrangement of indentors, the number of design variables here is equal to the number of indentors. Solving such a large scale optimization problem is highly prohibitive as it involves the evaluation of the objective function a few thousands of times by any of the first or second order optimization techniques.

An alternate procedure which can be attempted in this case is to identify and manipulate a group of indentors which are likely to improve the accuracy of realized shapes. Based on the error between the desired and realized surface shapes at any particular time, a single or a group of indentors can be identified. This involves scanning the error profile and identifying the high error zones and the indentors in the vicinity of these zones. Once the indentors are identified their heights can be manipulated in proportion to the error in their respective zones. This is a case of an interactive optimization. Such an approach will involve only a few objective function evaluations. This cycle can be repeated until the error is more or less uniform throughout the flexible sheet. Once the indentors to be manipulated are identified the optimization in this case reduces to that of a line search.

The accuracy of the realized shape can also be improved in some cases by moving all the indentors in either direction and keeping their relative configurations unchanged. Raising and lowering of all the indentors by an equal amount is equivalent to changing of the tension in the flexible sheet. Figure 5.1 shows this aspect for a two dimensional

case where the flexible sheet is made to stretch continuously as the indentors are raised without changing their relative heights.

5.4 Numerical Examples

Three numerical examples are presented in this section. The first example deals with the shape realization of a doubly curved surface patch. The parametric representation of this surface patch is given as,

$$z = 0.15 \left[1 - (5x/4)^2\right] \left[1 - (5y/4)^2\right] \tag{5.1}$$

$$\text{where } -0.5 \leq x \leq 0.5 \text{ and } -0.5 \leq y \leq 0.5$$

In this case, first the deformation analysis of the flexible sheet has been carried out by following the open-loop approach discussed in the last chapter. A 4.0 mm thick sheet and 81 indentors are used which are arranged in the form of a matrix of 9 by 9. A uniformly distributed load of 0.5 kPa has been applied on the flexible sheet. Figure 5.2 shows the error profile between the desired and realized surfaces patches for this case. It can be seen from the figure that the error in this case is equally distributed throughout the flexible sheet. This indicates that the improvement in the realizability of the shape is not likely to happen by varying the relative heights of the indentors. In this case all the indentors can be raised and lowered by the same height to see the effect on the realizability of this shape.

Figure 5.3 shows the effect of moving all the indentors on the accuracy of the realized shape in this case. It can be seen from Figure 5.3 that there exist an optimum height at which the best results can be obtained. At lower indentation heights, the tension in the flexible sheet is relatively small. In such case the effect of external loading on the realized shape is significant and responsible for relatively poor results. When the sheet is subjected to high tension values its ability to take the external load increases. However, at higher tensions, the tendency of the elastomeric sheet to form local areas of peaks and valleys increases (Fig 5.3).

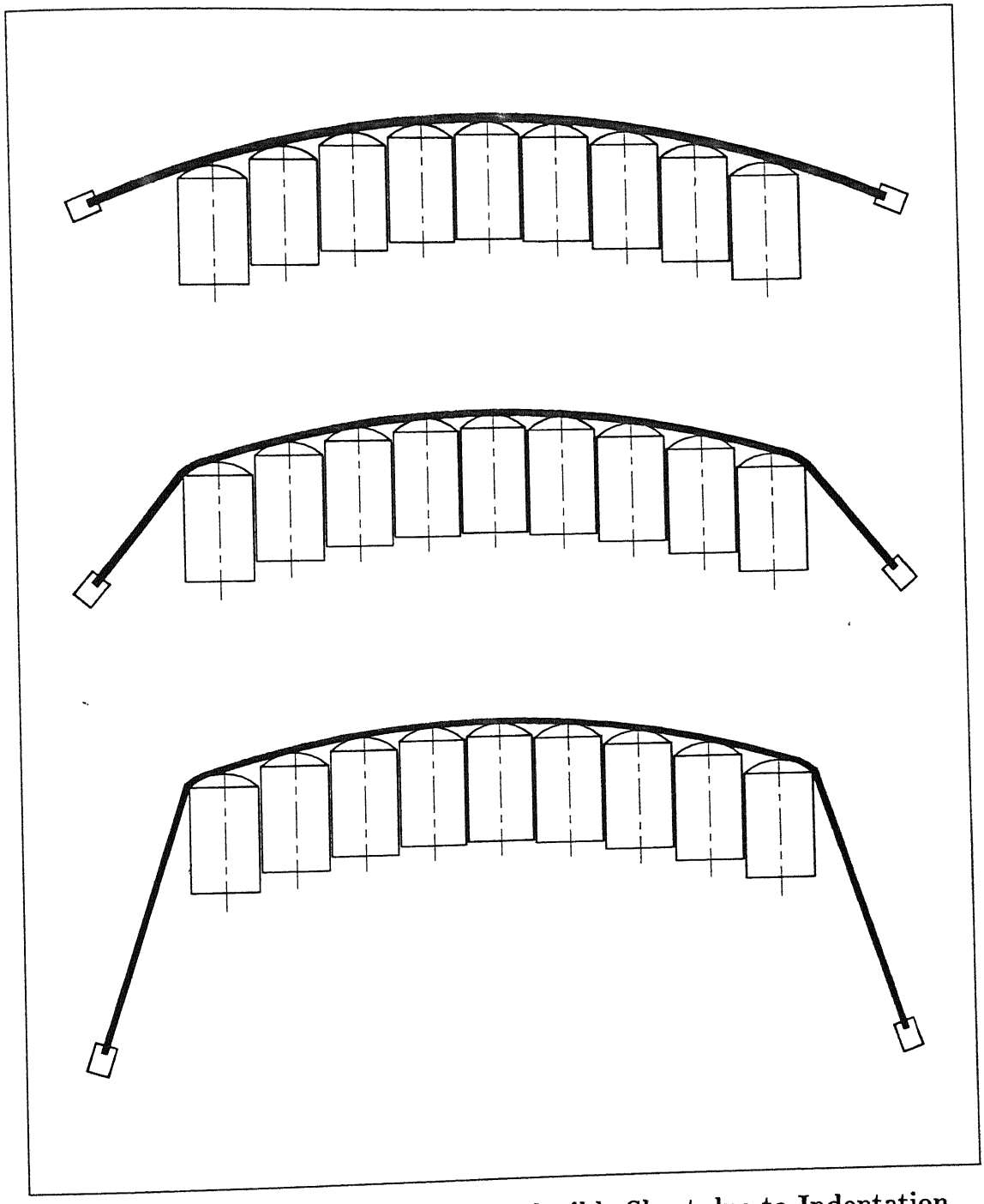

Figure 5.1. Continuous Stretching of Flexible Sheet due to Indentation.

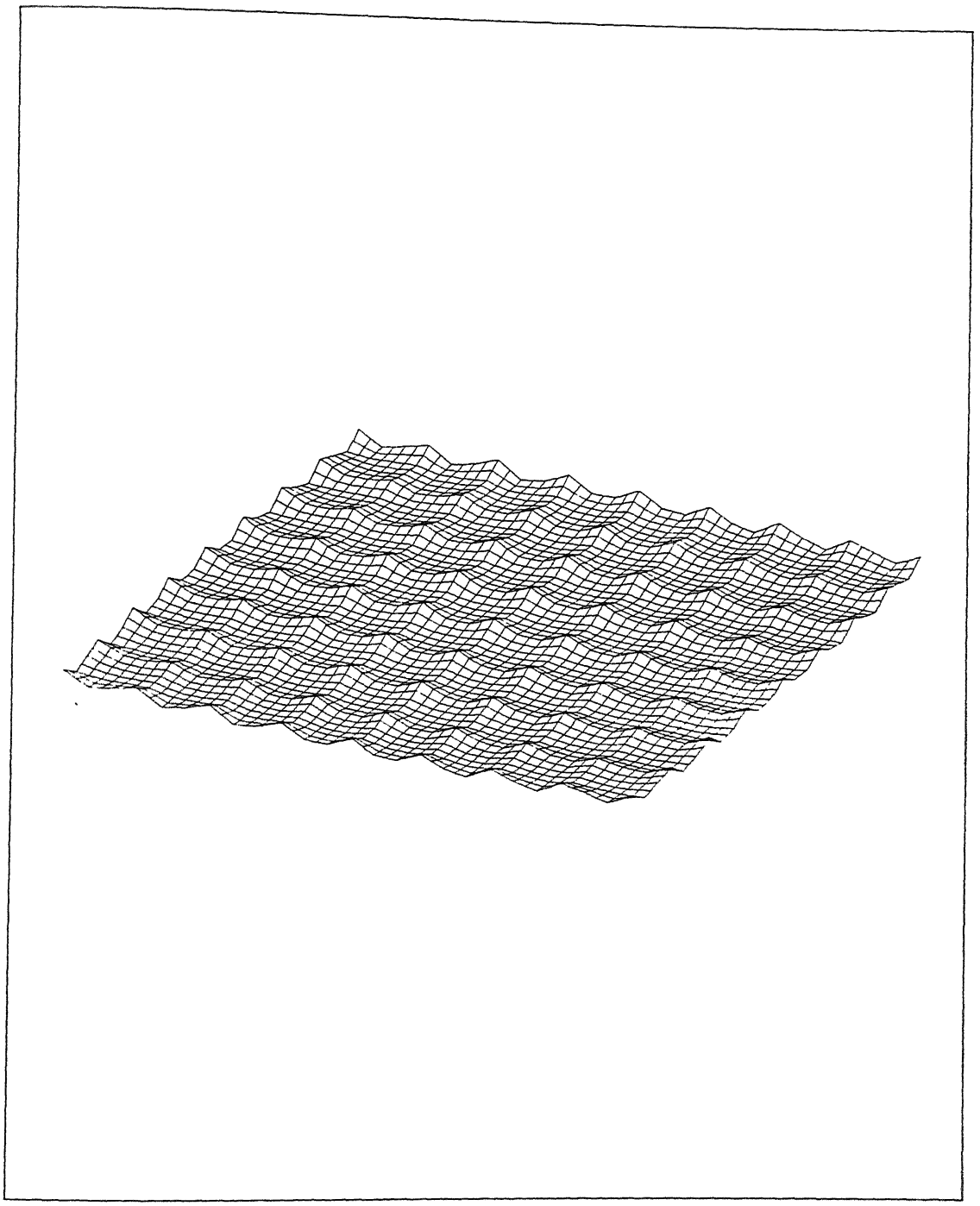

Figure 5.2. Error Profile (Numerical Example I).

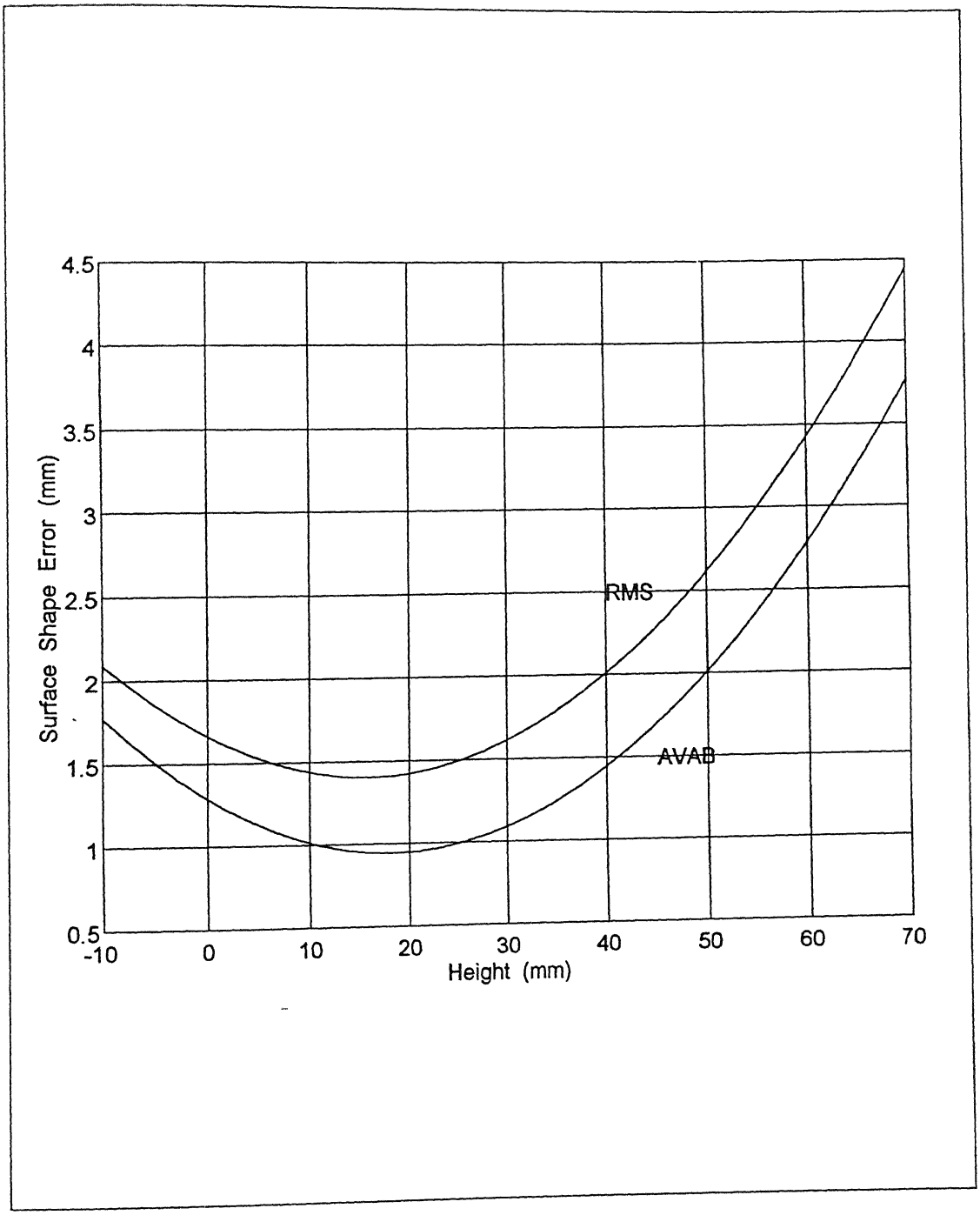

Figure 5.3. Static Shape Optimization for Indentation Height.

The second example is concerned with the realizability of another surface patch of compound curvature. The equation of the surface patch in this case is given as,

$$z = 0.1\left[(4x/3)^2 - 1\right]^2\left[(4y/3)^2 - 1\right]^2 \tag{5.2}$$

$$\text{where } -0.5 \leq x \leq 0.5 \text{ and } -0.5 \leq y \leq 0.5$$

The deformation analysis in this case is carried out with a total of 81 indentors and using a 5.0 mm thick elastomeric sheet. An UDL of 0.5 kPa has been applied on the flexible sheet in an area where the indentors are placed. Figure 5.4 shows the error profile between the desired and realized shapes. The error distribution in the flexible sheet here is not uniform. This is a case of an example where the relative movements of the indentors may lead to the improvement in the shape accuracy. A group of indentors is identified in the region of high error values and the sensitivity of the movement of these indentors is first carried out. Based on this, a search direction is evaluated and the optimization is carried out using a quadratic search. Table 5.1 presents the results for this surface patch after two iterations of interactive optimization. The improvement in the accuracy of the realized shape is evident from results.

Case	Average Absolute Error	Root Mean Square Error
Open-Loop Approach	1.2103 mm	1.5077 mm
Indentation Height Optimization	1.0922 mm	1.3949 mm
After First Iteration	0.8147 mm	1.0267 mm
After Second Iteration	0.7931 mm	1.0114 mm

Table 5.1 Results of Static Shape Optimization (Numerical Example II).

The last example of this section is concerned with the realization of a swept patch given by the following equation.

$$\begin{aligned} x &= 1.51625\, cos(u) \\ y &= 1.0 * v - 0.5 \\ z &= 0.758125\, sin(u) - 0.658125 \end{aligned} \tag{5.3}$$

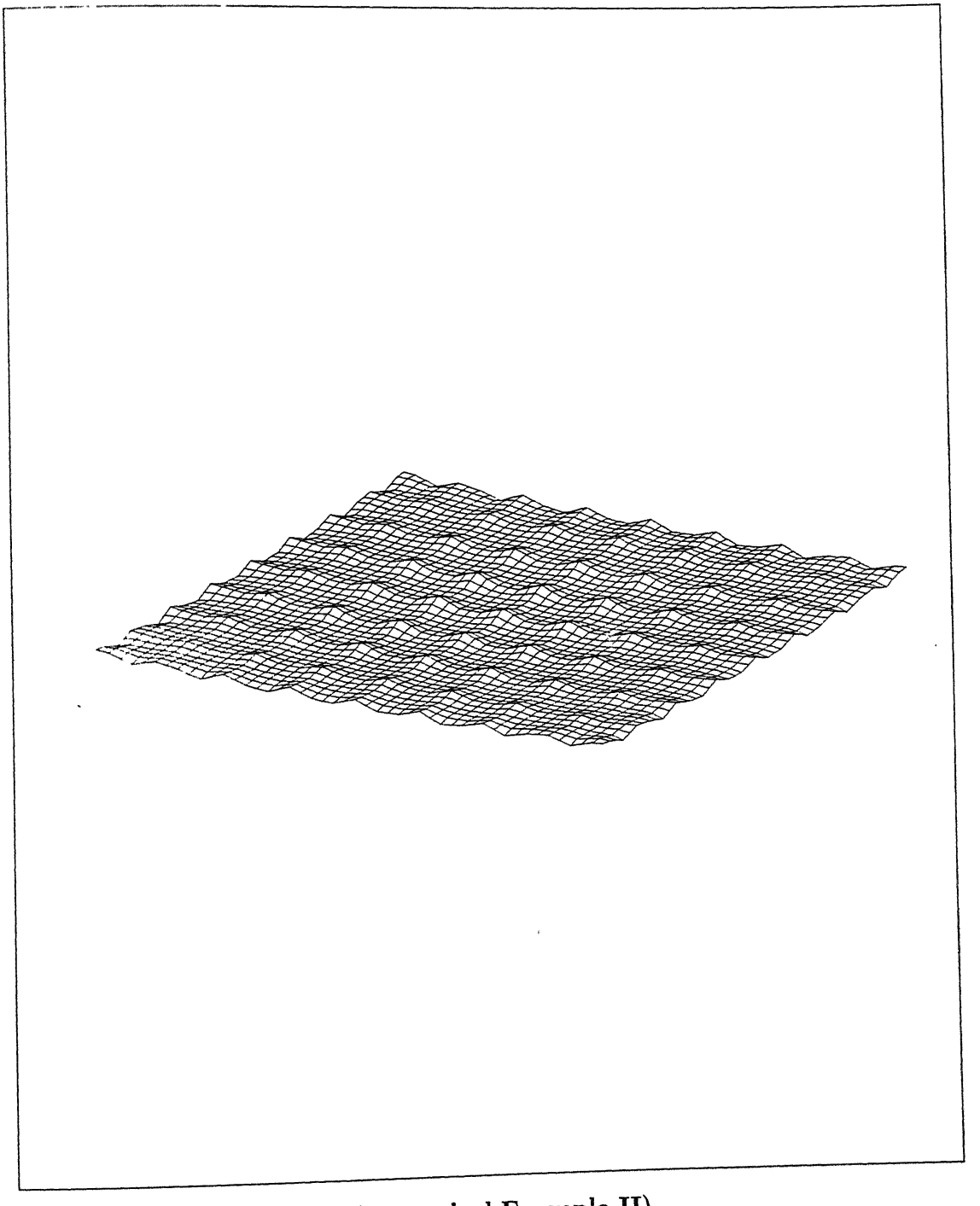

Figure 5.4. Error Profile (Numerical Example II).

$$\text{where } 1.0534 \leq u \leq 2.0882 \text{ and } 0.0 \leq v \leq 1.0$$

The deformation analysis is first carried out with a total of 81 indentors forming a matrix of 9 by 9. The layout of indentors in this case is shown in Figure 5.5. Figure 5.6 shows the realized surface patch and the error profile between the desired and realized surface patches when there is an external load of 0.25 kPa in the form of UDL.

The curvature of this surface patch varies only in one direction; the curvature in the direction of sweep being zero. All the indentors placed along the direction of sweep are raised by same height. This reduces the total number of design variables in this case to 9. The number of design variables further reduces to a value 5 as there is a symmetry in the shape to be realized and also in the placement of indentors. As the number of design variables here is small, the static shape optimization can be carried out in an automated manner. The conjugate gradient method(with Polak-Ribiere correction) is used for this optimization. The results of the same after two iterations are presented in Table 5.2.

Case	Average Absolute Error	Root Mean Square Error
Indentation Height Optimization	0.7990 mm	1.1024 mm
After First Iteration	0.7549 mm	1.0606 mm
After Second Iteration	0.7056 mm	0.9511 mm

Table 5.2 Results of Static Shape Optimization (Numerical Example III).

The relative performance of the three schemes of static shape optimization discussed above is found to vary from shape to shape. In the first two examples considered above, the RMS error between the desired and realized shapes have been minimized whereas, the average absolute error forms the objective function in the third case. In all the three cases, a relatively small number of indentors are used. This is done intentionally to reduce the excessive CPU time involved in these computations and also with an objective to reduce the number of indentors required for the realizability of the typical shapes discussed above.

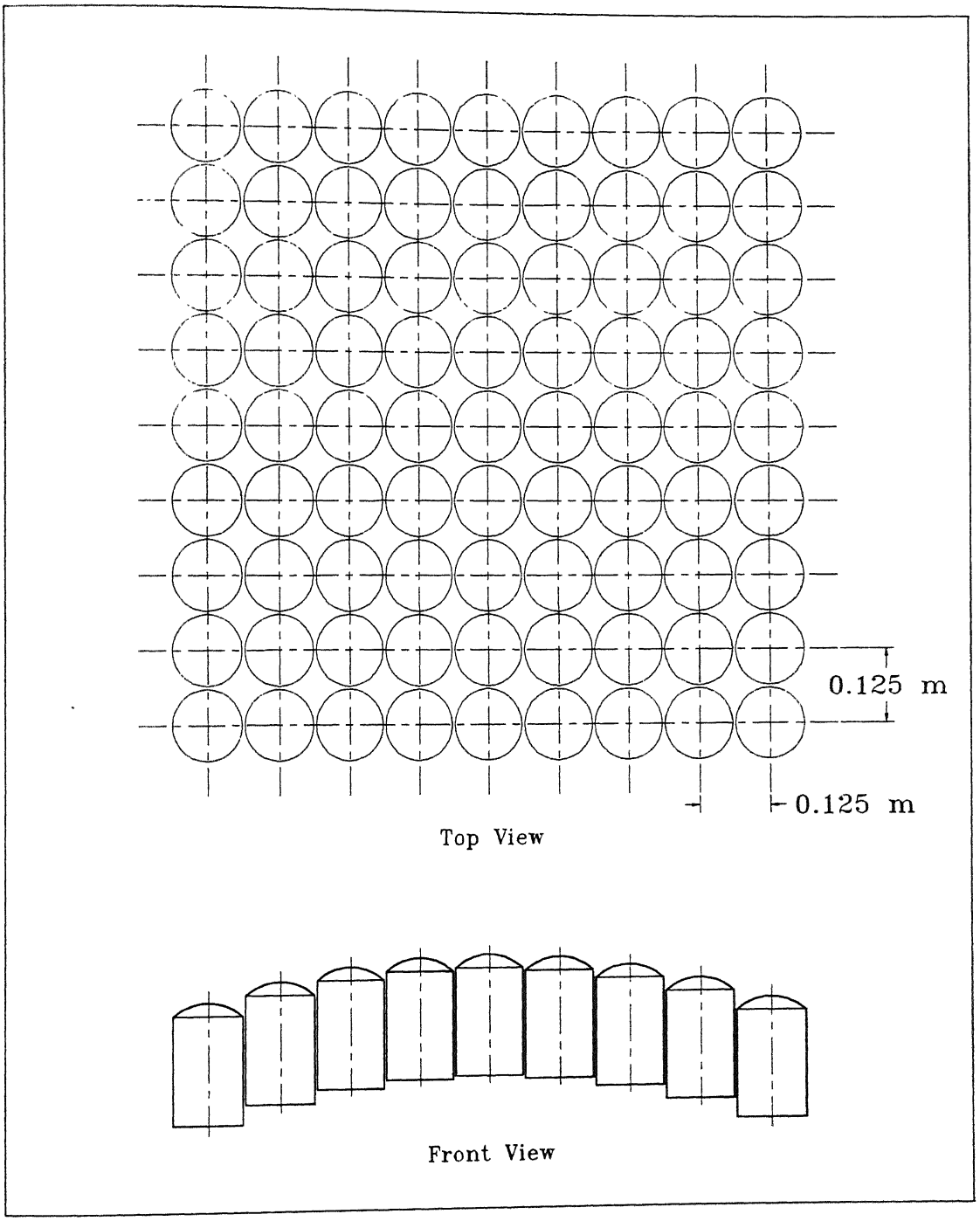

Figure 5.5. Indentor Layout (Numerical Example III).

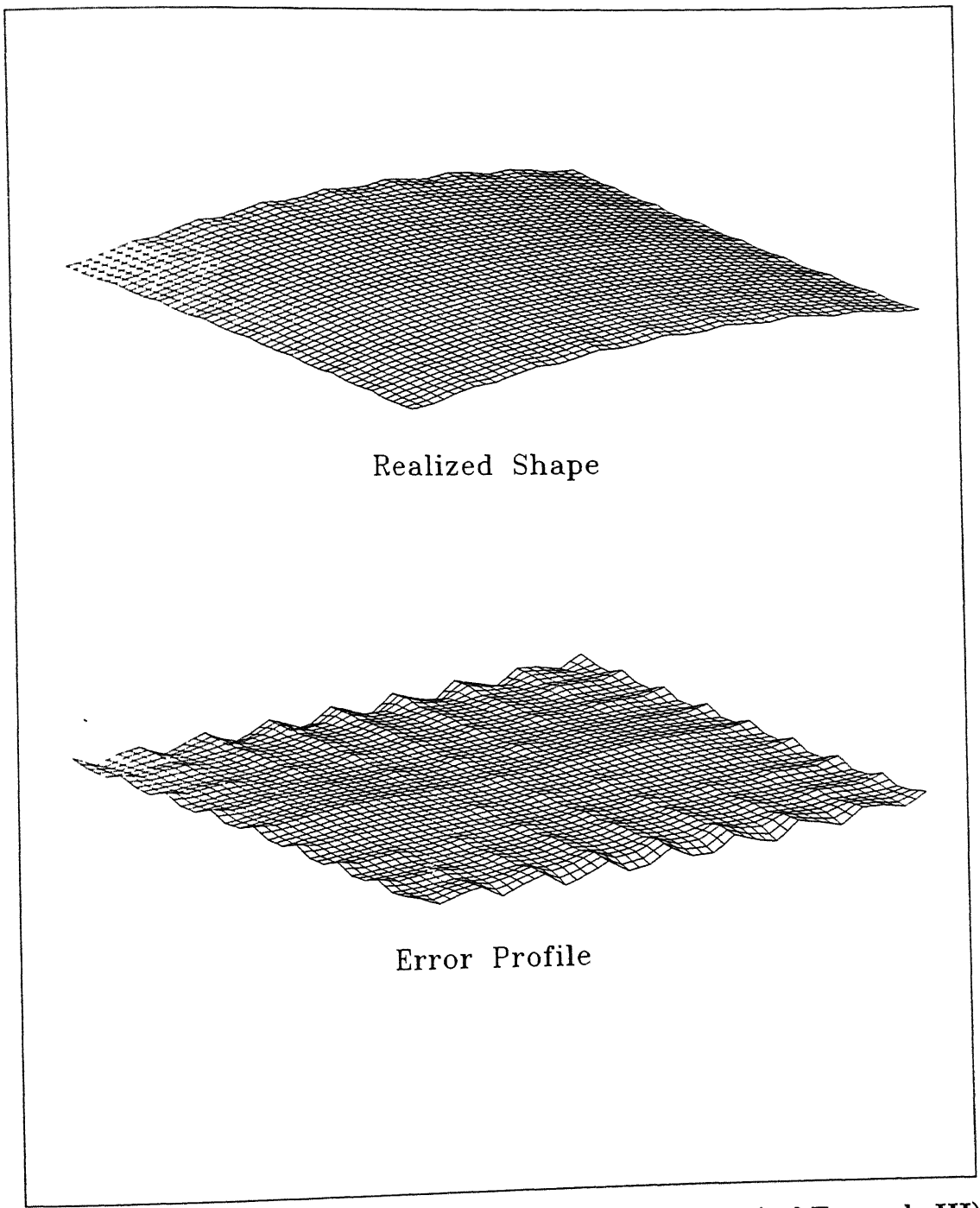

Figure 5.6. Realization of a Swept Surface Patch (Numerical Example III).

Chapter 6

FLEXIBLE SURFACE TOOLING WITH BONDED INDENTORS

6.1 Realizing Anticlastic Shapes

A flexible surface tooling in which there is no bonding between the indentors and the elastomeric sheet was the subject of last three chapters. The realizability of a certain class of shapes has been demonstrated with this version of tooling. The tooling is found to be effective for synclastic shapes with small curvature values. This version of tooling can also be used for anticlastic shapes with very small Gaussian curvature values. For example, the numerical examples 3 and 5 of Chapter 3 dealt with shapes which have both regions of elliptic and hyperbolic points. However, the nature of tooling does not allow the shapes with considerable negative Gaussian curvature to be realized. Figure 6.1 shows some typical shapes which cannot be realized with this version of tooling.

In order to extend the applicability of the flexible surface tooling for shapes with considerable negative Gaussian curvature, a second version of the tooling has been proposed. Figure 6.2 shows a conceptual sketch of this version of tooling. It consists of a matrix of indentors whose ends are bonded to a flexible sheet. In the base position,

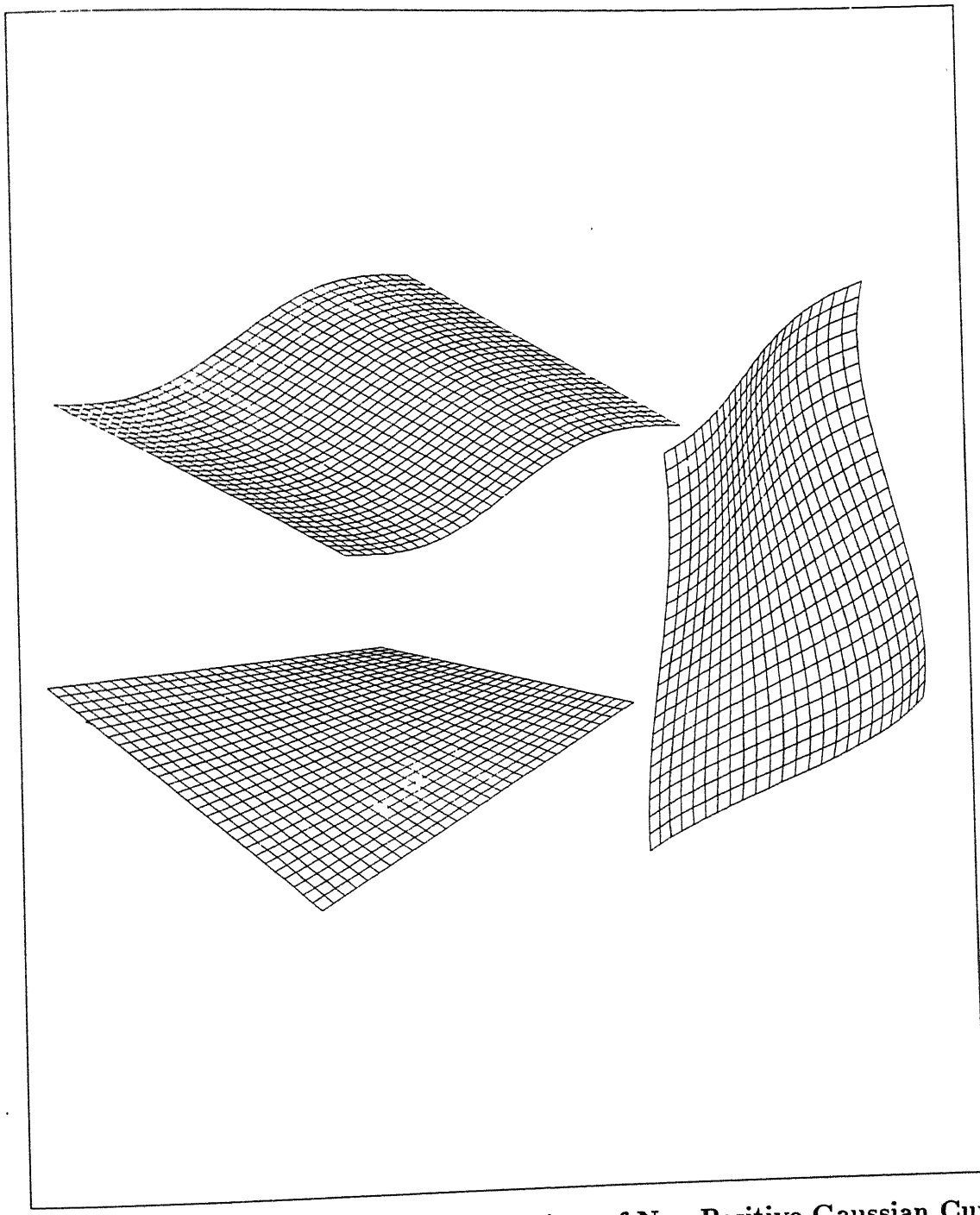

Figure 6.1. Surface Patches having Regions of Non-Positive Gaussian Curvature.

when all the indentors are at same height, the flexible sheet is in the undeformed state. When the indentors are raised by different heights, the sheet deforms to take a specific shape. The sheet can be made to deform to a desired shape by manipulating the indentor heights. A numerical study of the shape realizability by this version of tooling is the main subject of this chapter.

Unlike the earlier version of tooling, the indentors in this case are placed at some distance apart. This is necessary to allow the the portion of a sheet which is not in contact with the indentors to deform freely. As the indentors are placed a distance apart, their slenderness ratio is kept as low as possible to avoid any possible buckling due to reactive contact forces. The advantage of flexible surface tooling with bonded indentors is that it can be used for realizing shapes having positive or negative Gaussian curvature or both. However, the nature of tooling restricts the realizable shapes to those having small curvature values. This is due to flexible sheet being subjected to a high local straining in the regions of large curvatures.

The indentors can be bonded to flexible sheet either by some mechanical means or using suction jacks. When suction cups are used the process is similar to that of thermoforming. With a mechanical bonding, rotational degrees of freedom at the point of bonding can be incorporated. For the purpose of analysis, the contact between the the indentors and the flexible sheet can be treated as a point contact. The deformation analysis of the flexible sheet in this case involves finding of equilibrium shape of the sheet for certain positional constraints. The shape realization program described in Chapter 3 has been modified to account for this new boundary condition.

6.2 Numerical Examples

Five numerical examples are presented in this section. In order to compare this version of tooling with the earlier one, first two examples here are taken from that of Chapter 3. The first example is a linearly swept surface patch whose generatrix is an elliptic arc and the directrix is a line normal to the plane of generatrix curve. The parametric equation of the patch is reproduced here for the sake of convenience. It is given by,

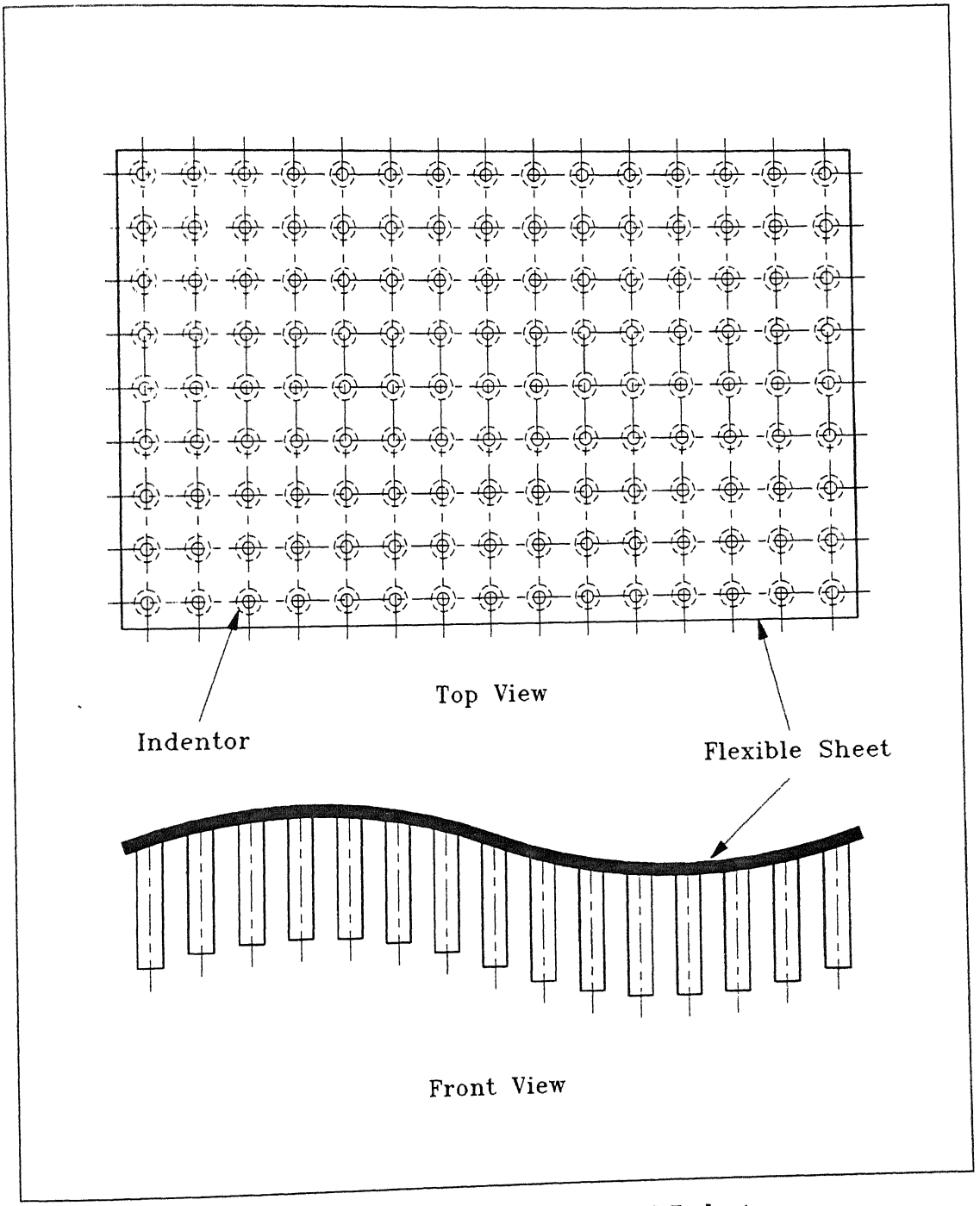

Figure 6.2. Flexible Surface Tooling with Bonded Indentors.

$$\begin{aligned} x &= 1.51625\ cos(u) \\ y &= v - 0.5 \\ z &= 0.758125\ sin(u) - 0.658125 \end{aligned} \tag{6.1}$$

$$\text{where } 1.0534 \leq u \leq 2.0882 \text{ and } 0.0 \leq v \leq 1.0$$

In order to realize this patch an elastomeric sheet of 1.1 m by 1.1 m and thickness 5.0 mm is used. The deformation analysis is carried out with a total of 121 indentors bonded to a flexible sheet. The layout of the indentors can be seen in Figure 6.3. The ratio of first and second Mooney constants, C_1/C_2 is taken as 4.0. The analysis has been carried out with a total of 1936 triangular elements (Fig. 6.4). The results of the analysis in terms of AVAB and RMS errors are given in Table 6.1. Figure 6.5 shows the realized shape and the error between the desired and realized shapes at higher magnification.

Indentor-Sheet Interaction	Average Absolute Error	Root Mean Square Error
Bonded	0.4817 mm	0.5521 mm
Unbonded	0.6936 mm	0.8611 mm

Table 6.1 AVAB and RMS Errors (Numerical Example I).

The second example is concerned with the realization of a doubly curved surface patch. The patch is defined by the following expression.

$$z = 0.25\ \left[1 - (5x/4)^2\right]\ \left[1 - (5y/4)^2\right] \tag{6.2}$$

$$\text{where } -0.5 \leq x \leq 0.5 \text{ and } -0.5 \leq y \leq 0.5$$

The analysis in this case is performed with a 4.0 mm thick sheet. The other input data for this analysis is same as that of previous example. The error between the desired and the deformed patches in this case is given in Table 6.2.

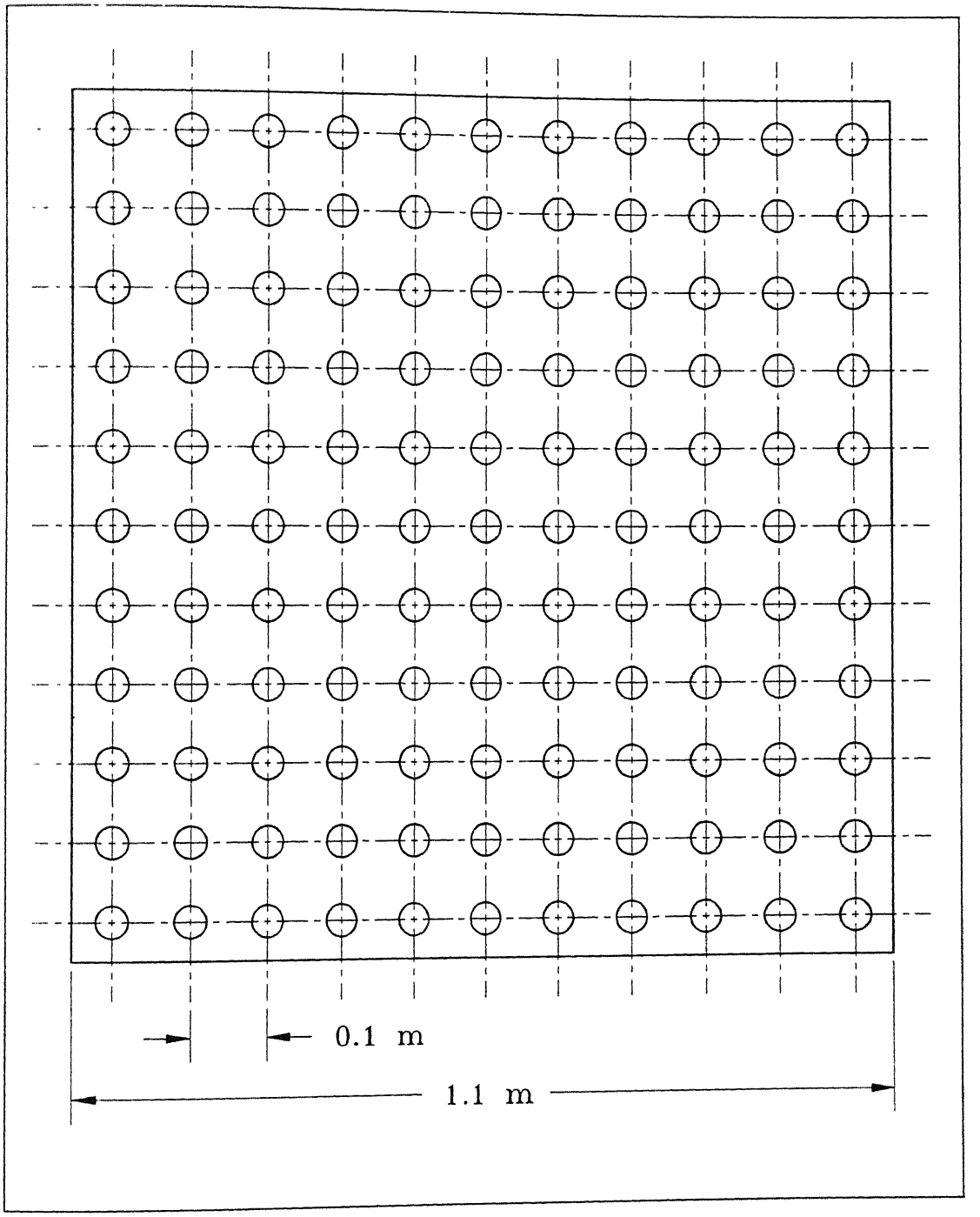

Figure 6.3. Indentor Layout (Numerical Example I).

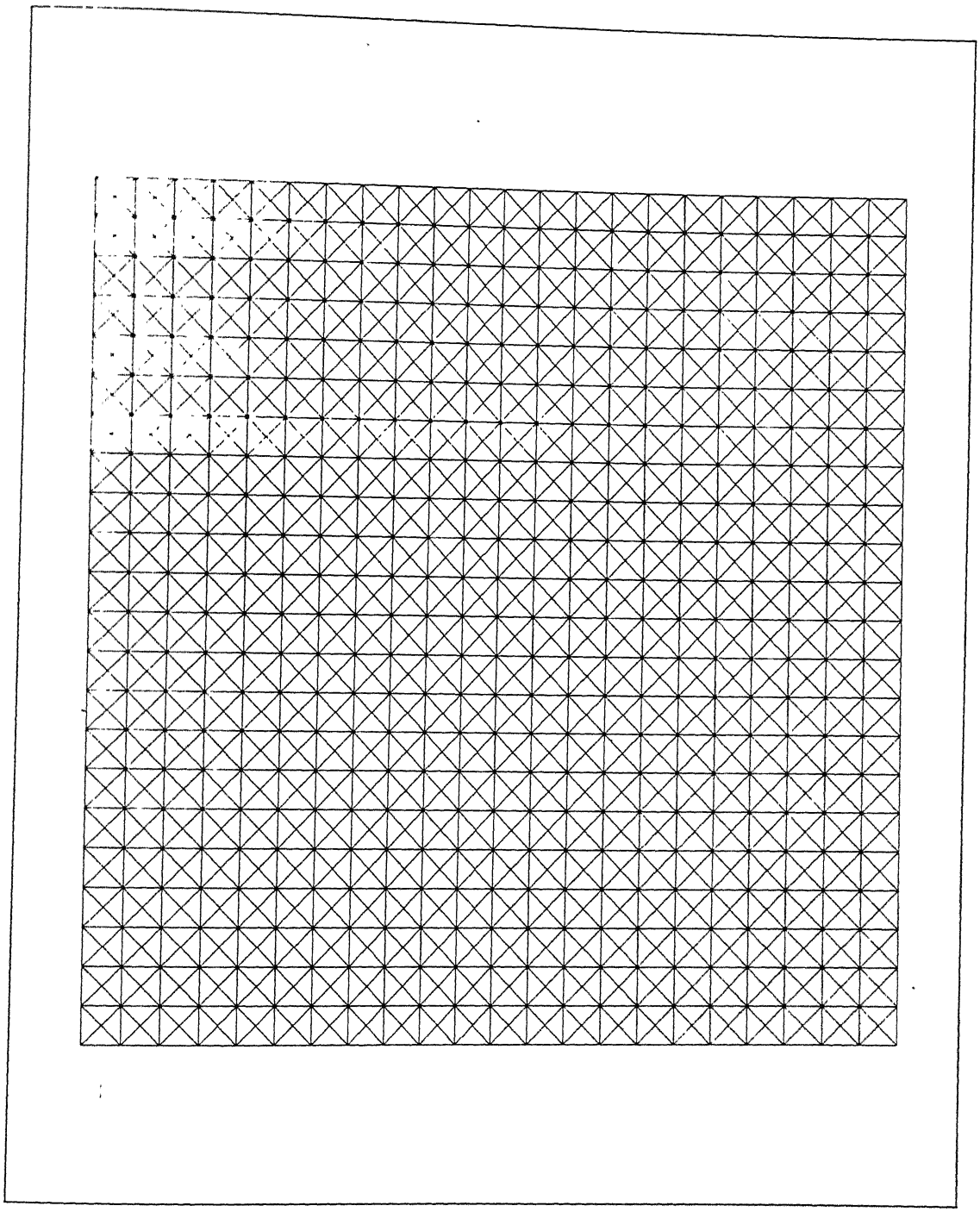

Figure 6.4. Finite Element Discretization (Numerical Example I).

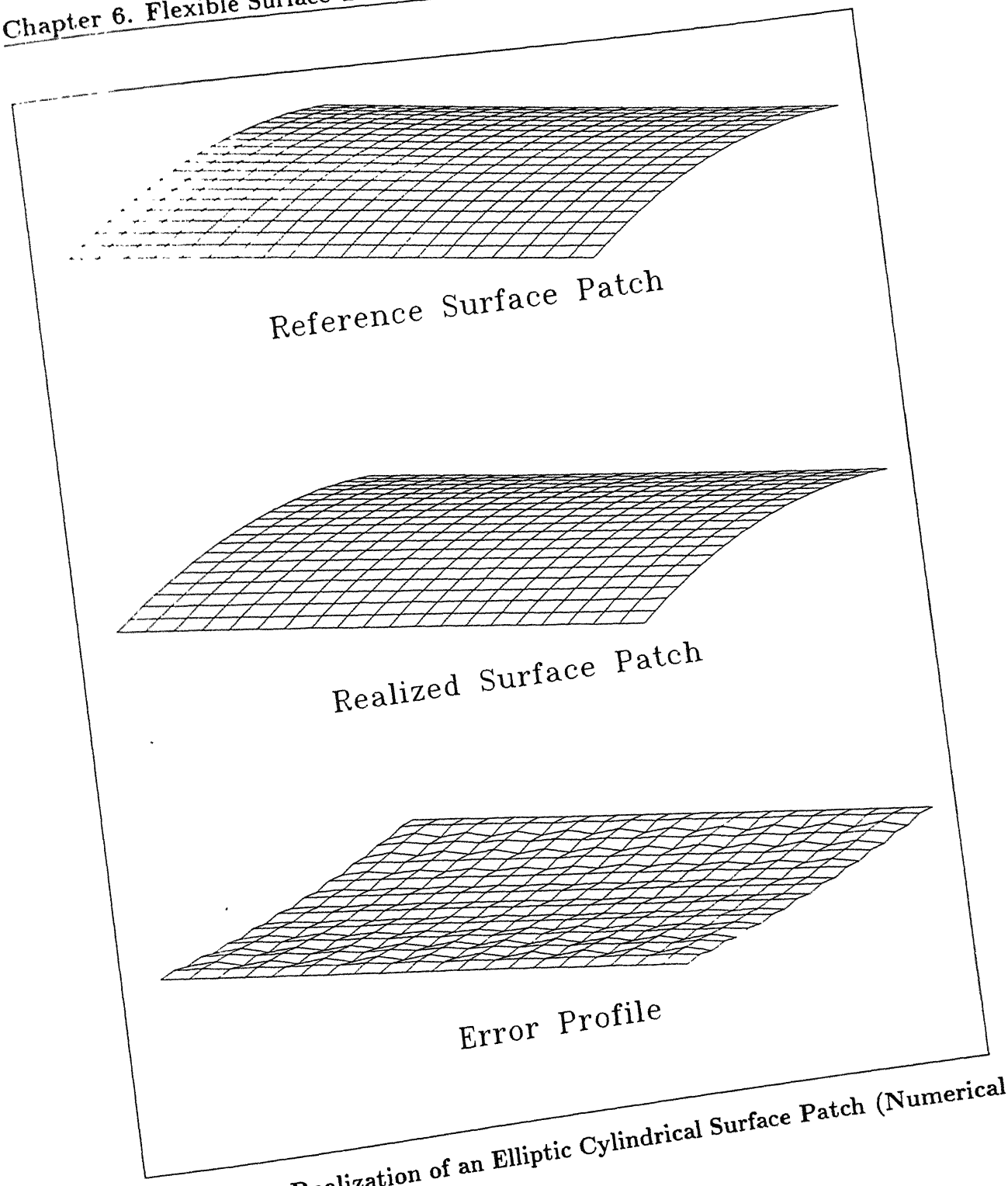

Figure 6.5. Realization of an Elliptic Cylindrical Surface Patch (Numerical Example I).

Indentor-Sheet Interaction	Average Absolute Error	Root Mean Square Error
Bonded	0.9911 *mm*	1.3243 *mm*
Unbonded	1.1948 *mm*	1.4755 *mm*

Table 6.2 AVAB and RMS Errors (Numerical Example II).

For the two surface patches discussed above better results were obtained with indentors bonded to flexible sheet. However, the results in practice may differ slightly from the reported values due to contact between the flexible sheet and the indentors being not a point contact.

The next two examples deal with the realization of shapes which have both synclastic and anticlastic regions. In the third example the results for a linearly swept surface patch are presented. The generatrix of the swept patch is a *sinusoidal* curve. The parametric equation of the patch is given as,

$$\begin{aligned} x &= u \\ y &= v \\ z &= A\, sin(2\pi u) \end{aligned} \tag{6.3}$$

$$\text{where } 0.0 \leq u \leq 1.0 \text{ and } 0.0 \leq v \leq 1.0$$

In this case, the analysis has been carried out for various values of A in the range of 0.02 to 0.2 m using a 5.0 mm thick sheet with 169 indentors. The realized surface patch and the error between desired and realized patches are shown in Figure 6.6. Figure 6.7 shows the variation of AVAB and RMS errors for this patch for various values of A. At smaller values of A which corresponds to surface patches with small curvature values, better results were obtained.

The next example is concerned with the realization of a bicubic Bezier patch. The parametric equation of the patch is given as,

$$\begin{aligned} x &= u - 0.5 \\ y &= v - 0.5 \end{aligned}$$

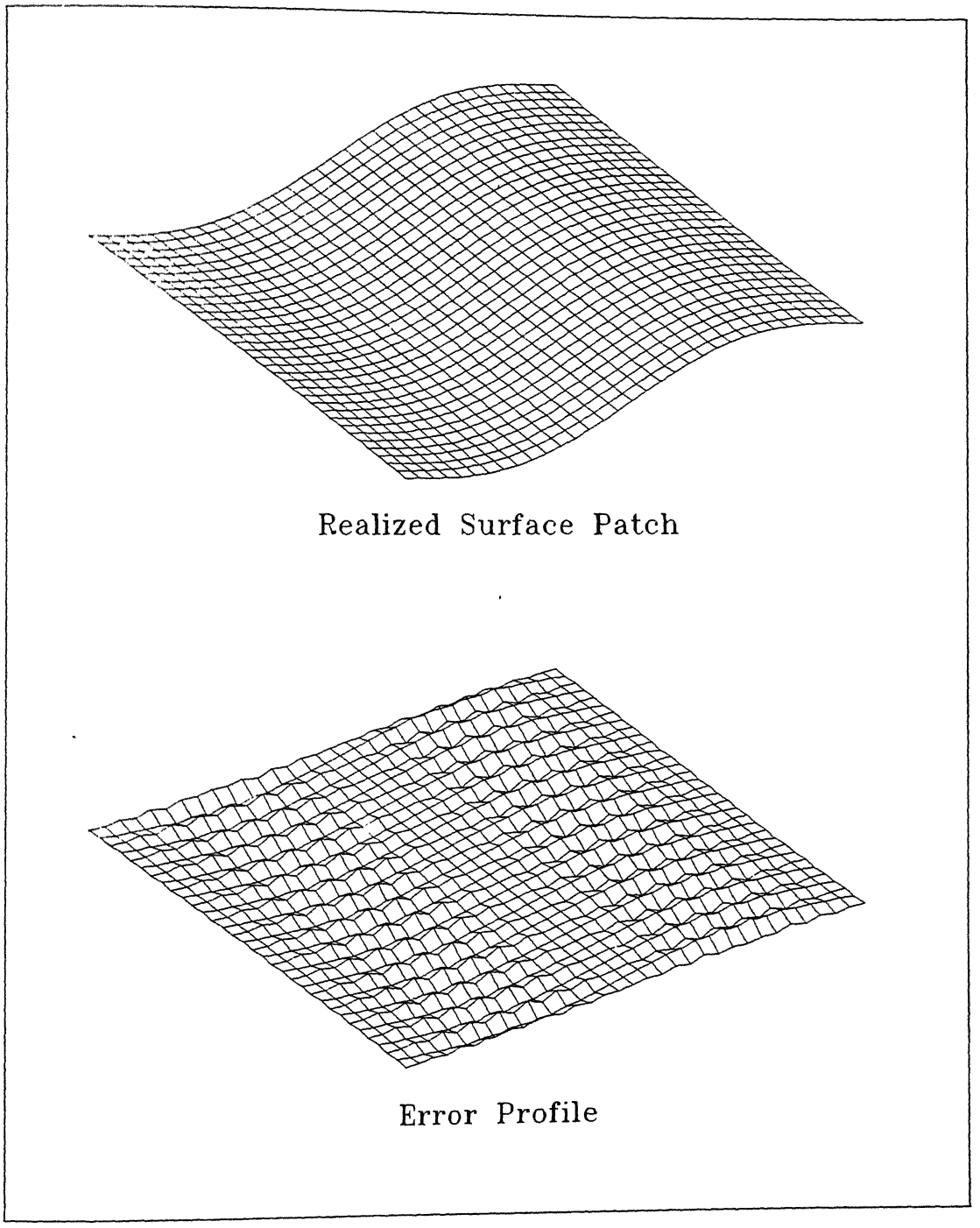

Figure 6.6. Realization of a Swept Surface Patch (Numerical Example III).

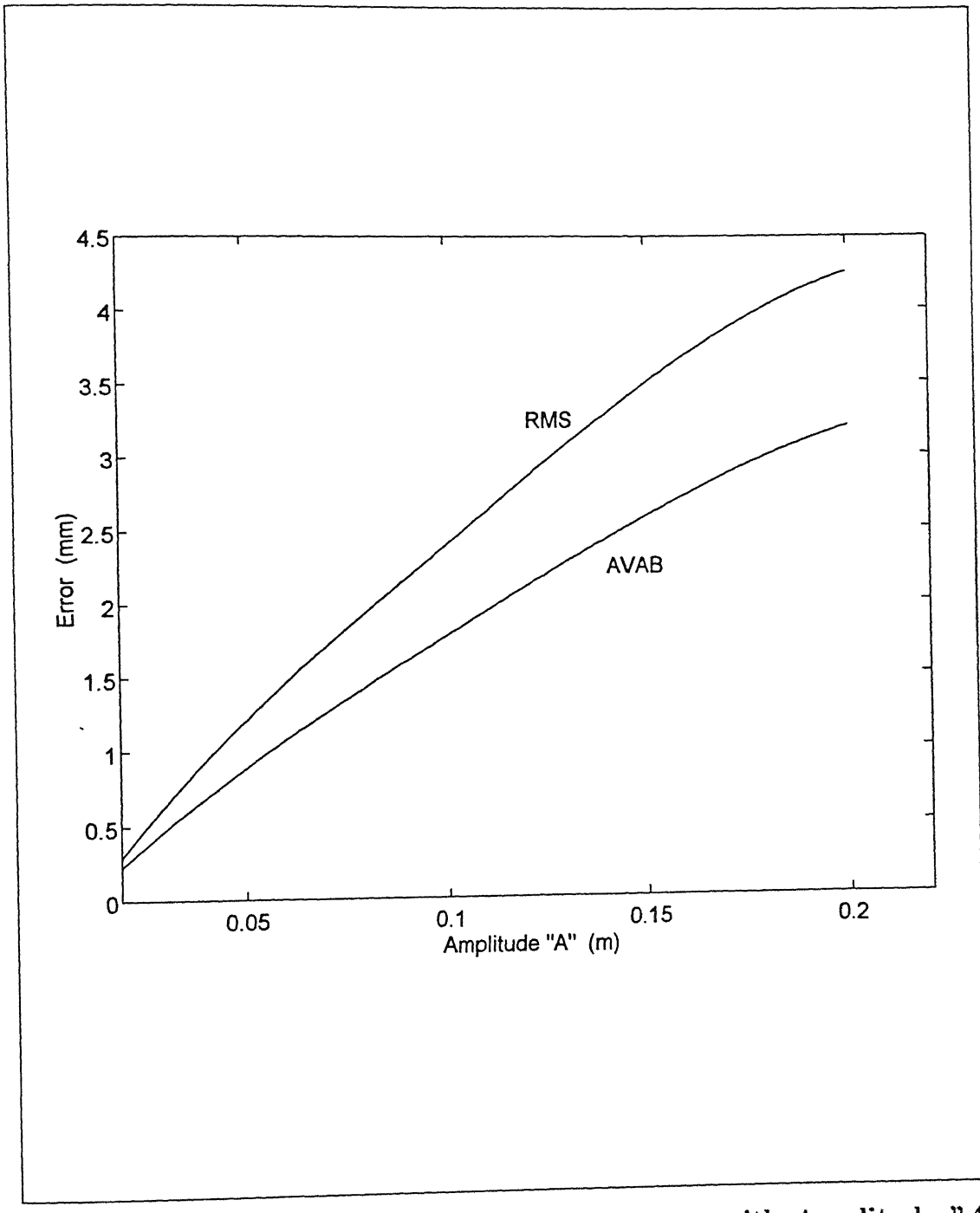

Figure 6.7. Variation of Realized Shape Accuracy with Amplitude "A" (Numerical Example III).

$$z = 20uv(1-u)(1-v)[-10+30u+25v-70uv] \tag{6.4}$$

$$\text{where } 0.0 \leq u \leq 1.0 \text{ and } 0.0 \leq v \leq 1.0$$

The results of the analysis for this patch are given in Table 6.3 and the realized shape is depicted in Figure 6.8. The error between the desired and realized surface patches at higher magnification is also shown in Figure 6.8. It can be seen from this figure that the distribution of shape error is not uniform throughout the flexible sheet. The error is more in the regions of high curvature.

Average Absolute Error	Root Mean Square Error
0.8861 *mm*	1.2718 *mm*

Table 6.3 AVAB and RMS Errors (Numerical Example IV).

The last example of this section is a hyperbolic paraboloid patch. This is an example of anticlastic surface patch. The parametric form of this surface patch is given below.

$$\mathbf{p}(u,v) = [1-u \;\; u] \begin{bmatrix} \begin{bmatrix} 0.0 & 0.0 & 0.00 \end{bmatrix}^T & \begin{bmatrix} 0.0 & 1.0 & 0.24 \end{bmatrix}^T \\ \begin{bmatrix} 1.0 & 0.0 & 0.24 \end{bmatrix}^T & \begin{bmatrix} 1.0 & 1.0 & 0.00 \end{bmatrix}^T \end{bmatrix} \begin{Bmatrix} 1-v \\ v \end{Bmatrix} \tag{6.5}$$

$$\text{where } 0.0 \leq u \leq 1.0 \text{ and } 0.0 \leq v \leq 1.0$$

The results for this surface patch are given in Table 6.4. The realized patch is shown in Figure 6.9. The results obtained for this patch are much superior than some of the earlier cases discussed above. Further numerical experiments related to realization of hyperbolic paraboloid patches which were carried out produced similar results. The better results obtained in the case of hyperbolic paraboloid patches can be explained in the following way.

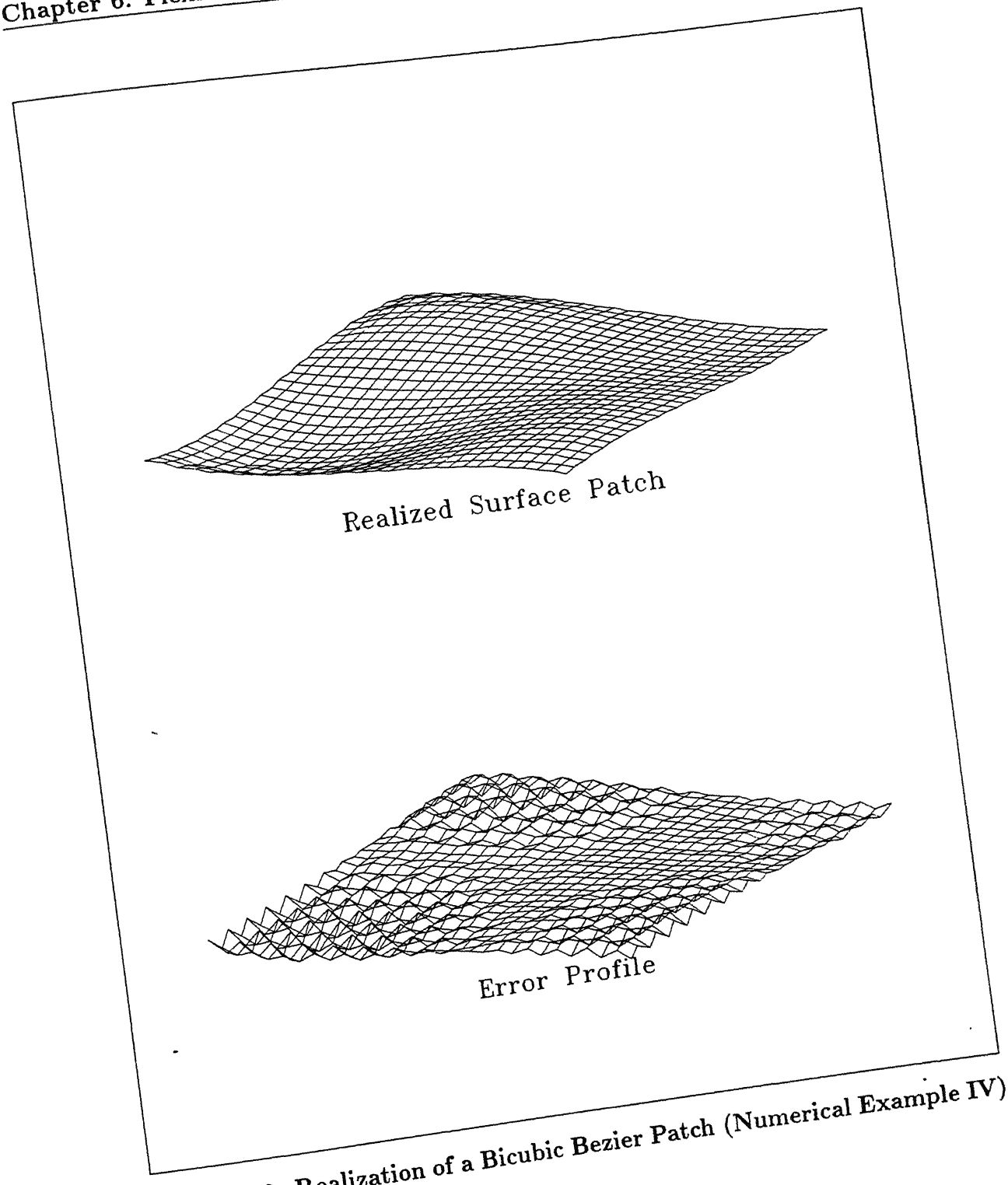

Figure 6.8. Realization of a Bicubic Bezier Patch (Numerical Example IV).

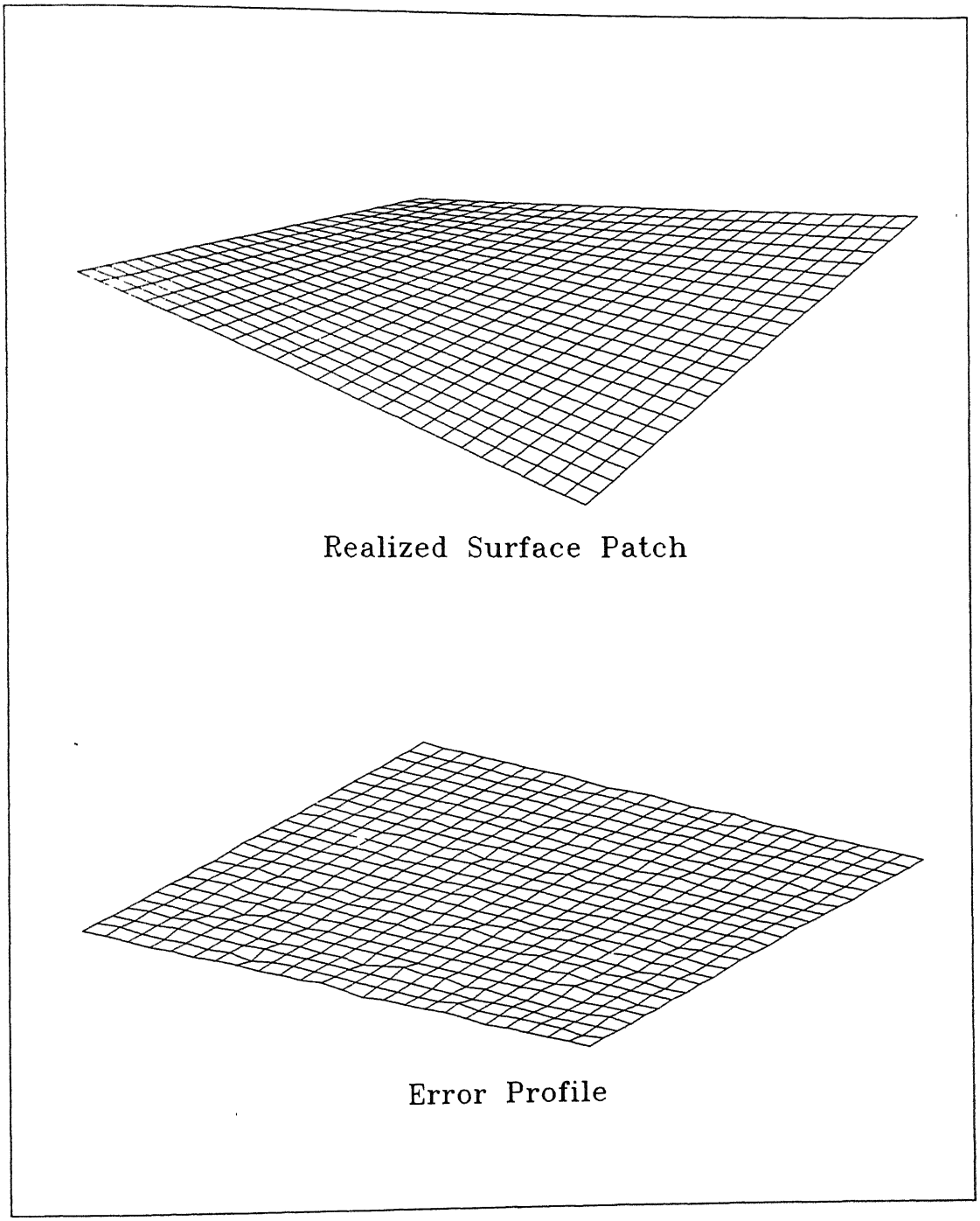

Figure 6.9. Realization of a Hyperbolic Paraboloid Patch (Numerical Example V).

Average Absolute Error	Root Mean Square Error
0.0486 *mm*	0.1158 *mm*

Table 6.4 AVAB and RMS Errors (Numerical Example V).

The deformed configuration of the flexible sheet in this version of tooling mainly depends on the displacement constraints imposed by the indentors. Considering a set of four adjacent indentors in the form of a rectangular grid, a boundary can be drawn by joining the four end points of these indentors by straight lines. An infinite number of surface patches can be constructed interpolating these four boundary edges. Among all these surface patches, the one which has a minimum surface area is the hyperbolic paraboloid defined by four end points of the indentors. As the rubber-like membrane has a tendency of deforming in a form minimizing its deformed surface area, superior results were obtained in the case of hyperbolic paraboloid (Callahan et al., 1988; Grundig, 1988; Hansen, 1993).

In the numerical examples discussed above, it is assumed that there is no external loading on the flexible sheet. The numerical experiments were carried out to study the effect of uniformly distributed load (UDL) on the surface shape error. The effect of external loading on a typical realized shape is shown in Figure 6.10. The error between the desired and realized surface shapes continuously increases with an increasing load.

6.3 Study of Tooling Parameters

The effect of tooling parameters on the accuracy of realizable shapes has been discussed in Chapters 3 and 4 for the flexible surface tooling in which there is no bonding between the flexible sheet and the indentors. Not all the tooling parameters discussed there are relevant in the present case. The effect of three tooling parameters on the the accuracy of realizable surface shapes are presented in this section. The parameters considered here are the sheet thickness, the sheet material and the indentor density.

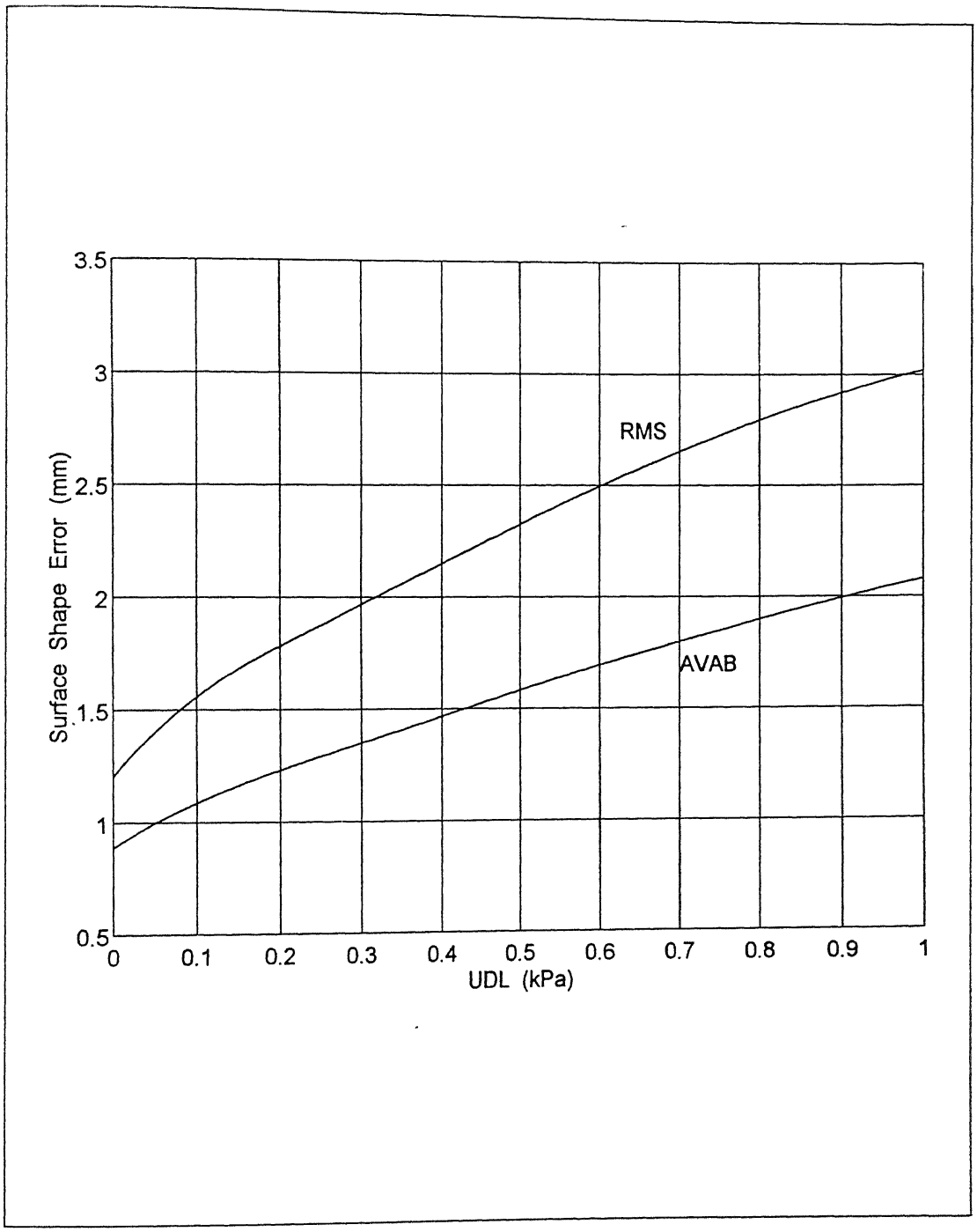

Figure 6.10. Effect of UDL on the Surface Shape Accuracy.

The shape realization experiments were performed with different sheet thickness in the range of 2.0 mm to 10.0 mm. Figures 6.11 and 6.12 present the effect of sheet thickness on the surface shape accuracy. In the absence of any external loading, the thickness does not effect the shape accuracy. This is due to membrane state of the flexible sheet. When there is an external load in the form of UDL acting on the sheet, the accuracy of realized shapes continuously increases with the increasing sheet thickness. The use of higher thickness of the sheet is advisable when there is a considerable external force acting on the flexible sheet. However, as the thickness increases the the reactive contact forces on the indentors bonded to flexible sheet also increases. A component of this recative contact force acting transversely on the indentor may lead to possible buckling if the slenderness ratio of the indentor is not high.

The effect of sheet material on the realizability of a typical shape is shown in Figure 6.13. The figure shows the variation of AVAB and RMS errors for an increasing values of C_1/C_2, where C_1 and C_2 are the first and second Mooney constants respectively. Unlike the earlier version of a flexible surface tooling discussed in Chapter 3, the effect of sheet material on the realizability of a shape is not much in the present case.

The number of indentors used for shape realization is another important factor which has been considered for the present study. Indentors in the range of 81(9 by 9) to 289(17 by 17) are used for the analysis. In each case the AVAB and RMS errors are plotted for number of indentors used (Fig. 6.14). The accuracy of realized shapes strongly depends on the number of indentors used. This is also true with the earlier version of the tooling discussed in Chapter 3.

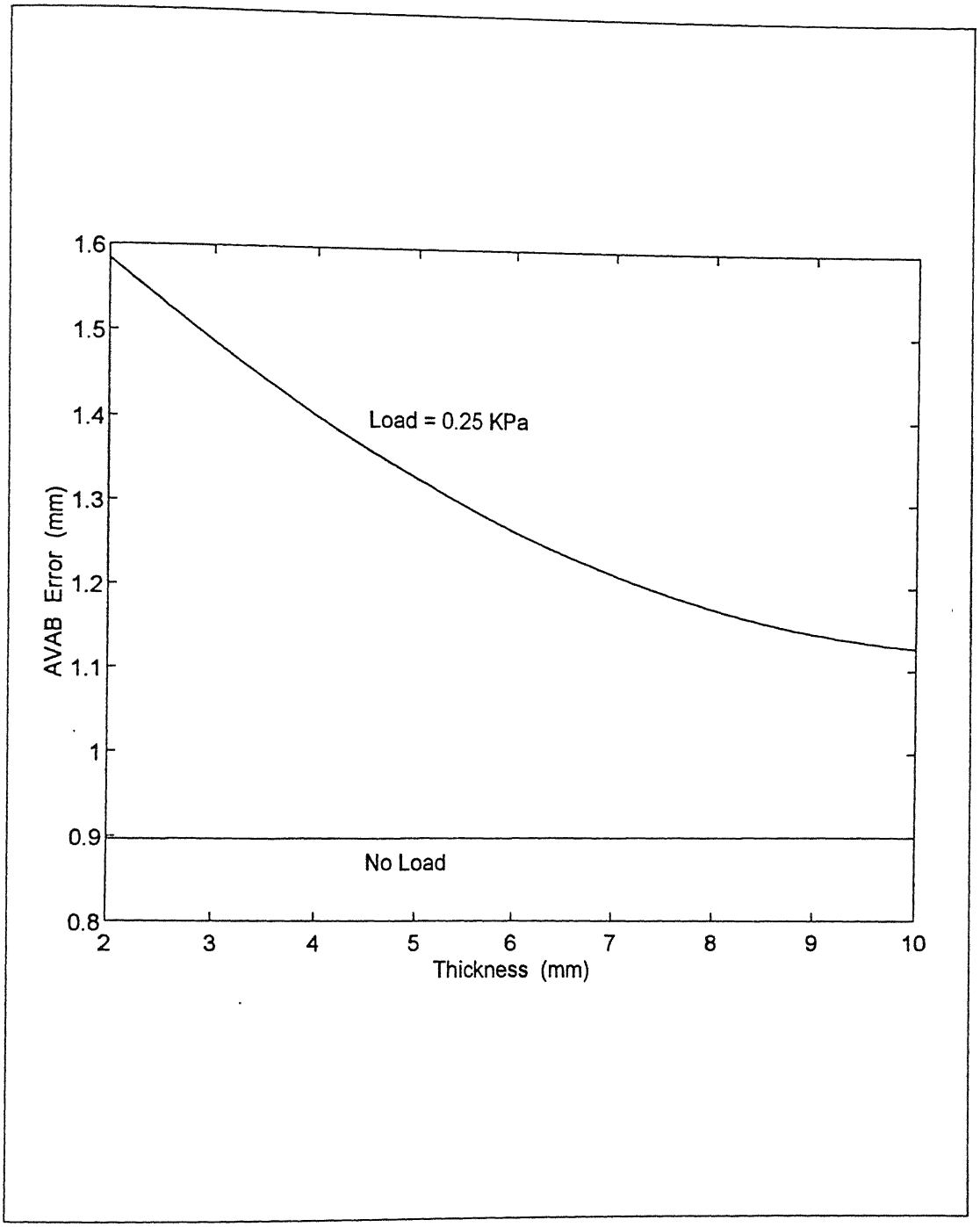

Figure 6.11. Effect of Sheet Thickness on AVAB Error.

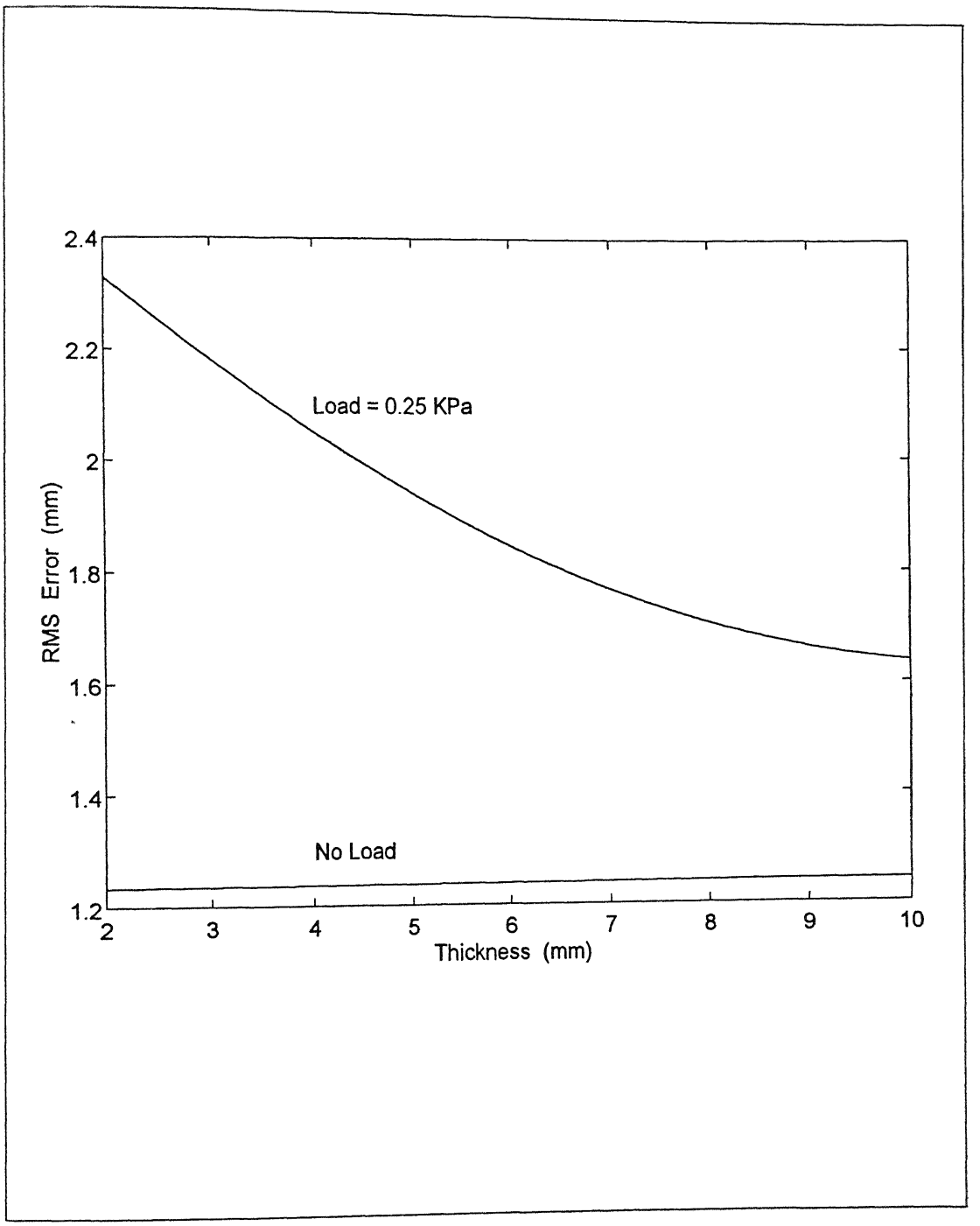

Figure 6.12. Effect of Sheet Thickness on RMS Error.

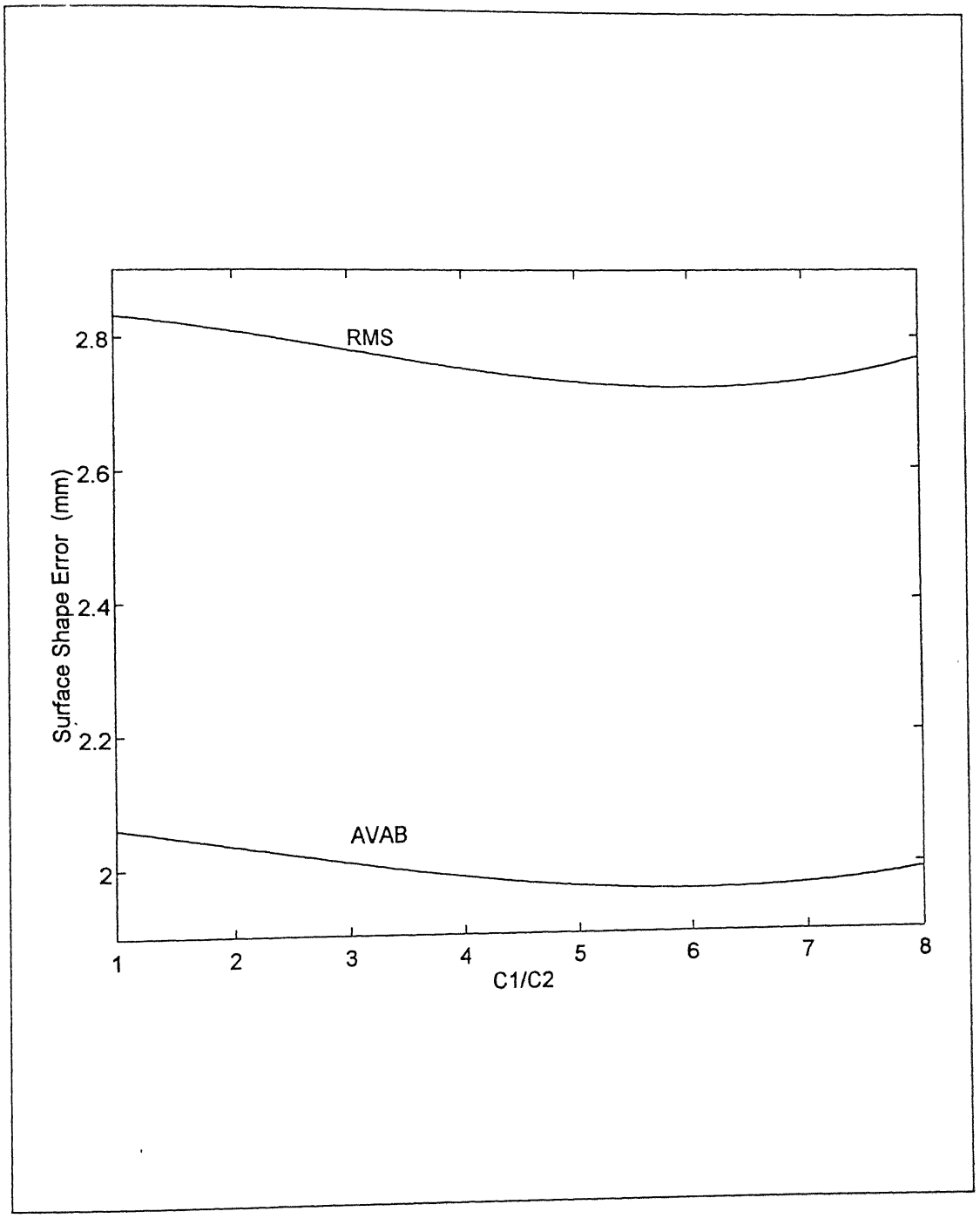

Figure 6.13. Effect of Sheet Material on Surface Shape Accuracy.

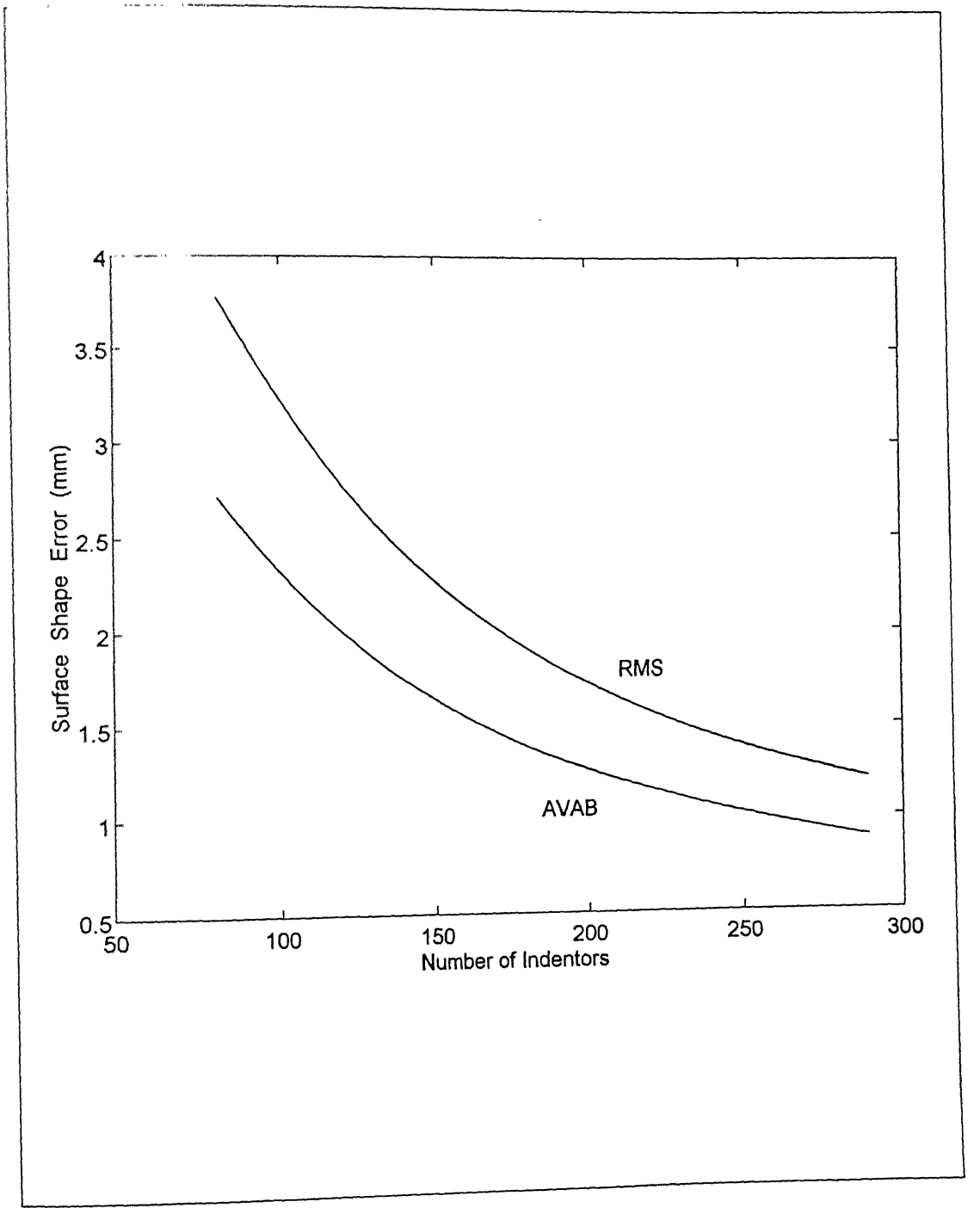

Figure 6.14. Effect of Indentor Density on Surface Shape Accuracy.

Chapter 7

CONCLUSIONS

7.1 Summary

In the present work, a flexible surface tooling system has been proposed for realizing free-form shapes. The tooling is based on the concept of discrete approximation to a continuous mold surface. This is a variation of the discrete surface tooling proposed earlier mainly for sheet metal forming. The applicability of the proposed tooling has been studied for shape conforming processes where a single finished surface is desired such as composite layup. Unlike the earlier investigations in this direction, which were based on laboratory experiments, the present approach is a computational one.

A computer code for the deformation analysis of rubber-like membranes in multiple contact has been developed for carrying out the proposed theoretical study. The effect of various parameters related to the proposed tooling on the realizability of a shape has been studied in order to identify a typical range of these values for a given application. The realizability studies have been carried out by two different approaches namely open and closed-loop approaches which are based on deciding the indentor heights in an off-line and on-line manners respectively. The range of realizable shapes by the proposed tooling include both synclastic and anticlastic shapes.

- The accuracy of realized shape can be considerably improved in some cases by following a closed loop approach which involves the manipulation of a single, a group or all the indentors after every deformation analysis run.

- The flexible surface tool in which the indentors are bonded to flexible sheet can be used for realizing anticlastic shapes with small curvature values.

7.3 Scope for Further Work

The present work is concerned with a numerical study of the shape realization using the proposed flexible surface tooling system. The concept can be extended to all the shape realization processes with appropriate modifications. Though the results presented here are quantitative in nature, the design inferences are more qualitative in nature. It has been felt that the numerical study of the proposed flexible surface tool can be improved by incorporating one or more of the following features.

1. Accounting for the contact friction between the flexible sheet and the indentors.
2. A viscoelastic analysis of the deformation process by including the thermal effects which are likely to be present in the case of processes like Layup.
3. Carrying out the deformation analysis with 3D finite elements or 2D elements with bending stiffness.
4. Extending the analysis to calculate the stresses in the flexible sheet and the possible deflections of the indentors in case of tooling with bonded indentors.

Most of the relevant tooling parameters which affect the realizability of a shape in the proposed tooling are covered as a part of the present work. However, a more detailed study of the these parameters using the concept of *design of experiments* is necessary in this case. The need for further numerical experiments to establish a close relation between the tooling parameters and the complexity of the shape to be realized was also

felt. The process of shape optimization discussed in Chapter 5 which was carried out interactively here, needs to be automated using an appropriate shape control algorithm.

In the present work of shape realization, no attempt has been made to compare the results of computational analysis with the physical experiments. This is necessary to get a more clear picture of the realizability of a shape by the proposed tooling. The efforts to build a flexible surface tooling system are already in progress and some of the lessons learnt from the computational analysis are being incorporated in this endeavor.

7.4 Scope for Related Work

Some of the concepts and techniques which are the outcome of the present work can be used in other areas of engineering. Two such applications which have similarities with the present problem of shape realization are geometric modeling of draped fabric surfaces and the shape finding of large spatial structures.

Geometric modeling of fabric-like objects has been an active area of research for the past one decade. The fabric-like materials when draped on support geometries, deform into complicated doubly curved surfaces which are aesthetically pleasing (Collier, 1990; Dowlen, 1976). The objective here is to model the shape of the deformed fabric when it is draped on the complicated support geometry. In another version of the problem the objective is to achieve a close conformance between the the fabric and the rigid surface on which it is draped (Aono et al., 1994; Hinds et al., 1991). These problems have applications in apparel design, fashion technology, computer animation and computer synthesized advertisements.

Initial attempts to model fabric-like objects were pure geometric in nature which did not yield realistic results. On the other hand, a finite element model accounting for the complex deformation process of the fabric-like materials is computationally intensive in nature (Lloyd, 1984). Thus attempts have been made to model cloth-like objects by hybrid geometric-physical deformable models (Coquillart, 1990; Michael, 1992; Terzopoulos, 1988; Thingvold and Cohen, 1990; Weil, 1986). The results of one such

model proposed by the author for fabrics is shown in Figure 7.1 (Dhande et al., 1993). The problem of finding the shape of a draped fabric can also be posed as a mechanics problem similar to the present case of deformation analysis of rubber-like flexible sheet. It can be further simplified by making some of the assumptions about the deformed geometry which are often used in the area of textile mechanics. Such an attempt has been made to model fabric-like objects in parallel to the present research work (Rao and Dhande, 1995).

Another area of research where some of the concepts proposed in the present work have applications, is the shape finding and shape optimization of the large shells and spatial structures (Berger, 1988; Fujikake et al., 1989; Ramm, 1992; Sclaich et al., 1989). The two geometric forms which are often used for large spatial structures such as roofs of large auditoriums and stadia are fabric membrane structures and pneumatic membrane structures. The first step in the design of these two forms of tensile membrane structures is the process of shape finding. Shape finding often involves deforming a flexible membrane under a controlled load case like pressure or dead load to a desired shape looking for a pure membrane stress state. It is common to use analytical, numerical and experimental methods for the process of shape finding. Often the shape of the spatial structure to be built is realized in a laboratory using models specifically built for this purpose (Aucouturier, 1966; Isler, 1993; Kirsh and Reiss, 1967). It is felt that a generic shape realization tool for realizing a variety of shapes is still lacking. Some of the lessons learnt from the shape realization experiments using flexible surface tool of the present work will be useful for building one such shape realization machine. Moreover, the present computational analysis too has many things in common with the shape finding of pneumatic membrane structures by numerical methods such as FEM.

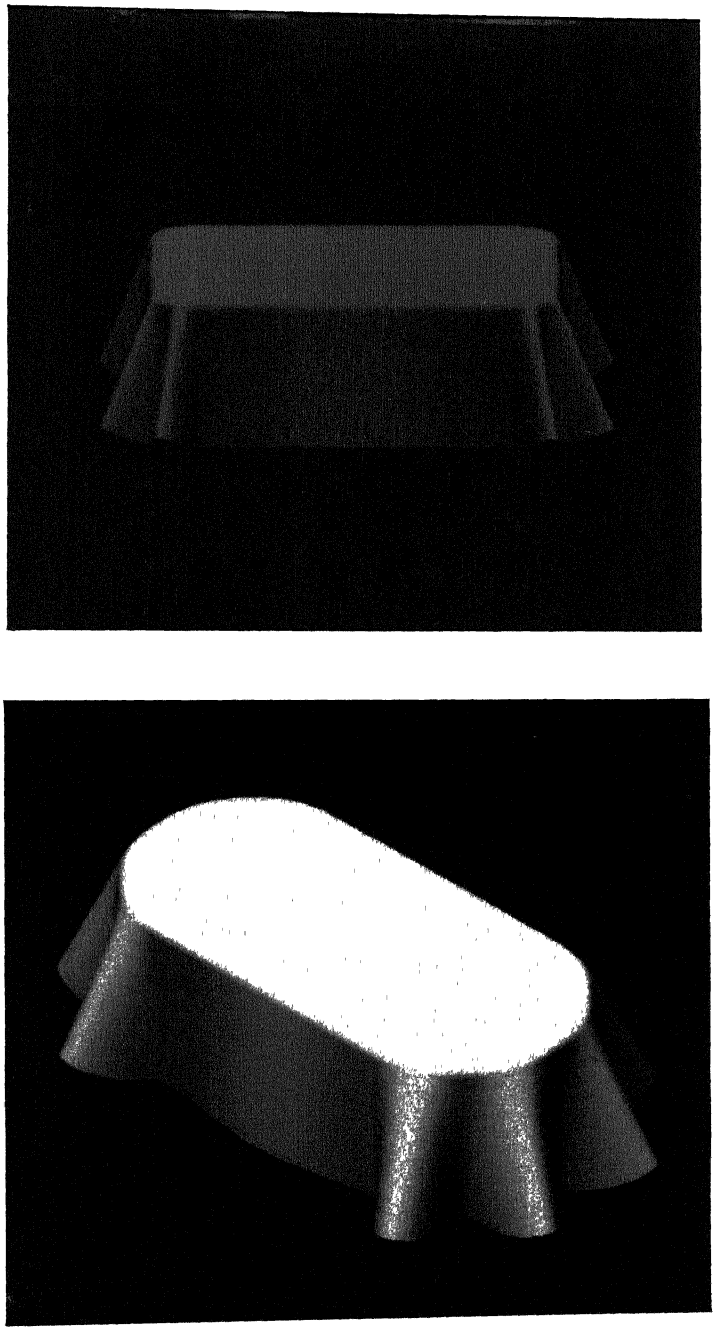

Figure 7.1. A Hybrid Geometric-Physical Deformable Model for Fabrics.

References

1. **Adkins, J. E. and Rivlin, R. S.**, *Large elastic deformations of isotropic materials IX - the deformation of thin shells*, Phil. Trans. Roy. Soc., Vol. A244, 1952, pp 505-531.

2. **Alting, L.**, *Manufacturing engineering processes*, Marcel Dekker, Inc., New York, USA, 1982.

3. **Aono, A., Breen, D. E. and Wozny, M. J.**, *Fitting a woven-cloth model to a curved surface: mapping algorithms*, Computer Aided Design, Vol. 26, No. 4, April 1994, pp 278-292.

4. *ASM Engineered Materials Handbook, Vol.1: Composites*, ASM International, OH, USA, 1988.

5. **Aucouturier, L.**, *Remarks on self-supporting shells*, Bulletin of the Intl. Association for Shell and Spatial Structures, September, 1966, pp 47-58.

6. **Bader, M. G., Smith, W., Isham, A. B., Rolston, J. A. and Metzner, A. B.**, *Delaware composites design encyclopedia, Volume 3 : Processing and fabrication technology*, Technomic Publishing Company, Inc., Lancaster, USA, 1990.

7. **Bass, J. M.**, *Three-dimensional finite deformation, rolling contact of a hyperelastic cylinder: Formulation of the problem and computational results*, Computers & Structers, Vol. 26, No. 6, 1987, pp 991-1004.

8. **Batra, R. C.**, *Quasistatic indentation of a rubberlike layer by a rigid cylinder*, Proc. of Intl. Conf. on Finite Elements in Computational Mechanics, Bombay, India, 2-6 December, 1985, pp 345-357.

9. **Beatty, M. F.**, *Topics in finite elasticity: hyperelasticity of rubber, elastomers, and biological tissues - with examples*, Applied Mechanics Review, Vol. 40, No. 12, 1987, pp 1699-1734.

10. **Becker, E. B.**, *Numerical solution of a class of problems of finite elastic deformation*, PhD thesis, University of California, Berkeley, 1966.

11. **Berger, H.**, *New developments in lightweight dome structures*, Invited Lecture at the IASS-MSU symposium on Domes from Antiquity to the Present, Istanbul, 1988.

12. **Callahan, M. J., Hoffman, D. and Hoffman, J. T.**, *Computer graphics tools for the study of minimal surfaces*, Communications of the ACM, Vol. 31, No. 6, 1988, pp 648-661.

13. **Carley, E. P., Dockum, J. F. and Jr. Schell, P. L.**, *Preforming for liquid composite molding*, Proc. of the Fifth Annual ASM/ESD Advanced Composites Conference, 25-28 September, Dearborn, Michigan, USA, 1989, pp 259-273.

14. **Chand, R., Haug, E. J. and Rim, K.**, *Analysis of unbonded contact problems by means of quadratic programming*, Journal of Optimization Theory and Applications, Vol. 20, No. 2, 1976, pp 171-189.

15. **Charrier, J. M., Shrivastava, S. and Wu, R.**, *Free and constrained inflation of elastic membranes in relation to thermoforming - axisymmetric problems*, Journal of Strain Analysis in Engineering Design, Vol. 22, No. 2, 1987, pp 115-125.

16. **Charrier, J. M., Shrivastava, S. and Wu, R.**, *Free and constrained inflation of elastic membranes in relation to thermoforming - non-axisymmetric problems*, Journal of Strain Analysis in Engineering Design, Vol. 24, 1989, pp 55-74.

17. **Cho, U. Y.**, *Plane strain finite element analysis of sheet forming operations including bending effects*, PhD thesis, Ohio State University, 1993.

18. **Collier, B. J.**, *Assessment of fabric drape*, FIT Review, Vol. 6, 1990, pp 40-43.

19. **Coquillart, S.**, *Extended free-form deformation: a sculpturing tool for 3D geometric modeling*. ACM Computer Graphics, Vol. 24, No. 4, August 1990, pp 187-196.

20. **deLorenzi, H. G. and Nied, H. F.**, *Blow molding and thermoforming of plastics: finite element modelling*, Computers & Structers, Vol. 26, 1987, pp 197-206.

21. **Dhande, S. G. and Karunakaran, K. P.**, *Realizability in computer aided design*, Proc. of the IFIP TC5/WG5.2/WG5.10 CSI International Conference on Computer Graphics - ICCG'93, Bombay, 24-26 February, Elsevier, Amsterdam, 1993, pp 259-270.

22. **Dhande, S. G., Rao, P. V. M., Tavakkoli, S. and Moore, C. L.**, *Geometric Modeling of Draped Fabric Surfaces*, Proc. of the IFIP TC5/WG5.2/WG5.10 CSI International Conference on Computer Graphics - ICCG'93, Bombay, 24-26 February, Elsevier, Amsterdam, 1993, pp 349-356.

23. **Dilintas, G., Gengoux, P. L. and Trystram, D.**, *A conjugate projected gradient method with preconditioning for unilateral contact problems*, Computers & Structers, Vol. 29, No. 4, 1988, pp 675-680.

24. **Dowlen, R.**, *Drape of apparel fabrics*, Technical Report, ARS-S-149, Agriculture Research Service, U.S. Department of Agriculture, September, 1976.

25. **Endo, T., Oden, J. T., Becker, E. B. and Miller, T.**, *A numerical analysis of contact and limit-point behaviour in a class of problems of finite elastic deformation*, Computers & Structers, Vol. 18, No. 5, 1984, pp 899-910.

26. **Farnham, S. E.**, *A guide to thermoformed plastic packaging*, Cahners Publishing Company, Inc., Boston, USA, 1972.

27. **Faux, I. D. and Pratt, M. J.**, *Computational Geometry for Design and Manufacture*, Ellis Horwood, Chichester, 1983.

28. **Feng, W. W. and Huang, P.**, *On the inflation of a plane nonlinear membrane*, Transactions of ASME Journal of Applied Mechanics, Vol. 41, No. 3, September 1974, pp 767-771.

29. **Feng, W. W. and Huang, P.**, *On the general contact problem of an inflated nonlinear plane membrane*, Intl. Journal of Solids & Structures, Vol. 11, 1975, pp 437-448.

30. **Feng, W. W., Tielking, J. T. and Huang, P.**, *The inflation and contact constraint of a rectangular Mooney membrane*, Transactions of ASME Journal of Applied Mechanics, Vol. 41, 1974, pp 979-984.

31. **Feng, W. W. and Yang, W. H.**, *On the contact problem of an inflated spherical nonlinear membrane*, Transactions of ASME Journal of Applied Mechanics, Vol. 40, 1973, pp 209-214.

32. **Foster, H. O.**, *Very large deformations of axially symmetrical membranes made of neo-Hookean materials*, International Journal of Engineering Science, Vol. 5, 1967, pp 95-117.

33. **Fujikake, M., Kojima, O. and Fukushima, S.**, *Analysis of fabric tension structures*, Computers & Structers, Vol. 32, No. 3-4, 1989, pp 537-547.

34. **Gadala, M. H.**, *Numerical solutions of nonlinear problems of continua - II. survey of incompressibility constraints and software aspects*, Computers & Structers, Vol. 22, 1986, pp 841-855.

35. **Gladwell, G. M. L.**, *Contact problems in the classical theory of elasticity*, Sijthoff & Noordhoff, Alphen aan den Rijn, 1980.

36. **Grundig, L.**, *Minimal surfaces for finding forms of structural membranes*, Computers & Structers, Vol. 30, No. 3, 1988, pp 679-683.

37. **Gruttman, F. and Taylor, R. L.**, *Theory and finite element formulation of rubberlike membrane shells using principal stretches*, International Journal for Numerical Methods in Engineering, Vol. 35, 1992, pp 1111-1126.

38. **Haftka, R. T. and Adelman, H. M.**, *An analytical investigation of shape control of large space structures by applied temperatures*, AIAA Journal, Vol. 23, No. 3, March 1985, pp 450-457.

39. **Haftka, R. T.**, *Integrated nonlinear analysis and design*, AIAA Journal, Vol. 27, 1989, pp 1622-1627.

40. **Haggblad, B. and Nordgren, G.**, *Automatic load incrementation for rubber-like bodies in contact*, Computers & Structers, Vol. 32, Nos. 3-4, 1989, pp 899-909.

41. **Ham, N. M. and Molitor, M. S.**, *Thermal analysis of composite tooling materials*, Proc. of the Fifth Annual ASM/ESD Advanced Composites Conference, Dearborn, Michigan, USA, 25-28, September, 1989, pp 161-165.

42. **Hansen, V. L.**, *Geometric in nature*, A. K. Peters Ltd., Wellesley, MA, USA, 1993.

43. **Hardt, D. E.**, *Closed-loop sheet metal forming processes*, Proc. of IFAC workshop on Intelligent Manufacturing Systems, Dearborn, Michigan, USA, 1992, pp 187-192.

44. **Hardt, D. E., Boyce, M. C., Ousterhout, K. B., Karafillis, A. and Eigen, G. M.**, *CAD-driven flexible forming system for three-dimensional sheet metal parts*, Proc. Sheet Metal and Stamping Symposium SAE Special Publications No. 944, SAE, Warrendale, PA, USA, 1993, pp 69-76.

45. **Hardt, D. E. and Gossard, D. C.**, *A variable geometry die for sheet metal forming*, Machine Design and Control, Proc. of Joint Automatic Control Conference, San Francisco, 1980.

46. **Hardt, D. E. and Webb, R. D.**, *Sheet metal die forming using closed-loop shape control*, Annals of the CIRP, Vol. 31, No. 1, 1982, pp 165-169.

47. **Hart-Smith, L. J.**, *Elasticity parameters for finite deformations of rubber-like materials*, ZAMP, Vol. 17, No. 39, 1966, pp 608-625.

48. **Hart-Smith, L. J. and Crisp, J. D. C.**, *Large elastic deformations of thin rubber membranes*, International Journal of Engineering Science, Vol. 5, 1967, pp 1-24.

49. **Hasan, S.**, *Physical modeling and finite element analysis of friction encountered in large deformation processes*, PhD thesis, Texas Tech. University, 1993.

50. **Hertz, H.**, *Uber die beruhrung fester elastischer korper*, J. fur Math., Vol. 92, 1882, pp 156-171.

51. **Hinds, B. K., McCartney, J. and Woods, G.**, *Pattern development for 3D surfaces*, Computer Aided Design, Vol. 23, No. 8, October 1991, pp 583-592.

52. **Hung, N. D. and Saxce, G. D.**, *Frictionless contact of elastic bodies by finite element method and mathematical programming technique*, Computers & Structers, Vol. 11, 1980, pp 55-67.

53. **Isler, H.**, *Generating shell shapes by physical experiments*, Bulletin of the Intl. Association for Shell and Spatial Structures, Vol. 34, No. 111, 1993, pp 53-63.

54. **Johnson, A. R. and Quigley, C. J.**, *Frictionless geometrically non-linear contact using quadratic programming*, International Journal for Numerical Methods in Engineering, Vol. 28, 1989, pp 127-144.

55. **Kamat, M. P. and Hayduk, R. J.**, *Energy minimization versus pseudo force technique for nonlinear structural analysis*, Computers & Structers, Vol. 11, 1980, 403-409.

56. **Karunakaran, K. P.**, *Geometric modeling of manufacturing processes using symbolic and computational conjugate geometry*, PhD thesis, Indian Institute of Technology, Kanpur, 1993.

57. **Khayat, R. E., Derdouri, A. and Garcia-Rejon, A.**, *Multiple contact and axisymmetric inflation of hyperelastic cylindrical membranes*, Proc. of Institution of Mechanical Engineers, Part C : Journal of Mechanical Engineering Science, Vol. 207, 1993, pp 175-183.

58. **Kikuchi, N. and Oden, J. T.**, *Contact problems in elasticity : A study of variational inequalities and finite element methods*, SIAM, Philadelphia, 1988.

59. **Kikuchi, N. and Song, Y. J.**, *Contact problems involving forces and moments for incompressible linearly elastic materials*, International Journal of Engineering Science, Vol. 18, 1980, pp 357-377.

60. **Kirsh, U. and Reiss, M.**, *Experimental study of regular hexahyps*, Bulletin of the Intl. Association for Shell and Spatial Structures, December, 1967, pp 41-48.

61. **Klingbeil, W. W. and Shield, R. T.**, *Some numerical investigations on empirical strain energy functions in large axi-symmetric extensions of rubber membranes*, ZAMP, Vol. 15, 1964, pp 608-629.

62. **Lee, G. B. and Kwak, B. M.**, *Formulation and implementation of beam contact problems under large displacement by a mathematical programming*, Computers & Structers, Vol. 31, No. 3, 1989, pp 365-376.

63. **Levinson, M.**, *The application of the principle of stationary potential energy to some problems in finite elasticity*, Transactions of ASME Journal of Applied Mechanics, Vol. 32, No. 3, September 1965, pp 656-660.

64. **Lloyd, D. W.**, *The mechanics of drape*, In Flexible Shells, **Axelrad, E. L. and Emmerling, F. A. (eds.)**, Springer Verlag, Berlin, 1984, pp 271-282.

65. **Lord, E. A. and Wilson, C. B.**, *The mathematical description of shape and form*, Ellis Horwood, Chichester, England, 1984.

66. **Mallick, P. K. and Newman, S.(Eds.)**, *Composite materials technology : Processes and properties*, Hanser Publishers, New York, 1990.

67. **May, O. H.**, *The conjugate gradient method for unilateral problems*, Computers & Structers, Vol. 12, No. 4, 1986, pp 595-598.

68. **Michael, C., Ying, Y., Thalmann, N. M. and Thalmann, D.**, *Dressing animated synthetic actors with complex deformable cloths*, ACM Computer Graphics, Vol. 26, No. 2, July 1992, pp 99-104.

69. **Misra, B. K.**, *Geometric modeling of virtual cutter and swept surfaces generated by nontraditional manufacturing processes*, PhD thesis, Indian Institute of Technology, Kanpur, 1993.

70. **Mooney, M.**, *A theory of large elastic deformation*, Journal of Applied Physics, Vol. 11, 1940, pp 582-592.

71. **Mortenson, M. E.**, *Geometric Modeling*, John Wiley, USA, 1985.

72. **Nakajima, N.**, *A newly developed technique to fabricate complicated dies and electrodes with wires*, Bulletin of JSME, Vol. 12, No. 54, 1969, pp 1546-1554.

73. **Oden, J. T.**, *Analysis of large deformation of elastic membranes by the finite element method*, Proc. of IASS Intl. Congress of Large-Span Shells, Leningrad, 1966.

74. **Oden, J. T.**, *Numerical formulation of nonlinear elasticity problems*, Journal of structural division, Proc. of the ASCE, Vol. 93, No. ST3, 1967, pp 235-255.

75. **Oden, J. T.**, *Finite plane strain of incompressible elastic solids by the finite element method*, Aeron. Quart., Vol. 19, 1968, pp 254-264.

76. **Oden, J. T.**, *Finite elements of nonlinear continua*, McGraw Hill, USA, 1972.

77. **Oden, J. T. and Carey, G. F.**, *Finite elements : Special problems in solid mechanics*, Vol. 5, Prentice-Hall, Inc., New Jersey, 1984.

78. **Oden, J. T. and Key, J. E.**, *Numerical analysis of finite axisymmetric deformation of incompressible elastic solids of revolution*, International Journal Solids & Structures, Vol. 6, 1970, pp 497-518.

79. **Oden, J. T. and Key, J. E.**, *Analysis of finite deformations of elastic solids by the finite element method*, Proc. of IUTAM Colloq. High Speed Computing Elastic Struct. Liege, 1971.

80. **Oden, J. T. and Sato, T.**, *Finite strains and displacements of elastic membranes by the finite element method*, International Journal Solids & Structures, Vol. 3, 1967, pp 471-488.

81. **Orozco, C. E. and Ghattas, O. N.**, *Jacobian and hessian sparsity in simultaneous and nested structural optimization*, Collection of Technical Papers, Part I, AIAA/ASME/ASC/AHS/ASC 32nd Structures, Structural Dynamics and Materials Conference, Baltimore, MD, USA, April 8-10, 1991, pp 413-423.

82. **Ousterhout, D. C.**, *Design and control of a flexible process for three-dimensional sheet metal forming*, PhD thesis, Massachusetts Institute of Technology, 1991.

83. **Padula, S. L., Adelman, H. M., Bailey, M. C. and Haftka, R. T.**, *Integrated structural electromagnetic shape control of large space antenna reflectors*, AIAA Journal, Vol. 27, No. 6, June 1989, pp 814-819.

84. **Pham, B.**, *Offset curves and surfaces: a brief survey*, Computer Aided Design, Vol. 24, No. 4, April 1992, pp 223-229.

85. **Potter, K. D.**, *Fabrication techniques for advanced composites*, Proc. of Institution of Mechanical Engineers, Part G : Journal of Aerospace Engineering, Vol. 203, 1989, pp 25-30.

86. **Ramm, E.**, *Shape finding methods of shells*, Bulletin of the Intl. Association for Shell and Spatial Structures, Vol. 33, No. 109, 1992, pp 89-99.

87. **Rao, P. V. M. and Dhande, S. G.**, *Computer Aided Apparel Design*, Paper under preparation for IEEE Computer Graphics & Applications.

88. **Reklaitis, G. V., Ravindran, A. and Ragsdell, K. M.**, *Engineering optimization methods and applications*, Wiley, New York, 1983.

89. **Rigbi, Z. and Hiram, Y.**, *An approximate method for the study of large deformations of membranes*, International Journal of Mechanical Science, Vol. 23, 1981, pp 1-10.

90. **Rivlin, R. S.**, *Large elastic deformations of isotropic materials. IV*, Phil. Trans. Roy. Soc., Vol. A241, 1948, pp 379-397.

91. **Sayegh, A. F. and Tso, F. K.**, *Treatment of frictionless contact boundaries by direct minimization*, Computers & Structers, Vol. 22, No. 6, 1986, pp 905-915.

92. **Schlaich, J., Bergermann, R. and Sobek, W.**, *Tensile membrane structures*, Invited Lecture in the IASS-Congress in Madrid, September, 1989.

93. **Schuldt, S. B., Gabriele, G. A., Root, R. R., Sandgren, E. and Ragsdell, K. M.**, *Application of a new penalty function method to design optimization*, Transactions of ASME Journal of Engineering for Industry, Vol. 99, 1977, pp 31-36.

94. **Shukla, J.**, *Fabrication of aircraft structures from thermoplastic drapeable preforms*, Advanced Materials: The Big Payoff, National SAMPE Technical Conference, Vol. 21, SAMPE, Covina, CA, 1989, pp 700-704.

95. **Steenkamer, D. A., Wilkins, D. J. and Karbhari, V. M.**, *Resin transfer molding : part I materials and preforming*, Processing of Advanced Materials, Vol. 3, 1993, pp 89-105.

96. **Strong, A. B.**, *High performance and engineering thermoplastic composites*, Technomic Publishing Company, Inc., Lancaster, PA, USA, 1993.

97. **Struik, D. J.**, *Lectures on Classical Differential Geometry*, Addison-Wesley, Massachusetts, USA, 1950.

98. **Sussman, T. and Bathe, K. J.**, *A finite element formulation for nonlinear incompressible elastic and inelastic analysis*, Computers & Structers, Vol. 26, No. 1-2, 1987, pp 357-409.

99. **Tavakkoli, S.**, *Intrinsic geometry for shape design*, PhD thesis, Virginia Polytechnic Institute and State University, 1991.

100. **Terzopoulos, D. and Fleischer, K.**, *Deformable Models*, Visual Computer, Vol. 4, 1988, pp 306-331.

101. **Thingvold, J. A. and Cohen, E.**, *Physical modeling with B-spline surfaces for interactive design and animation*, ACM Computer Graphics, Vol. 24, 1990, pp 129-137.

102. **Tielking, J. T. and Feng, W. W.**, *The application of the minimum potential energy principle to nonlinear axisymmetric membrane problems*, Transactions of ASME Journal of Applied Mechanics, Vol. 41, No. 2, June 1974, pp 491-496.

103. **Van West, B. P.**, *A simulation of the draping and a model of the consolidation of commingled fabrics*, PhD thesis, University of Delaware, 1990.

104. **Voruganti, R. S.**, *Symbolic and computational conjugate geometry for design and manufacturing applications*, Master's thesis, Virginia Polytechnic Institute and State University, 1990.

105. **Webb, R. D.**, *Spatial frequency based closed-loop control of sheet metal forming*, PhD thesis, Massachusetts Institute of Technology, 1987.

106. **Webb, R. D. and Hardt, D. E.**, *A transfer function description of sheet metal forming for process control*, Transactions of the ASME Journal of Engineering for Industry, Vol. 113, No. 1, 1991, pp 44-52.

107. **Weil, J.**, *The synthesis of cloth objects*, ACM Computer Graphics, Vol. 20, No. 4, 1986, pp 49-54.

108. **Westbrook, D. R.**, *Contact problem for the elastic beam*, Computers & Structers, Vol. 15, No. 4, 1982, pp 473-479.

109. **Yang, W. H. and Hsu, K. H.**, *Indentation of a circular membrane*, Transactions of ASME Journal of Applied Mechanics, Vol. 38, 1971, pp 227-230.

110. **Zamani, N. G., Watt, D. F. and Esteghamatian, M.**, *Status of the finite element method in the thermoforming process*, International Journal for Numerical Methods in Engineering, Vol. 28, 1989, pp 2681-2693.

111. **Zhong, Z. H.**, *Finite element procedures for contact-impact problems*, Oxford University Press Inc., New York, 1993.

112. **Zhou, D.**, *Development and testing of a new algorithm for FEM of sheet forming*, PhD thesis, Ohio State University, 1993.

Date Slip

This book is to be returned on the date last stamped.